ABSTRACT

HU, GANG. Adsorption and Activity of Cellulase Enzymes on Various Cellulose Substrates. (Under the direction of Professor John A. Heitmann and Associate Professor Orlando J. Rojas.)

The objective of this research is to understand the interfacial behavior in cellulose hydrolysis by cellulase enzymes. This research began with an investigation on the in-situ monitoring of cellulose hydrolysis using a piezoelectric quartz crystal microbalance. The real-time kinetic behavior was modeled using a dose-response model. The adsorption indicated by the drop in resonance frequency followed a Langmuir model. Another important part of this research was the development of a new cellulase activity assay based on the piezoelectric technique. This assay provides an easier and more user-friendly method to measure cellulase activity. It also helped to clarify an element in the interpretation of frequency shift after injection of cellulase solutions for the hydrolysis of cellulose thin films, which has been neglected in previous efforts. Interfacial adsorption of cellulase proteins was also investigated using the depletion method. The effects of substrate properties, primarily the crystallinity, which was characterized using X-ray diffraction, were investigated. The effect of surface areas, which were measured using laser light scattering and BET gas adsorption techniques, on cellulase adsorption were also investigated. It was found that both crystallinity and surface areas played an important role in cellulase adsorption on the substrates studied. In the characterization of cellulosic substrates, the water retention value was also investigated. The results indicated that substrates with lower crystallintiy had higher water retention ability. The cellulase adsorption and desorption were also studied by using sodium dodecyle sulphate polyacrylamide gel electrophoresis (SDS-PAGE). The adsorption results followed the same trend as indicated by the depletion methods. The various isozymes demonstrated a uniform adsorption and desorption in proportion to their concentrations. Higher pH was found to produce higher desorption for the cellulases and substrates studied. It was also found that cellulases from *Trichoderma reesei* had higher affinity than those from *Aspergillus niger* in terms of their affinity with the cellulosic substrates used in this work.

Adsorption and Activity of Cellulase Enzymes on Various Cellulose Substrates

by
Gang Hu

A dissertation submitted to the Graduate Faculty of
North Carolina State University
in partial fulfillment of the
requirements for the Degree of
Doctor of Philosophy

Wood and Paper Science

Raleigh, North Carolina

2009

APPROVED BY:

Dr. John A. Heitmann Committee Chair	Dr. Orlando J. Rojas Co-chair
Dr. Dimitris S. Argyropoulos	Dr. Joel J. Pawlak

DEDICATION

I would like to dedicate this dissertation to my parents, Yuguo Hu and Huizhen Wang, and to those who love and supported me with their patience.

BIOGRAPHY

Gang Hu was born in Chongqing, China on June 3, 1974. He lived there until finished high school. In 1997, he graduated from Shanghai Jiaotong University with a B.S. of Applied Chemistry and a B.S. of Applied Electronics. He started to work as a shift manager in a polyester plant. He moved to work as a chemical technician and then the chief engineer in the research and development section of a multinational paper company in Shanghai. He had also worked in South Korea and Thailand for some time. Gang Hu is a certified engineer since 2003. He began his Ph.D. study in January 2005 in the Department of Forest Biomaterials (formerly the Department of Wood and Paper Science) at North Carolina State University.

ACKNOWLEDGEMENTS

First and foremost, I would like to give my utmost appreciation to Dr. John A. Heitmann for his precious advice, patience, encouragement and support in the accomplishment of this research. I also sincerely appreciate every bit of education/suggestions he made in all our weekly meetings. Most of them will be my invaluable wealth that leads me to success. I also thank his family for being host at many special holidays. This research was partially funded by Proctor & Gamble and we appreciate this financial support.

I would like to thank Dr. Orlando Rojas and Dr. Martin Hubbe for their priceless advice, suggestions and help with this research and my student career in this department. They are also thanked for many other issues. I also acknowledge Dr. Dimitris Argyropoulos and Dr. Joel Pawlak for their valuable suggestions, comments and encouragement in finishing this research. Dr. Steve Kelley is thanked for his leadership, trust and encouragement. Dr. Hou-min Chang and Dr. Michael J. Kocurek are thanked for their interview in Shanghai and their many criticisms that helped me grow.

I would also thank Kelley Spence and Rachel Ernest for their friendship and discussions on many cultural issues. There are also many other people, including my Chinese folks in this department, to whom I express my acknowledgement but not be able to mention their names in a short paragraph. I would like to give my special acknowledgement to Ning Wu, who had accompanied me to learn swimming. She is also thanked for her support when I was in a hard time.

Finally, I thank my parents for their understanding, patience and unending encouragement. I also thank them for allowing me to have most of their advantages and few disadvantages. Thanks them for their unselfish love.

TABLE OF CONTENTS

LIST OF TABLES

List of Figures

Chapter 1 General background

Biotechnology plays a key role in development of natural sustainable materials for human use. The applications of such materials range from foodstuff, beverages and garments to synthetic materials and energy. The exploitation of renewable natural resources for energy and materials has become a crucial issue due to the depletion and increasing cost of petroleum reserves. Lignocellulosic biomass has long been a focus of both scientific research and industrial development since it is the largest energy reservoir in nature. Cellulase enzymes are one of the key elements in converting lignocellulosic biomass to simple sugars, which serve as starting materials for either bioenergy in the form of ethanol or synthesis of polymers. This dissertation focuses on some of the basic principles concerning how the cellulase enzyme converts lignocellulosic biomass to reducing sugars. The dissertation starts with the introduction of the structural and chemical properties of lignocellulosics and proposed mechanism of hydrolysis of cellulose substrates. Different techniques were used to monitor the activity of cellulase enzymes. To help understand the mechanism of enzymatic hydrolysis, the adsorption and desorption behaviors of cellulases were also studied from the perspective of the effect of the nature of the substrates. Future potential for research in this area will also be discussed. The following studies are included:

In-situ monitoring of cellulase activity using a piezoelectric system

Quantification of cellulase activities using a quartz crystal microbalance with dissipation

The effect of cellulose crystallinity and surface areas on water retention value of cellulose substrate

Exploration of the effects of cellulose particle size and surface area on cellulase adsorption and desorption

Differentiation of isozyme adsorption and desorption of cellulase by SDS-PAGE

Chapter 2 The structural and chemical characteristics and properties of lignocellulosic biomass

Abstract

The chemical structures of the major components in lignocellulosic biomass, namely cellulose, hemicelluloses and lignin were reviewed in the chapter.

1. Introduction

Lignocellulosic materials (biomass) are widely available on a sustainable basis in large quantities and at low cost. Species including trees, flowers, grass, fruits and other plants compose the main families for lignocellulosics. Cellulose, hemicelluloses and lignin are the major three natural polymers in most lignocelluloses. Extractives, proteins and starches may also be present in some species. Cellulose and hemicelluloses form a natural carbohydrate reservoir in nature, which contains six carbon sugars such as glucose, mannose and galactose and five carbon sugars such as xylose and arabinose. Lignins are biosynthesized from the phenylpropane monomer. It is believed that lignocellulosic biomass is the most abundant renewable resources that can be converted for fuel and chemical applications by various conversion approaches.[1, 2] There is about 1.3 billion tons of renewable biomass in the US alone that can be employed to produce ethanol or chemicals to replace those from petroleum sources.[3] It is important to know the composition and chemical structure and properties of different components in lignocellulosic materials in order to utilize them efficiently and in an

environmentally friendly way. This chapter will review the structural characteristics of the major species which exist in some important lignocellulosic materials.

2. Wood and Wood components

Trees are the direct sources for wood and wood components. Wood is generally classified into two categories: hardwood and softwood, the former is from angiosperm trees, most of which are deciduous, while softwood comes from coniferous trees. Hardwood has generally a higher density and hardness than softwood, but considerable variation usually takes place in both groups in terms of their hardness, with a great amount of overlap. For example, some hardwoods such as balsa are softer than most softwood, while yew is an example of hard softwood.[4] The property differences can be traced back to the difference in chemical compositions and structural organizations of the wood.

All wood is composed of cellulose, hemicelluloses, lignin, extractives and small amounts of components such as proteins. Starch is a major component in wood leaves but does not commonly exist in wood fibers. The ratio of major components are different in hardwood and softwood as show in the following table:[5]

Table 2-1. Chemical component ratios in hardwood and softwood

	Hardwood	Softwood
Cellulose	$45 \pm 2\%$	$42 \pm 2\%$
Hemi-cellulose	$30 \pm 5\%$	$27 \pm 5\%$
Lignin	$20 \pm 4\%$	$28 \pm 4\%$
Extractives	$5 \pm 3\%$	$3 \pm 2\%$

2.1 Cellulose

Both cellulose and hemicelluloses are composed of carbohydrates (sugar polymers). Cellulose is the natural polymer formed by D-glucose, which exists in a chair configuration connecting with its neighboring units through β-1-4 glucosidic bonds. Conformational analysis of cellulose indicates that cellobiose (4-O-β-D-glucopyranosyl-β-D-glucopyranose) rather than the glucose is its basic structural unit.[6] The cellulose chain has a linear form which forms hydrogen bonds with its neighboring chains and which results in a sheet formation. The neighboring glucose residues form an intra-molecular hydrogen bond, which brings rigidity to cellulose fiber chains. Figure 1 shows the structure of cellulose. Cellulose chain length varies between 100 and 14,000 residues.[7] Inter-molecular hydrogen bonds consolidate cellulose chains into bundles called microfibrils as shown in Fig. 2-1. Cellulose is believed to have both amorphous region and crystalline regions. The crystallinity index has been broadly used to characterize the relative crystalline cellulose contents in several natural cellulose materials.[8, 9] Raman spectroscopy and solid-state C-NMR have shown that the crystalline cellulose occurs in different forms. Cross sectional dimensions of micro-fibrils range from 3-4 nm for higher plants up to 20 nm for the microfibrils of the alga Valonia macrophysa, which contains up to several hundred cellulose chains.[7]

The crystalline form of native cellulose is designated as type I, which can be converted to type II cellulose by strong alkali treatment called mercerization. Four different forms of cellulose have been proposed and most of these forms can change into each other under

different conditions. Figure 2-2 schematically represents the interchange of different cellulose forms.

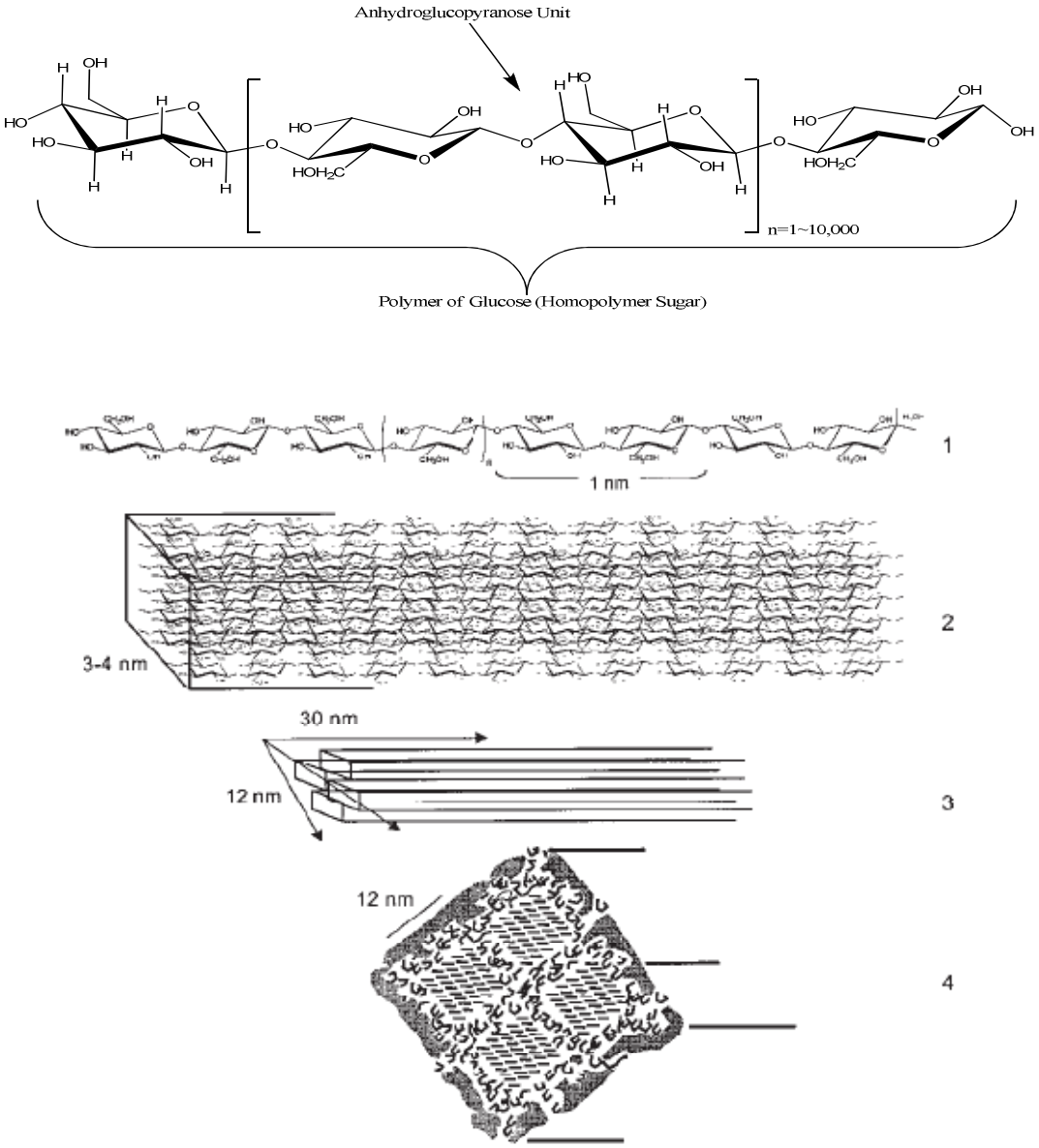

Figure 2-1. Chemical association in plant cell wall: (1) the cellulose backbone (2) framework of cellulose chains in the elementary fibril. (3) cellulose crystallite (4) microfibril cross section. [10]

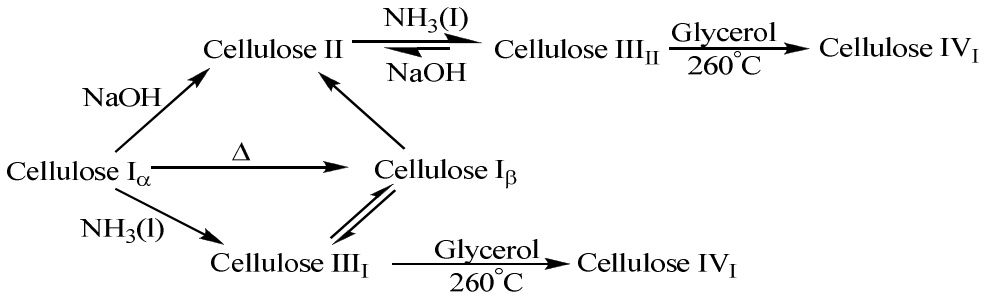

Figure 2-2. The interchange of different cellulose forms.

2.2 Softwood hemicellulose

Cellulose is a homopolymer of anhydrocellobiose but hemicelluloses are copolymer of several sugars and sugar derivatives. Many hemicelluloses are extensively branched and are readily soluble in water; they have a much less crystalline structure than cellulose. Hemicelluloses have more variations in its monomer component than cellulose. The 5-carbon sugar D-xylose constitutes a large portion of softwood hemicelluloses. Other sugar residues such as D-mannose, D-galactose, D-arabinose and L-rhamnose are also present in the hydrolysis products of hemicelluloses. Sugar derivatives such as D-glucuronic acid, 4-O-methyl-glucuronic acid and D-galacturonic acid also are often found in acid hydrolysis products of hemicelluloses. The degree of polymerization of most hemicelluloses is in the order of about 200.[11]

The amount of hemicelluloses in softwood and hardwood are different. The relative ratio of hemicelluloses in softwood and hardwood are indicated in Table 2-1. The principle hemicelluloses in softwood are galactoglucomanns, whose backbone is formed by β-D-glucopyranose and β-D-mannopyronose through β-1-4 glycosidic bonds (Fig. 2-3)

Galactoglucomannas can be divided into two fractions that have different galactose contents. In the fraction that has a low galactose content the galactose:glucose:mannose ratio is about 0.1:1:4 whereas the galactose-rich fraction has the corresponding ratio of 1:1:3. The one of lower galactose ratio is usually referred to as glucomann. The α-D-galactopyranose residue is linked through a $1 \rightarrow 6$ ester bond to the main chain. A significant feature of this hemicellulose is that the hydroxyl groups at C-2 and C-3 positions in the chain units are partially substituted by O-acetyl groups, in a proportion of one O-acetyl group per 3 or 4 hexose units. The galactomannans are readily decomposed by acid hydrolysis and the bond between galactose and the main chain is easily labile. The acetyl groups are more easily hydrolyzed by alkali than by acid.[11]

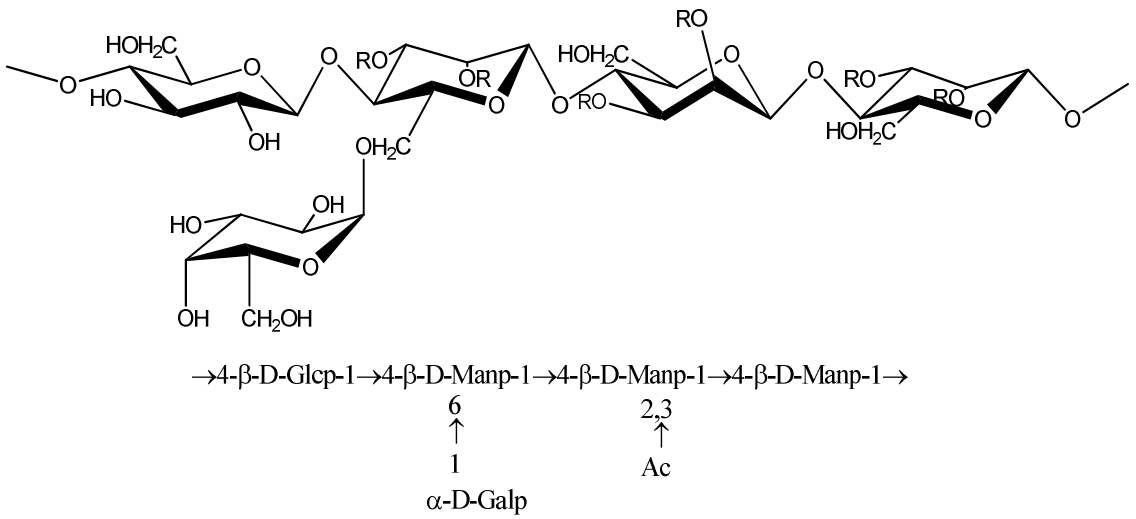

Figure 2-3. Principle structure of softwood hemicelluloses galactoglucomanns. The upper drawing is the chemical structure and the lower one is the abbreviated formula representing the proportion of the units. Sugar units: Glcp =β-D-glucopyranose; Manp = β-D-mannopyranose; Galp = β-D-galactopyranose; R= CH_3CO or H.

Besides galactoglucomanns, most SW also contain 5~10% arabinoglucuronoxylan. The framework of arabinoglucuronoxylan is composed of β-1-4 linked D-xylopyranose units, some of whose C-2 hydroxyl groups are substituted by 4-O-methyl-α-glucuronic acid groups (Fig. 2-4). The substitution ratio is on average two residues per 10 xylose units. The framework also contains arabinofuranose residues; its average ratio is about 1.3 residues in every 10 xylose units. The furanosidic structure of arabinose side chains makes it easily hydrolysable by acids, but both the arabinose and uronic acid substitutes are stable against alkali-catalyzed degradation.

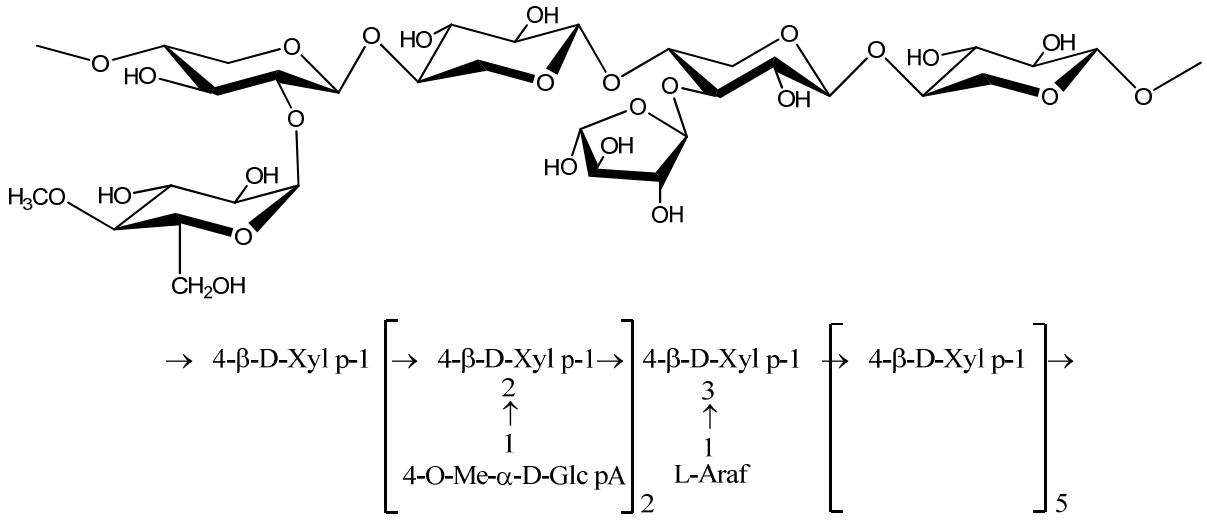

Figure 2-4. Principle structure of SW hemicelluloses arabinoglucuronoxylan. Upper part is the chemical structure drawing; the lower part is an abbreviated formula showing the relative proportions of the different units. Xyl P = β-D-xylopyranose; Glc pA = 4-O-methyl-α-glucopyranosyluronic acid; Ara f = α-L-arabinofuranose.

Most wood species also contain a small amount of water-soluble arabinogalactan. β-D-galactopyranose forms its backbone by 1→3 linkage. It is highly branched at C-6, where a 1→6 linkage is either connected with either β-D-galactopyranose or L-arabinose (Fig. 5). This heavily branched structure makes arabinogalactan highly soluble in water and the resultant solution has a low viscosity.

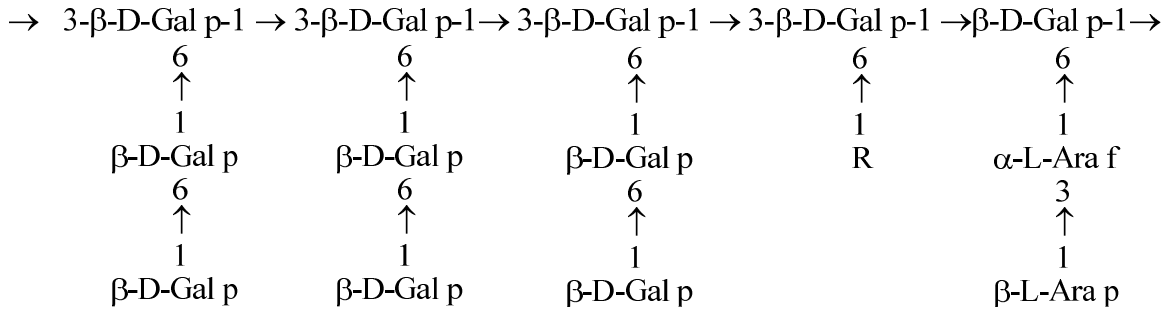

Figure 2-5. Abbreviated structure of arabinogalactan. Gal p = β-D-galactopyranose; Ara P = α-L-arabinopyranose; Ara f = α-L-arabinofuranose; R= β-D-galactopyranose or α-L-arabinopyranose or β-D-glucopyranosyluronic acid residue.

In addition to these three polysaccharides, there are other species such as pectic polysaccharides. The typical component of pectic polysaccharides include galacturonans, rhamnogalacturonans, arabinans and galactans, they are mainly located in the primary cell wall and middle lamella.[11]

2.3 Hardwood hemicelluloses

The hemicelluloses in different hardwoods vary from species to species, but the major hemicellulose component is an O-acetyl-4-O-methylglucurono-β-D-xylan. It is often called glucuronoxylan for simplicity. In general, the xylose-related hemicelluloses in both SW and

HW are simply named xylan. These comprise about 15-30% of the dry wood. In addition to xylan, hardwood also contains a small portion of glucomann (2%~ 5%).

Xylan in hardwood has a backbone consisting of β-D-xylopyranose units, linked by the β-1-4 glycosidic bonds (Fig. 2-6). Most xylose residues contain an acetyl group at their C-2 or C-3 carbons; the average substitution is about 7 acetyl groups for each 10 xylose residues. The backbone also contains one 4-O-methyl-α-D-glucopyranosyluronic acid residue at its C-2 carbon for each 10 xylose residues. The glycosidic bonds in the backbone are easily hydrolysable by acids and the acetyl group is readily hydrolyzed by alkali, whereas the bonds between the uronic acid and xylose residues are very resistant to acid hydrolysis.

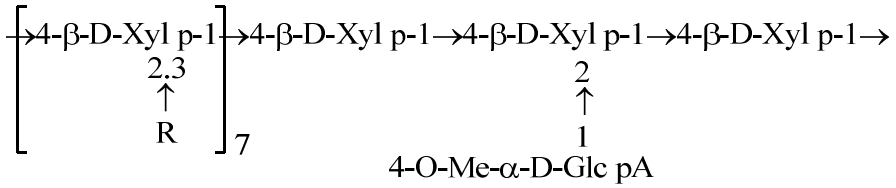

Figure 2-6. An abbreviated illustration of glucuronoxylan structure. Xyl p = xylopyranose; Glc pA=4-O-methyl-α-D-glucopyranosyluronic acid. R=CH_3CO

The minor hemicelluloses glucomannan in HW is composed of β-D-glucopyranose and β-D-mannopyranose linked by β-1-4 glycosidic bonds (Fig. 2-7). The relative ratio of mannose to glucose is between 1:1 and 2:1 in different HW species. The mannose-related glycosidic bonds are easier to be hydrolyzed than glucosidic bonds, and acids can easily depolymerize glucomann.

→4-β-D-Glc p-1→4-β-D-Man p-1→4-β-D-Glc p-1→4-β-D-Man p-1→4-β-D-Man p-1→

Figure 2-7. An abbreviated illustration of chemical structure of glucomann. Glc p=4-β-D-glucose; Man p=4-β-D-glucose

There are also some other minor hemicelluloses in HW, as those presents in SW hemicelluloses.

2.4 Lignin

Lignin is found with the highest amount in plant cell walls although the greatest ratio of lignin is present in the middle lamellae, which binds cells together. The various functions of lignin can be described as providing mechanical support for plants, resisting biochemical stress such as microbial attacks, implanting to plants antioxidant properties, giving plants flame retarding properties and providing other properties such as waterproofing, water balance and water transport et al.[12]

The properties that lignin implant to plants are determined by its structures. Lignin is an amorphous, phenylpropanoid polymer with a molecular weight of about 10^5 Daltons. It has a highly branched three dimensional structure with no typical repeating unit. The elucidation of lignin structure is a challenge; part of the reason is because it is hard to completely separate lignin from carbohydrates. In general, the intermonomeric linkages are believed to be carbon-carbon bonds or relatively inert ether or ester bonds. The bonds between the basic units are very stable.

The basic forming units of lignin contain coumaryl, conliferyl, sinapyl substituents at different ratios. Their ratios vary depending on the species of plants. Fig. 2-8 shows an example of lignin structure.

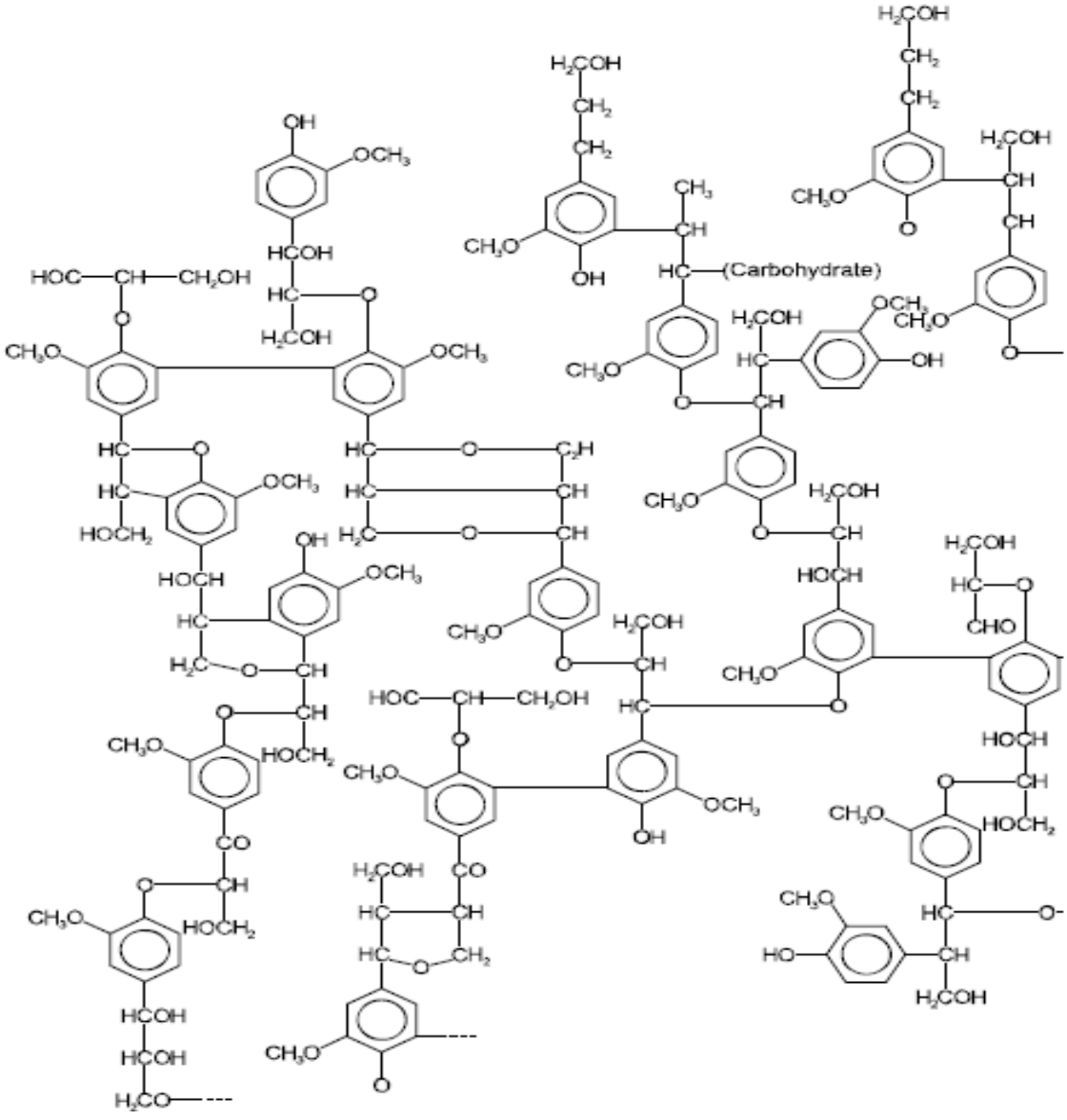

Figure 2-8. Formulation of lignin

3. Concluding remarks

Plants have been utilized since the beginning of civilization. The complexity of plants involve not only their chemical structure, it also involves such aspects as physical properties, biological properties, morphology and other respects. The efficient biological utilization of biomass will require us to understand these aspects as much as possible. The review in this dissertation is preliminary aimed at the chemical aspects so that they can help understand what may be significant in this research results as well as the basic mechanism between cellulose and the corresponding cellulase enzyme.

Reference

1. Lynd, L.R. et al. How biotech can transform biofuels. Nat. Biotechnol. **26**, 169-172 (2008).

2. Ragauskas, A.J. et al. The Path Forward for Biofuels and Biomaterials. Science **311**, 484-489 (2006).

3. Christensen, C.H. The renewable chemical industry: Optimal use of biomass resources. Abstracts of Papers, 235th ACS National Meeting, New Orleans, LA, United States, April 6-10, 2008, FUEL-094 (2008).

4. Rowell, R.M. Handbook of wood chemistry and wood composites. (CRC Press, Boca Raton, Fla.; 2005).

5. Smook, G.A. Handbook for pulp & paper technologists. (Angus Wilde Publications, Vancouver ; Bellingham, WA; 1992).

6. Fengel, D. & Grosser, D. Chemical composition of softwoods and hardwoods. Bibliographical review. Holz Roh- Werkst. **33**, 32-34 (1975).

7. Pierre Béguin, J.-P.A. The biological degradation of cellulose. FEMS Microbiology Reviews **13**, 25-58 (1994).

8. Segal, L., Creely, J.J., Martin, A.E., Jr. & Conrad, C.M. An Empirical Method for Estimating the Degree of Crystallinity of Native Cellulose Using the X-Ray Diffractometer. Textile Research Journal **29**, 786-794 (1959).

9. Cowling, E.B. & Kirk, T.K. Properties of cellulose and lignocellulosie materials as substrates for enzymatic conversion processes. Biotechnol. Bioeng. Symp. ; Vol/Issue: 6, Pages: 95-123 (1976).

10. Ramos, L.P. The chemistry involved in the steam treatment of lignocellulosic materials. Quim. Nova **26**, 863-871 (2003).

11. Sjeostreom, E. Wood chemistry: fundamentals and applications. (Academic Press, San Diego; 1993).

12. Betts, W.B. Biodegradation: natural and synthetic materials. (Springer-Verlag, London ; New York; 1991).

Chapter 3 Cellulase enzyme systems, cellulase adsorption and mechanism of enzymatic hydrolysis

Abstract

Cellulase enzyme systems will be reviewed in this article. The different cellulase systems will be introduced, including the sources, culture conditions and the properties of the cellulase systems. The adsorption and hydrolysis mechanism of general cellulase systems on cellulose substrates will also be discussed.

1. General cellulase systems

Cellulase has long ago evolved as part of nature's carbon cycle. Microbial cellulose utilization is responsible for one of the largest flow of materials in the biosphere and is of interest in relation to analysis of carbon flux at both local and global scales. [1] Only recently, hydrolysis and utilization of cellulose by microorganisms in amounts sufficient to provide usable energy has received global attention. Different organisms produce cellulase systems with different and/or similar isozymes. For microorganisms to hydrolyze and metabolize insoluble cellulose, extracellular cellulases must be produced that are either free or cell-associated. It is generally believed that there are three major types of isozymes in cellulase systems based on their structural properties: (i) Endogluconases or 1, 4-β-D-glucan-4-glucanohydrolases (EC 3.2.1.4). Endogluconases cleave cellulose polysaccharide chains at

internal amorphous regions and generate oligosaccharides of different length, thus providing new chain ends. (ii) Exoglucanase, including 1,4-β-D-glucan glucanohydrolase (EC 3.2.1.74) and 1,4-β-D glucan cellobiohydrolases (cellobiohydrolases). Exoglucanases attack cellulose fragments from either their reducing or non-reducing ends, releasing either glucose or cellobiose as their major products. Exoglucanse can also hydrolyze the crystalline region of native cellulose by peeling the cellulose chains. (iii) β-glucosidases or β-glucoside glucohydrolases (EC 3.2.1.21). β-glucosidases hydrolyze soluble cellobiose and other cellodextrins to glucose. Cellulases are distinguished by their ability to hydrolyze β-1-4-glucosidic bonds within the cellulose chains. Figure 3-1 is a schematic representation showing the synergistic function of different cellulase isozymes during cellulose hydrolysis.

There are in general two different cellulase systems that have been categorized. One is the so-called non-complexed cellulase system and the other one is the complexed cellulase system. Non-complexed cellulase systems are generally developed by anaerobic fungi. The non-complexed cellulase system produced by such microorganisms is a “free” cellulase, which may or may not have cellulose binding modules (CBMs), is sufficient to hydrolyze cellulose without forming high molecular weight complexes. In contrast, anaerobic bacteria that lack the ability to penetrate cellulosic material have to find an alternative mechanism for the degradation of cellulose and access the cellulose hydrolysis products in the presence of competing microorganisms. These bacteria have limited ATP for cellulase synthesis. A cellulase system in such situations is termed a “complexed” cellulase system or

"cellulosomes", which have cellulase-producing cells at the hydrolysis sites. Such systems have been observed in clostridia and ruminal bacteria. Cellulosome are protuberances formed on the cell wall of cellulolytic bacteria while growing on cellulosic substrates. In our research, the cellulase system used belongs to the non-complexed family and therefore the discussion will be focused on the non-complexed cellulose system. For more information about complexed cellulase system, see the review by Lynd et al, 2002.[1]

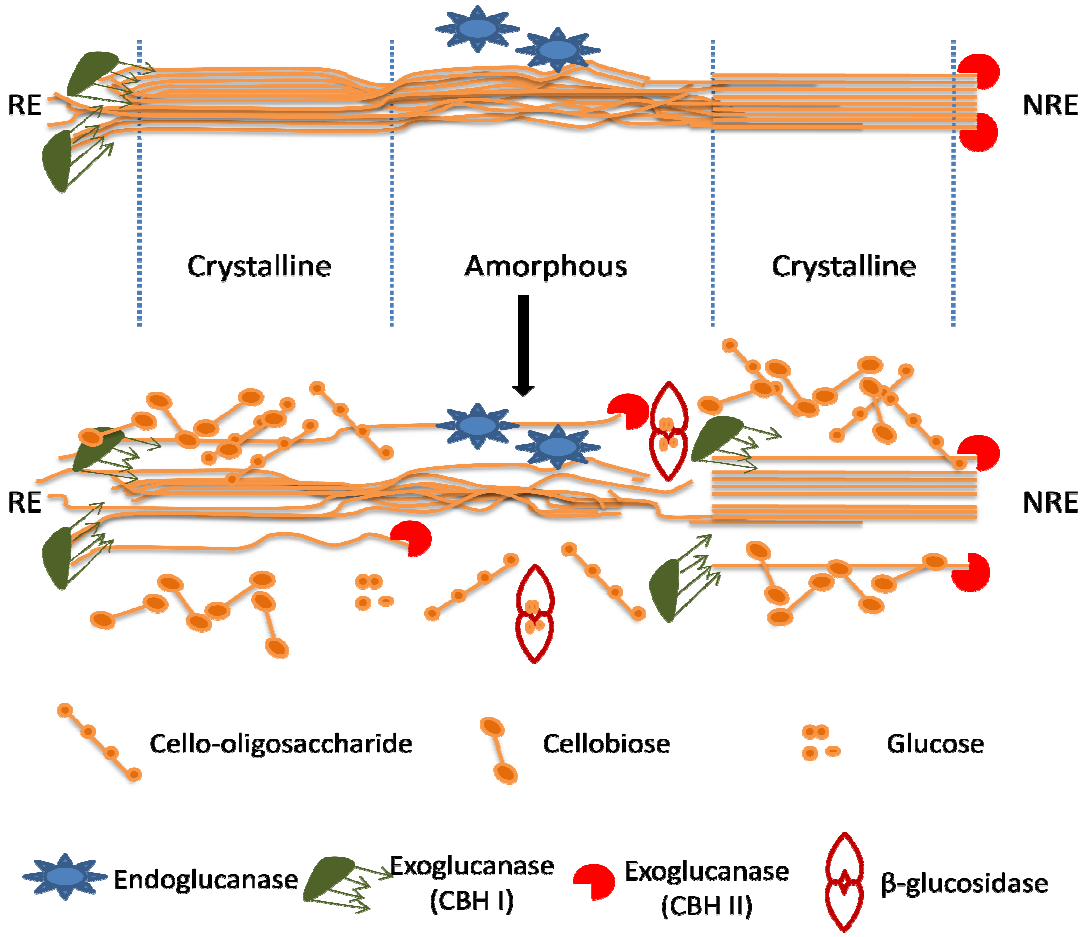

Figure 3-1. Schematic representation of the hydrolysis of cellulose by non-complexed cellulase system[1].

One of the most widely studied non-complexed systems is the fungal cellulase system from *Trichoderma reesei* (T. *reesei*). In most situations, T. *reesei* produces at least two exoglucanases (CBH I and CBHII), five endoglucanases (EGI, EGII, EGIII, EGIV, and EGV), and two β-glucosidases (BGLI and BGLII). CBHI attacks preferentially the reducing end of cellulose while CBHII attacks the non-reducing end of cellulose chains (Figure 3-1). Synergisms have been observed between CBHI and CBHII. The three dimensional structures of the two CBHs have been elucidated by crystallography. CBHI has a tunnel of 50Å in length that is formed by the four surface loops, while CBHII contains two surface loops that give rise to a tunnel of 20 Å.[1] In contrast, EGI has short surface loops that form a groove instead of a tunnel, a similar groove was also found in the structure of EGIII. The tunnels in CBHs are essential for them to progressively hydrolyze cellulose from both chain ends, the grooves in EGs are thought to allow the side entry of cellulose chains for subsequent cleavage in the middle of the chain. CBHs are proven to be the major component of *Trichoderma reesei* cellulase, CBHI and CBHII representing 60% and 20% of the total cellulase protein mass. However, CBHs by themselves hydrolyze cellulose very slowly; the reduction in degree of polymerization of cellulose is not substantially fast since they can only attack cellulose chains from the chain ends. The creation of chain ends is a necessity to increase hydrolysis rate. Endoglucanases are believed to be responsible for the rapid decrease of the DP of cellulose by their random cleavage of amorphous regions, which creates the synergism between exoglucanase and endoglucanse. Several works show the synergism between cellobiohydrolase and EGI,[2] and EGII,[3] and EGIII.[4] No research has shown

synergism between EGs; however, there is evidence showing the synergism between CBHs.[5] Two β-glucosidases have been proven to exist in cellulase mixtures from *T. reesei*.[6] There are other fungi such as *Aspergillus niger* that produce higher level of β-glucosidases.[7] The β-glucosidases from *Aspergillus niger* is more tolerant of glucose while the ones from *Trichoderma reesei* are subject to end product inhibition by glucose.[1] β-glucosidases from *Aspergillus niger* are used to supplement the cellulase system from *Trichoderma reesei* in current industrial applications.[8]

The cellulase systems from other sources such as the thermophilic fungus *H. insolens* and the white rot fungus *Phanerochaete chrysosporium* possess isozymes similar to the ones obtained from *T. reesei* and *Asperigillus niger*, but with differences in the structure of isozymes and relative ratios, [9, 10] for example, the EGI and EGIII from *H. insolens* do not have cellulose binding module (CBM). The enzyme systems from *P. Chrysosporium* also contain hemicellulase and lignin-degrading enzymes besides cellulase. The complex array of these enzymes constitutes an efficient degradation of the three major components of plant cell walls.[11, 12] The cellulase systems from *P. Chrysosporium* contain CBHII and six CBHI-like homologues, of which CBHI-4 is the major cellobiohydrolase.[1, 13, 14] In addition, *P. Chrysosporium* also produces cellobiose dehydrogenase that oxidizes cellobiose to cellobiolactone in the presence of oxygen.[15, 16]

Aerobic bacteria that have been most studied for producing cellulase enzyme belongs to the genera *Cellulomonas* and *Thermobifida*.[1] The cellulases produced by *Cellulomonas* resemble aerobic fungal cellulases and contain cellulose binding modules (CBM); there are

also cellulose-like protuberance noted on the *Cellulomonas* cell wall when cellobiose and cellulose are used as carbon sources.[17, 18] *Thermobifida fusca* is a thermophilic filamentous bacterium that serves as a major cellulose decomposer in soil. Three endoglucanases (E1, E2, E5) and two exoglucanases (E3, E6), as well as an usual cellulase with both endoglucanase and exoglucanase activity(E4) have been isolated from *Thermobifida fusca* cellulase.[19] Kim et al have proven that E4 has the highest synergistic effect with the addition of CBHI from *T. reesei*.[20] A family III CBM is contained in the E4 isozyme that increases the activities of cellulases.[21]

Some hyperthermophilic prokaryotes have been found to have cellulolytic characteristics.[22] Only two aerobic thermophilic bacteria have been found to be able to produce cellulases: *Acidothermus cellulolyticus* and *Rhodotherms*.[23, 24] These species grow at temperatures that may exceed 100°C. Archaea can grow on cellobiose and degrade such polysaccharides as starch, chitin and xylan, but cellulolytic thermophic archaea have not been isolated yet.[1, 25, 26]

2. Characterization of cellulolytic hydrolysis of cellulose

The different isozymes are complementary to each other in cellulose hydrolysis, or in some cases form multiple protein complexes. Because of this, different isozymes may behave differently when they are employed in combination with each other than when they are present individually. Cellulosic substrates are typically insoluble macromolecules with varying morphology in terms of their size, shape, or crystallinity; in some situations, the chemical composition of the substrates may vary as well.[27] Both natural cellulose and pretreated cellulose typically contain either hemicelluloses or lignin or both, to which many

cellulase can bind. The existence of hemicelluloses can impede the access of cellulases to β-1-4 glycosidic bonds, and the degradation of hemicelluloses often requires the application of hemicellulases. The substrate can undergo changes in the course of hydrolysis in terms of adsorption, affinity, and substrate reactivity, chemical and physical properties. Figure 3-1 shows the general schematics of insoluble cellulose hydrolysis, but does not include the adsorption steps. We will give a general review about cellulase adsorption and its characterization in the next section.

2.1 Cellulase adsorption

Cellulose binding modules (CBM), also called cellulose binding domains (CBD), readily adsorb on cellulosic substrates to form a substrate-enzyme complex through non-covalent bonding. The catalytic domain (CD) of some isozymes may also adsorb specifically to cellulose independent of the cellulose binding domain, but it is less significant in the light of understanding cellulose hydrolysis. Cellulase may also adsorb on lignin, but it is nonspecific.[28] The formation of a cellulose-cellulase complex constitutes a significant step for the conceptual understanding of quantitative model for cellulose hydrolysis. Cellulose hydrolysis rate has been shown to have strong correlation with the adsorption equilibrium constant.[29]

A description of cellulase adsorption to cellulose typically involves such variables as cellulase-cellulose complex concentration, total cellulase concentration/initial cellulase and free cellulase or equilibrium concentrations. For pure cellulose substrates, the kinetic adsorption/desorption equilibrium between cellulase and its substrate can be expressed as

follows:

$$\begin{array}{lccc} & C & + \; E & \rightleftharpoons \; CE \\ t_0: & [S_T] & [E_T] & 0 \\ t: & & [E_F] & [CE] \end{array} \qquad (1)$$

$$[CE] = [E_T] - [E_F] \qquad (2)$$

where in equation (1), [CE] is the concentration of cellulose-cellulase complex, $[E_T]$ is the concentration of total binding sites on the cellulase enzymes and $[E_F]$ is the concentration of binding sites on the cellulases that have not been adsorbed to cellulose. It is well known that the binding of cellulase CBM/CBD to cellulose is a heterogeneous process and cellulose is not included in the equation (2). Other variables such as temperature and ionic strength are not included in the expression, but they definitely affect the relative concentrations of the species in equation (1).

Equilibrium is typically assumed in cellulase adsorption, which is often justified by the observation that a short time is required for $[E_F]$ to reach a constant value when compared to the time required for substrate hydrolysis. Research has shown that the time for equilibrium is typically shorter than 90 minutes.[30-35] The simplest characterization for adsorption equilibrium is to use an equilibrium constant, K_d, which can be derived as follows:

$$R_a = \frac{d[E_F]}{dt} = k_a[E_F][C],\ R_d = \frac{d[CE]}{dt} = k_d[CE] \qquad (3)$$

at equilibrium, $R_a = R_d$, which leads to $K_d = \frac{k_d}{k_a} = \frac{[E_F][C]}{[CE]}$, where [C] is the concentration of available binding sites on cellulose that have not been occupied by cellulase, R_a and R_d represent the rates of cellulase adsorption and desorption respectively and k_a and k_d are the adsorption and desorption rate constants. The units for K_d, [C], $[E_F]$, [CE] and $[E_T]$ are often micromoles per liter; other units can also be used for convenience. From the viewpoint of chemical balance, adsorption and desorption is a dynamic equilibrium, although researchers have demonstrated that enzymes can stay bound to the substrate for a significant period, during which hundreds of catalytic events occur. [1, 36-38]

The above derivation for adsorption-desorption equilibrium constants used available binding sites for substrates, which is directly related to the concentration of substrate $[S_T]$ (milligram per milliliter or gram per liter). The binding site on substrates has a linear relationship with binding capacity β, which describes the relative ratio of reactive cellulose sites for cellulase-cellulose complexes. For soluble substrates, this number is unity while it is far less than unity for most heterogeneous cellulase-cellulose systems (β<0.001 for most pure heterogeneous systems involving insoluble substrates). The relationship between accessible binding sites and available binding must be considered from the perspective of mass balance:

$$\beta [S_T] = [C] + [CE] \qquad (4)$$

Substituting [C] into the equilibrium constant gives the Langmuir equation

$$[CE] = \frac{\beta [S_T][E_F]}{K_d + [E_F]} \qquad (5)$$

The Langmuir isotherm has been broadly employed to describe cellulase adsorption in literature. Such studies have both applied to individual isozymes[39, 40], and multi-component non-complexed systems and commercial mixtures.[41]

Equation (4) states the relationship between bounded enzyme and free enzyme without including total enzyme. Putting equation (2) and equation (4) into the equilibrium constant K_d gives a quadratic equation indicating the relationship between bound enzyme, total enzyme, and total solids used and binding capacity:

$$[CE]^2 - (\beta\,[S_T] + E_T + K_d])[CE] + \beta\,[S_T][E_T] = 0 \qquad (6)$$

Equation (6) has two roots, $[\mathrm{CE}]_1 = \frac{1}{2}([\mathrm{E_T}] + \mathrm{K_d} + \beta\mathrm{S_T} - \sqrt{(-\mathrm{E_T} - \mathrm{K_d} - \beta\mathrm{S_T})^2 - 4\beta\mathrm{S_T}\mathrm{E_T}}$ and $[\mathrm{CE}]_2 = \frac{1}{2}([\mathrm{E_T}] + \mathrm{K_d} + \beta\mathrm{S_T} + \sqrt{(-\mathrm{E_T} - \mathrm{K_d} - \beta\mathrm{S_T})^2 - 4\beta\mathrm{S_T}\mathrm{E_T}}$. With the one restriction of $0 \le [CE] \le \frac{[E_T]}{[S_T]}$, only $[\mathrm{CE}]_1$ has physical meaning. The effective root of [CE] gives two important features:

1) [CE] approaches a constant value when $[S_T]$ is increased at a constant $[E_T]$ or $[E_T]$ is increased at a constant $[S_T]$, which correspond to saturation with either substrate or enzyme.

2) The concentration of substrate $[S_T]$ required to reach an arbitrary degree of saturation in the concentration of substrate-enzyme complex [CE] is a function of total enzyme concentration $[E_T]$ applied, which means a larger amount of substrate requires a higher total enzyme concentration to achieve a saturation adsorption. Adsorption experiments have provided support for these behaviors.[42, 43]

The description of adsorption behavior of cellulase with multiple isozymes may involve

solutions of several equations describing the isotherms for each individual component. Competitive adsorption amongst different isozymes has been identified.[44, 45] the binding sites on substrates may be unique to some isozymes, but others may be common to different isozymes. Adsorption synergism has been observed in cellulase mixtures from pure isozymes when compared to their individual adsorption at similar conditions.[44, 45] On the other hand, the presence of lignin can competitively adsorb celluase and therefore decrease the hydrolysis of natural cellulosic materials. Experimental results have shown that the presence of lignin decreased hydrolysis rate by sevenfold and stopped the hydrolysis even before cellulose is exhausted.[46] Cellulase adsorption still follows Langmuir adsorption kinetics even in the presence of lignin.[1]

It is noteworthy that the assumption of a Langmuir model is ideal; the binding sites on substrates are treated as non-uniform and the interaction between adsorbates are thought to be common. Other models, such as a combined Langmiur-Freundlich model has been proposed to describe negative or positive binding cooperativity.[3, 47] The complexes formed may exist in different status and the proteins may also change their conformation upon adsorption. The Langmuir adsorption equation implies a reversible adsorption, which is shown in the derivation. However, irreversible or less fully reversible binding has been proposed in the literature.[3, 31, 48, 49]

Other noticeable features for Langmuir adsorption model is that no substrate change or negligible substrate reaction has been accounted for. There is evidence that cellulase adsorption is a fast process. The change of celluase charge has been found to have no

obvious effect on the time required to reach adsorption equilibrium.[50, 51] The structure of cellulose changes during the course of cellulose hydrolysis, requiring different enzymes at different time.[52]

2.2 Hydrolysis mechanism

Figure 3-1 schematically shows the hydrolysis of cellulose by cellulase. A deeper understanding of the hydrolysis mechanism requires better knowledge of the biochemical structure of cellulase isozymes. Gene sequence analysis of cellulase and their biochemical characteristic have shown distinct domains in both wild type and truncated enzymes.[52, 53] The sequence similarities define domains. Domains from the same family share similar biochemical properties. Understanding the biochemical structure is of significance in understanding the reaction mechanism involved in cellulose hydrolysis. Henrissat et al. have introduced the classification of 21 cellulolytic and xylanolytic enzymes into six families by identifying their amino acid sequences.[54] There have also been research conducted to study the protein folding and three dimensional structures of cellulases enzymes using X-ray diffraction and/or NMR. Such three dimensional structure studies have determined the folding pattern of cellulases and xylanases from various sources.[55, 56 57-59] The secondary structure of *T. Reesei* CBHII, in other words, the protein folding in CBHII, is composed of one 7-stranded β-barrel. Two extended loops at the C-terminal end of the barrel forms the active site. For the *C. thermocellum* CelD, the protein folding comprises an N-terminus composed of two β-sheets, and one large C-terminal catalytical domain of an α-barrel formed by 12 helices. The active site is formed by three loops connected with six of the α-barrels on the same side of the barrel.[52]

The geometry of the active sites of different isozymes provides an explanation for their behaviors. From the perspective of biochemical catalysis, it is generally believed that the hydrolysis is catalyzed via an acid-base pair mechanism involving two residues.[52, 60] The first residue serves as an acid catalyst and protonates the oxygen of the osidic bond. The second one often interacts with the oxocarbonium intermediate for retaining the enzymes or boosts the formation and a hydroxide ion (OH^-) from a water molecule for inverting the enzyme (Figs 3-2 and 3-3).[52, 60] The configuration retention suggests a two step mechanism, which involves a double inversion of the configuration at the anomeric carbon and the formation of a oxocarbonium intermediate.[60] An example of this type of mechanism is the mechanism for lysozyme (Fig. 3-2). The inversion of configuration is catalyzed by a single nucleophilic substitution (Fig. 3-3).

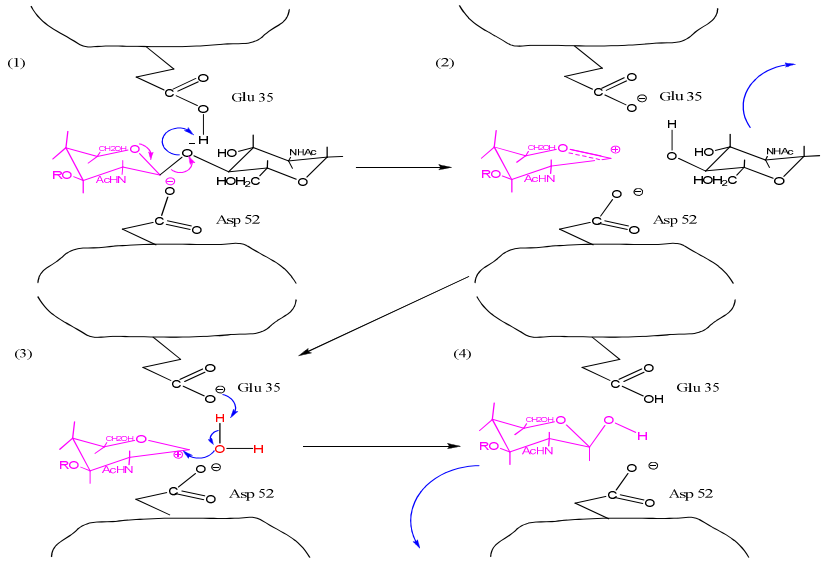

Figure 3-2. Reaction mechanism of lysozyme as an example of β-glycanase acting to retain the anomeric carbon conformation. (1) Attack of the glycosidic bond between the left

acetylmuramate residue and the right acetylglucosamine is initiated by the proton provided by glutamate (Glu-35) residue of the enzyme. (2) Breaking of glycosidic bond leads to the release of fragment with a new non-reducing end group (here carried by the acetylglucosamine on the right) and the formation of an oxocarbonium intermediate (carried by the acetylmuramate on the left). The positive oxocarbonium intermediate interacts with the negative charges carried by the Aspartate residue of the enzyme (Asp-52). (3)A water molecule supplies a hydroxide ion (OH^-) reacting with the oxocarbonium and a hydrogen ion (H^+) to regenerate the proton lost by the glutamate residue (Glu-35). (4) The liberation of the fragment with a new anomeric carbon.[52]

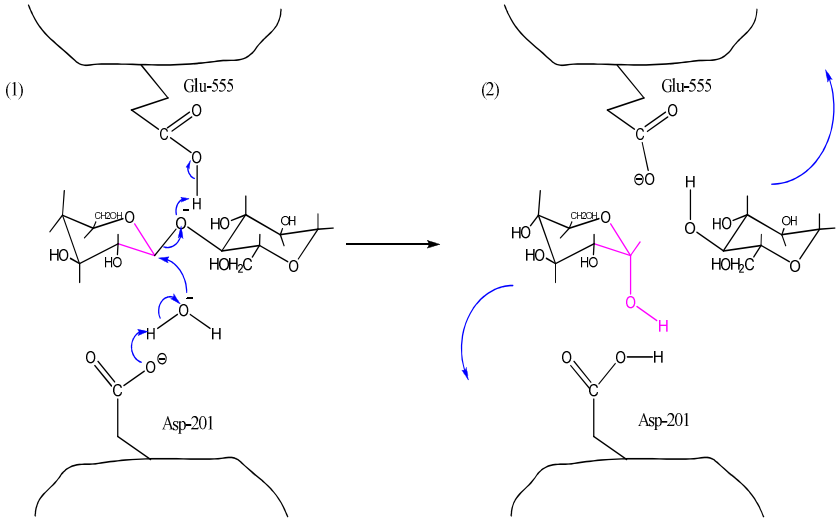

Figure 3-3. Catalytic mechanism of C. *thermocellum* endoglucanase CelD as an example of β-glucanase acting with the inversion of the anomeric carbon configuration. A glutamate residue (Glu-555) provides a proton to protonate the glycosidic oxygen. Meanwhile, the negatively charged Aspartate (Asp-201) residue boosts the ionization of a water molecule.

The leaving hydroxide ion (OH^-) reacts with the newly formed anomeric carbon, which leads to a nucleophilic substitution and to the inversion of configuration.[52]

2.3 Nomenclature and characteristics of cellulase isozymes

Since Henrissat and Bairoch gave the modern classification for glycosyl hydrolases[61, 62] and his subsequent new designation for cellulase and hemicelluase enzymes[63], there also have been discussion and additions to this designation system.[37, 64] Table 3-1 shows examples of cellulases of different origin by this new nomenclature system. In this nomenclature, glycosyl hydrolases were classified into families according to the related amino acid sequence in the molecules, the similarity of three dimensional folding and the stereospecificities of hydrolysis on different substrates. Compared to the IUMBM classification, the nomenclature system still uses three letters to denote the corresponding substrates the enzyme hydrolyzes, followed by a number to signify the family, then a subsequent letter for the discovery sequence of the corresponding enzyme. The molecular characteristics were proposed to be denoted by their catalytic domains and cellulose binding domain, from an N-terminus to C-terminus sequence. It was also suggested that the source of enzymes be denoted by the initial letter abbreviation at the beginning of notation. Others suggestions include the molecular weights and isoelectric points (pI) of different isozymes[1, 37, 64]. It should be noted that β-glucosidase is not included in this nomenclature.

Table 3-1. Cellulase nomenclature according to Henrissat et al. [61, 63]

Organism and its abbreviation	Enzyme		EC 3.2.1	Former abbreviation	New abbreviation	Examples of designation of modular structure
Trichoderm reesei (Tr)	Cellobiohydrolase	I	91	CBHI	Cel7A	CD7/CBD1
		II	91	CBHII	Cel6A	CBD1/CD6
	Endoglucanase	I	4	EGI	Cel7B	CD7/CBD1
		II	4	EGII	Cel5A	CBD1/CD5
		III	4	EGIII	Cel12A	CD12
		IV	4	EGIV	Cel61A	CD61/CBD1
		V	4	EGV	Cel45A	CBD1/CD45
Trichoderm reesei (Tr)	Mannanase		78	Man	Man5A	CD45/CBD1
	Xylanse	I	8	XynI	Xyn11A	CD11
		II	8	XynI	Xyn11B	CD11
Cellulomonas fimi (Cf)	Cellobiohydrolase	A	91	CbhA	Cel6B	CD6/(FN3)3/CBD2
		B	91	CbhB	Cel48A	CD48/(FN3)3/CBD2
	Xylanse /Exoglucanase		Aug-91	Cex	Xyn10A	CD10/CBD2
	Endoglucanase	A	4	CenA	Cel6A	CBD2/CD6
		B	4	CenB	Cel9A	CD9/CBD3/(FN3)3/CBD2
		C	4	CenC	Cel9B	(CBD4)2/CD9/?/?
		D	4	CenD	Cel5A	CD5/(FN3)2/CBD2
	Mannanase		78	-	Man26	CD26/SL1/?/?
	Xylanse	B	8	XynB	Xyn10B	(NodB-AXE)/(TST-XBD)/CD10/(CBD9)2
		C	8	XynC	Xyn11A	CD11/CBD2/(NodB-AXE)/CBD2

Table 3.1 Continued

Clostridium thermocellum (Ct)	Cellobiohydrolase	A	91	CelA	Cel48A	CBD4/CD9(1)(FN3)2/CBD3/D1
		O	91	CelO	Cel9E?	CBD3/CD5/D
		S	91	CelS	Cel5F	
Clostridium thermocellum (Ct)	Endoglucanase	B	4	CelB	Cel5A	Not given
		C	4	CelC	Cel5B	
		C	4	CelC	Cel5C	
		G	4	CelG	Cel5D	
		H	4	CelH	Cel26A-Cel5E	
		A	4	CelA	Cel8A	
		D	4	CelD	Cel9A	
		F	4	CelF	Cel9B	
		I	4	CelI	Cel9C	
		J	4	CelJ	Cel9D-Cel44A	
		M	4	CelM	Cel60A	
Thermomonospora fusca (Tf)	Celluase	K	4/91?	CelK	Cel9F?	CBD4/CD9/D1
	Lichenase	B	73	LicB	Lic16A	
	Xylanase		X	XynX	Xyn10A	Not given
			Y	XynY	Xyn10B	
			X	XynZ	Xyn10c	
	Endoglucanase		4	E1	Cel9B	
			4	E2	Cel6A	
			4	E4	Cel9A	
			4	E5	Cel5A	
	Cellobiohydrolase		91	E3	Cel6B	
			91	E6	Cel48A	

It should be noted that this nomenclature is based on the current understanding and experimental results about molecular structures, most of which were obtained using X-ray diffraction and supplemented by NMR information[13, 22, 37, 65, 66]. The architecture of many cellulases can be schematically depicted as a catalytic domain linked to cellulose-binding domain by a linker (Fig. 3-4). For most of the fungal cellulase, the active sites of catalytic domains contain aspartate (Asp or D) or glutamate (Glu or E) which interact with the substrate by an acid-base pair mechanism. The cellulose-binding domains may contain basic amino acid residues such as lysine, arginine etc, and these residues may form hydrogen bonds with the oxygen of the hydroxyl groups on lignocellulosic substrate surfaces.[67] Both the catalytic domain and linker may be glycosylated by carbohydrates, either via O-glycosylation or N-glycosylation depending on the section to which carbohydrates are attached.[68] Glycosylation may hinder cellulase activity on crystalline cellulose whereas it has negligible effect on its activity to soluble substrates.

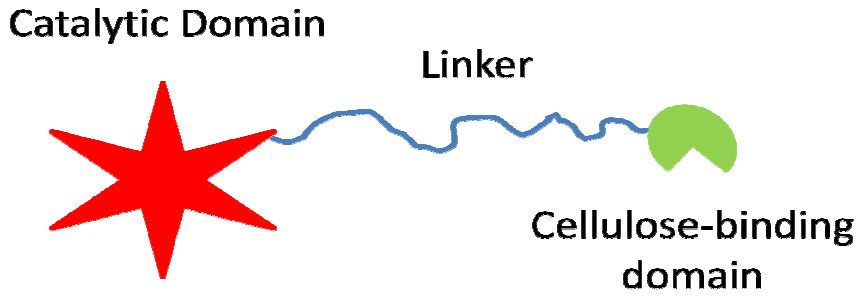

Figure 3-4. Schematic drawing for many cellulase architecture.[68]

Most commercial cellulase products for research are probably from fungal sources since these products belong to the non-complexed cellulase. A supplement to table 3-1 gives the

iso-electric points and molecular weights of fungal cellulase isozymes found in the literature (Table 3-2).

It should be pointed out that most organisms that can produce cellulase may probably produce hemicellulases, such as xylanases and mannases, as well as pectinases and other enzymes.[69-71] It may therefore be more difficult to have a pure cellulase mixture than to have pure cellulase isozymes. The latter could be obtained using electrophoresis and other techniques, many of which have been applied by researchers who study these enzymes from the perspective of molecular biology.

Table 3-2. A summary of the characteristics of common fungal cellulase isozymes from literature

Cellulase isozymes	EC #	New Nomenclature[1]		MW (kDa)	pI	Glycosylation (%)[2]	Reference
		Abbreviation	Designation of modular structure				
CBHI	3.2.1. 91	Cel7A	CD7/CBD1	42~72	3.5~4.2	1.4~10.4	[72]
CBHII	3.2.1. 91	Cel6A	CBD1/CD6	50~58	5.0~6.3	8~18%	[73]
EGI	3.2.1.4	Cel7B	CD7/CBD1	54	4.0~4.7	4	[74]
EGII	3.2.1.4	Cel5A	CBD1/CD5	48~50	5.5	6~15	[72]
EGIII	3.2.1.4	Cel12A	CD12	20~23.5	7.4~7.7	---	[75]
EGIV	3.2.1.4	Cel61A	CD61/CBD1	---	---	---	
EGV	3.2.1.4	Cel45A	CBD1/CD45	---	---	---	
XynI	3.1.2.8	Xyn11A	CD11	14~40	4~9.5	---	
XynI	3.2.1.8	Xyn11B	CD11	---	---	---	

3. Concluding remarks

Numerous efforts have been dedicated the study of the mechanisms of different isozymes and their synergisms, as well as the molecular structure of these enzymes. Process or application researchers have also given much attention to the utilization of celluase in different fields including energy conversion, fiber modification and energy reduction in the paper industry, and finishing treatments in textile. The techniques used range from traditional chemical methods to X-ray chyrstallography (such as small angle X-ray scattering-SAXS), to transmission electron microscopy (TEM) and other techniques in the different fields. With the introduction or wider application of more techniques, such as atomic force microscopy (AFM), surface plasma reflection (SPR) and quartz crystal microbalance (QCM) in related fields, researchers will be able to develop more comprehensive understanding of cellulase systems and their interaction on substrates, as well as the interaction between different isozymes. Recently, there has been some work using AFM and QCM to explore interaction between cellulase and cellulose[50, 76-78].

Reference

(1) Lynd Lee, R.; Weimer Paul, J.; van Zyl Willem, H.; Pretorius Isak, S. Microbiology and molecular biology reviews : MMBR **2002**, 66, 506-577, table of contents.

(2) Väljamäe, P.; Sild, V.; Pettersson, G.; Johansson, G. European Journal of Biochemistry **1998**, 253, 469-475.

(3) Medve, J.; Karlsson, J.; Lee, D.; Tjerneld, F. Biotechnol. Bioeng. **1998**, 59, 621-634.

(4) Nidetzky, B.; Steiner, W.; Hayn, M.; Claeyssens, M. Biochemical Journal **1994**, 298, 705-710.

(5) Palonen, H.; Tenkanen, M.; Linder, M. Appl. Environ. Microbiol. **1999**, 65, 5229-5233.

(6) Messner, R.; Hagspiel, K.; Kubicek, C. P. Archives of Microbiology **1990**, 154, 150-155.

(7) Réczey, K.; Brumbauer, A.; Bollók, M.; Szengyel, Z.; Zacchi, G. Appl Biochem Biotechnol **1998**, 70-72, 225-235.

(8) Sternberg, D.; Vijayakumar, P.; Reese, E. T. Canadian journal of microbiology **1977**, 23, 139-147.

(9) Schülein, M. J. Biotechnol. **1997**, 57, 71-81.

(10) Broda, P.; Birch, P.; Brooks, P.; L., J.; Copa-Patiñio; Sinnott, M. L.; Tempelaars, C.; Wang, Q.; Wyatt, A.; Sims, P. FEMS Microbiology Reviews **1994**, 13, 189-195.

(11) Broda, P.; Birch, P. R. J.; Brooks, P. R.; Sims, P. F. G. Molecular Microbiology **1996**, 19, 923-932.

(12) Copa-Patiño, J. L.; Kim, Y. G.; Broda, P. Appl. Microbiol. Biotechnol. **1993**, 40, 69-76.

(13) Covert, S. F.; Vanden Wymelenberg, A.; Cullen, D. Appl. Environ. Microbiol. **1992**, 58, 2168-2175.

(14) Vanden Wymelenberg, A.; Covert, S.; Cullen, D. Appl. Environ. Microbiol. **1993**, 59, 3492-3494.

(15) Vallim, M. A.; Janse, B. J. H.; Gaskell, J.; Pizzirani-Kleiner, A. A.; Cullen, D. Appl. Environ. Microbiol. **1998**, 64, 1924-1928.

(16) Henriksson, G.; Johansson, G.; Pettersson, G. J. Biotechnol. **2000**, 78, 93-113.

(17) Lamed, R.; Naimark, J.; Morgenstern, E.; Bayer, E. A. J. Bacteriol. **1987**, 169, 3792-3800.

(18) Vladut-Talor, M.; Kauri, T.; Kushner, D. J. Archives of Microbiology **1986**, 144, 191-195.

(19) Irwin, D. C.; Spezio, M.; Walker, L. P.; Wilson, D. B. Biotechnology and Bioengineering **1993**, 42, 1002-1013.

(20) Kim, E.; Irwin, D. C.; Walker, L. P.; Wilson, D. B. Biotechnology and Bioengineering **1998**, 58, 494-501.

(21) Irwin, D.; Shin, D.-H.; Zhang, S.; Barr, B. K.; Sakon, J.; Karplus, P. A.; Wilson, D. B. J. Bacteriol. **1998**, 180, 1709-1714.

(22) Bergquist, P. L.; Gibbs, M. D.; Morris, D. D.; Te'o, V. S. J.; Saul, D. J.; Morgan, H. W. FEMS Microbiology Ecology **1999**, 28, 99-110.

(23) Sakon, J.; Adney, W. S.; Himmel, M. E.; Thomas, S. R.; Karplus, P. A. Biochemistry **1996**, 35, 10648-10660.

(24) Halldórsdóttir, S.; Thórólfsdóttir, E. T.; Spilliaert, R.; Johansson, M.; Thorbjarnardóttir, S. H.; Palsdottir, A.; Hreggvidsson, G. Ó.; Kristjánsson, J. K.; Holst, O.; Eggertsson, G. Appl. Microbiol. Biotechnol. **1998**, 49, 277-284.

(25) Driskill, L. E.; Kusy, K.; Bauer, M. W.; Kelly, R. M. Appl. Environ. Microbiol. **1999**, 65, 893-897.

(26) Sunna, A.; Moracci, M.; Rossi, M.; Antranikian, G. Extremophiles **1997**, 1, 2-13.

(27) Hu, G.; Heitmann, J. A.; Rojas, O. J. BioResouces **2008**, 3, 270-294.

(28) Ooshima, H.; Burns, D. S.; Converse, A. O. Section Title: Fermentation and Bioindustrial Chemistry **1990**, 36, 446-452.

(29) Klyosov, A. A. Biochemistry **1990**, 29, 10577-10585.

(30) Banka, R. R.; Mishra, S. Enzyme and Microbial Technology **2002**, 31, 784-793.

(31) Nidetzky, B.; Steiner, W. Biotechnology and Bioengineering **1993**, 42, 469-479.

(32) Boerjesson, J.; Engqvist, M.; Sipos, B.; Tjerneld, F. Enzyme Microb. Technol. **2007**, 41, 186-195.

(33) Boussaid, A.; Saddler, J. N. Enzyme and Microbial Technology **1999**, 24, 138-143.

(34) Converse, A. O.; Girard, D. J. Biotechnol. Prog. **1992**, 8, 587-588.

(35) Hoshino, E.; Kanda, T.; Sasaki, Y.; Nisizawa, K. Section Title: Enzymes **1992**, 111, 600-605.

(36) Rabinovich, M. L.; Klesov, A. A.; Grigorash, S. Y.; Kalnina, I. A.; Chernoglazov, V. M. Bioorganicheskaya Khimiya **1982**, 8, 84-95.

(37) Rabinovich, M. L.; Melnick, M. S.; Bolobova, A. V. Biochemistry (Moscow) **2002**, 67, 850-871.

(38) Yuldashev, B. T.; Rabinovich, M. L.; Rakhimov, M. M. Prikladnaya Biokhimiya i Mikrobiologiya **1993**, 29, 233-243.

(39) Gerber, P.; Joyce, T.; Heitmann, J.; Siika-Aho, M.; Buchert, J. Cellulose **1997**, 4, 255-268.

(40) Wu, S.; Ding, S.; Li, Z. In New Technologies in Non-Wood Fiber Pulping and Papermaking, [International Conference on Non-Wood Fiber Pulping and Papermaking], 5th, Guangzhou, China, Nov. 8-10, 2006, 2006, pp 436-439.

(41) Steiner, W.; Sattler, W.; Esterbauer, H. Biotechnology and Bioengineering **1988**, 32, 853-865.

(42) Lynd, L. R.; Grethlein, H. E. Biotechnology and Bioengineering **1987**, 29, 92-100.

(43) Wald, S.; Wilke, C. R.; Blanch, H. W. Biotechnology and Bioengineering **1984**, 26, 221-230.

(44) Kyriacou, A.; Neufeld, R. J.; MacKenzie, C. R. Biotechnology and bioengineering **1989**, 33, 631-637.

(45) Ryu, D. D. Y.; Kim, C.; Mandels, M. Biotechnology and Bioengineering **1984**, 26, 488-496.

(46) Chernoglazov, V. M.; Ermolova, O. V.; Klyosov, A. A. Enzyme and Microbial Technology **1988**, 10, 503-507.

(47) Medve, J.; Ståhlberg, J.; Tjerneld, F. Appl Biochem Biotechnol **1997**, 66, 39-56.

(48) Beldman, G.; Voragen, A. G. J.; Rombouts, F. M.; Leeuwen, M. F. S.-v.; Pilnik, W. Biotechnology and Bioengineering **1987**, 30, 251-257.

(49) Suvajittanont, W.; McGuire, J.; Bothwell, M. K. Biotechnology and Bioengineering **2000**, 67, 12-18.

(50) Turon, X.; Rojas, O. J.; Deinhammer, R. S. Langmuir **2008**, 24, 3880-3887.

(51) Rojas, O. J.; Jeong, C.; Turon, X.; Argyropoulos, D. S. ACS Symp. Ser. **2007**, 954, 478-494.

(52) Béguin, P.; Aubert, J.-P. FEMS Microbiology Reviews **1994**, 13, 25-58.

(53) Pérez, J.; Muñoz-Dorado, J.; Rubia, T. d. l.; Martínez, J. International Microbiology **2002**, 5, 53-63.

(54) Henrissat, B.; Claeyssens, M.; Tomme, P.; Lemesle, L.; Mornon, J. P. Gene **1989**, 81, 83-95.

(55) Rouvinen, J.; Bergfors, T.; Teeri, T.; Knowles, J. K.; Jones, T. A. Science **1990**, 249, 380-386.

(56) Joliff, G.; Beguin, P.; Juy, M.; Millet, J.; Ryter, A.; Poljak, R.; Aubert, J.-P. Nat Biotech **1986**, 4, 896-900.

(57) Divne, C.; Sinning, I.; Ståhlberg, J.; Pettersson, G.; Bailey, M.; Siika-aho, M.; Margolles-Clark, E.; Teeri, T.; Jones, T. A. Journal of Molecular Biology **1993**, 234, 905-907.

(58) Divne, C.; Stahlberg, J.; Reinikainen, T.; Ruohonen, L.; Pettersson, G.; Knowles, J. K.; Teeri, T. T.; Jones, T. A. Science **1994**, 265, 524-528.

(59) Bedarkar, S. Journal of Molecular Biology **1992**, 228, 693.

(60) Sinnott, M. L. Chemical Reviews **1990**, 90, 1171-1202.

(61) Henrissat, B. Biochemical Journal **1991**, 280, 309-316.

(62) Henrissat, B.; Bairoch, A. Biochemical Journal **1996**, 316, 695-696.

(63) Henrissat, B.; Teeri, T. T.; Warren, R. A. J. FEBS Letters **1998**, 425, 352-354.

(64) Rabinovich, M. L.; Melnik, M. S.; Boloboba, A. V. Appl. Biochem. Microbiol. **2002**, 38, 305-321.

(65) Klesov, A. A.; Rabinovich, M. L.; Nutsubidze, N. N.; Todorov, P. T.; Ermolova, O. V.; Chernoglazov, V. M.; Mel'nik, M. S.; Kude, E.; Dzhafarova, A. N.; et al. Biotekhnologiya **1987**, 3, 152-168.

(66) Davies, G.; Henrissat, B. Structure **1995**, 3, 853-859.

(67) Henrissat, B. Cellulose **1994**, 1, 169-196.

(68) Knowles, J.; Lehtovaara, P.; Teeri, T. Trends Biotechnol. **1987**, 5, 255-261.

(69) Bhat, M. K. Biotechnology advances **2000**, 18, 355-383.

(70) Senior, D. J.; Mayers, P. R.; Saddler, J. N. Biotechnology and bioengineering **1991**, 37, 274-279.

(71) Eriksson, L. A.; John A. Heitmann, J. In Pulping Conference, 1998, pp 1301-1312.

(72) Goyal, A.; Ghosh, B.; Eveleigh, D. Bioresource Technology **1991**, 36, 37-50.

(73) Kyriacou, A.; MacKenzie, C. R.; Neufeld, R. J. Enzyme and Microbial Technology **1987**, 9, 25-32.

(74) Bhikhabhai, R.; Johansson, G.; Pettersson, G. Journal of applied biochemistry **1984**, 6, 336-345.

(75) Beldman, G.; Leeuwen, M. F.; Rombouts, F. M.; Voragen, F. G. J. European Journal of Biochemistry **1985**, 146, 301-308.

(76) Wallace, J. T., North Carolina State University, Raleigh, 2006.

(77) Ahola, S.; Turon, X.; Österberg, M.; Laine, J.; Rojas, O. J. Langmuir **2008**, 24, 11592-11599.

(78) Jeong, C.; Maciel, A. M.; Pawlak, J. J.; Heitmann, J. A.; Argyropulous, D. S.; Rojas, O. J., Auckland, New Zealand, 16-19 MAY 2005.

Chapter 4 In-situ monitoring of cellulase activity with the quartz microbalance technique (QCM)

Abstract

Various techniques have been employed to investigate the interaction between cellulases and cellulose substrates. The application of quartz crystal microbalance techniques provide new insights for the understanding of such interactions, namely the adsorption and desorption between the enzymes and the substrates. It also provides in-situ, real time monitoring of the kinetics of cellulose hydrolysis. In this chapter, model cellulose films from microcrystalline cellulose (Avicel® PH101) were applied to a gold-coated silica sensor for quartz crystal microbalance with dissipation, from which both the cellulase adsorption and hydrolysis rates were obtained. A new interpretation of kinetics is proposed using the dose-response model. The frequency shift concomitant with cellulase injection was fitted using a Langmuir model. Parameters from the hydrolysis kinetic model and frequency changes can be used to estimate substrate information, interfacial adsorption and liquid properties. We report that cellulase adsorption may not be a prerequisite for amorphous cellulose hydrolysis.

Keywords: QCM, QCM-D, cellulose hydrolysis, cellulase adsorption, Langmuir, dose-response model, cellulose hydrolysis kinetics

1. Introduction

The broad application of piezoelectric quartz crystal techniques started long after Marie Curie discovered this property of crystals. At present, the quartz crystal microbalance is becoming a major technique that can be used to study interfacial phenomena in different fields. Since Sauerbrey first reported that the mass sensitivity of a quartz crystal could be used to measure the thickness of vacuum-deposited metal, significant progress has been made in understanding other interaction mechanisms between acoustic devices and contacting media.[1] The various applications include the setup of theoretical models,[2, 3] thin film deposition,[4, 5] electrochemical QCM,[6, 7] application in biological/biochemical research,[8] cellulose hydration,[9] adsorption and adhesion,[10] and enzyme kinetic rate of hydrolysis of cellulose films.[11-13]

According to the Sauerbrey equation,[14] when a crystal is loaded with a uniform rigid film that has a mass which is much smaller than that of the quartz resonator, the change of the resonance frequency and mass are linearly related:

$$\Delta f = -\frac{2f^2}{v_q \rho_q} m = -\frac{f}{\rho_q t_q} m = -Cm \qquad (1)$$

Where ρ_q and v_q are the specific density and the shear wave velocity in the quartz respectively; t_q is the thickness of the quartz crystal, and m is the mass per unit area of the added film. The minus sign in this formula shows that a decrease of mass will result in an increased frequency. For rigid films, C is a constant that is determined by the dimensions of

the crystal disc resonator, e.g., C is 17.7 $ng.Hz^{-1}.cm^{-2}$ for a 5 MHz crystal sensor in our setup.

For soft films, equation (1) is not exactly obeyed due to viscoelastic dissipation. Dissipation is used to characterize more comprehensively and accurately the film viscoelasticity. The dissipation factor, which measures the energy dissipation in the dampening of the oscillation as it its vibration amplitude decays exponentially, can be expressed as:

$$D = \frac{E_{dissipated}}{2\pi E_{stored}}, \qquad (2)$$

Equation (2) describes the viscoelecticity of thin films in terms of the energy dissipation. Interpretation of film mass changes should include the viscoelastic contribution. The mass change under this situation does not follow a linear relationship with frequency as described in equation (1); instead, the dissipation should be considered.

The QCM technique provides real time monitoring of the mass change on its crystal sensors and the change of liquid properties in the test chamber. This allows one to monitor cellulose hydrolysis after the cellulose is anchored on the crystal sensors. The deposition of cellulose films has been successfully practiced for the study of cellulase activity and other related aspects.[15-17] Real-time monitoring of cellulose hydrolysis provides information about both the enzyme adsorption and substrate hydrolysis. The maximum adsorption, initial hydrolysis velocity, and maximum hydrolysis rate may be obtained by analyzing the time-course response of frequency with the QCM-D. The activation energy of cellulose hydrolysis

can also be obtained using the Arrhenius equation. In this report, microcrystalline cellulose was dissolved in NMMO/DMSO solution. Cellulose films were prepared from this solution for enzyme activity monitoring using the QCM-D. A pseudo-Langmuir model was adapted to fit the frequency change to cellulase charge and the kinetic process was investigated using a dose-response model. The activation energy was also estimated based on the maximum rate constant from the dose-response model used.

2. Experimental

2.1 Materials

Microcrystal cellulose (MCC, Avicel®PH-101) was purchased from Fluka. N-methylmorpholin-N-oxide (NMMO) and dimethylsulfoxide (DMSO) were supplied by Aldrich. Polyvinylacrylamide (PVAm) was supplied by BASF. DyAdic EXP Cellulase was supplied by DyAdic (Jupiter, FL). This cellulase was a yellow powder and dissolved in buffer solution before use. Another commercial cellulase (Celluclast) was purchased from Sigma Aldrich Inc. This cellulase was produced from *Trichoderma reesei*. The Modified Lowry Assay Kit was supplied by Pierce (Rockford, IL). Glacial acetic acid and sodium acetate were used in the preparation of buffer solutions (pH 4.8, ionic strength 100mM). Crystal sensors coated with silicon dioxide (QSX303) were purchased from Q-Sense (Baltimore, Q-sense, US). A Milli-Q® Gradient system was the source of water (resistivity > 18 MΩ) used in all experiments.

2.2 Preparation of cellulose film on sensor disks

The silica sensor disks were cleaned by exposure to an ultraviolet-ozone (UVO) for 10 minutes followed by soaking in a sodium dodecyl-sulfate solution for 30 minutes. A dilute polyvinyl amide PVAm (100ppm) solutions were used to pre-coat the quartz disks by immersion for 10 minutes. After rinsing with water, the excess solution was removed through drying with a gentle jet of filtered air, and then the crystal sensors were dried in an oven at 40 º C for 20 minutes. Microcrystalline cellulose (MCC) was dissolved in NMMO at the concentration of 2% at 115 ºC. Care was addressed that the temperature did not exceed 130 ºC. A small amount of DMSO was carefully added to improve the dispersion, viscosity and solubility. Additional DMSO was added so that the final concentration of cellulose in the solution was 0.5%. The cellulose solution was then spin-coated on the PVAm-coated resonator using a spin coater (Laurell Technologies model WS-400A-6NPP) at 5000rpm for 40 seconds.[16] The resulting cellulose-coated resonator was heated in an oven at 80°C for two hours, followed by washing with milli-Q water for 1 hour. The water was replaced with fresh water and the disks were soaked for another 3 hours.

2.3 Protein Assay with Lowry Kit

Based on the work done by Lowry et al,[18] the modified Lowry Protein Assay Kit (product no. 23240) using bovine serum albumin (BSA) as a standard for the assay of protein content. Two cellulase samples, one with a concentration 0.06% and the other one with a concentration of 0.1%, as well as the BSA standards were treated with the protein assay and Folin-Ciocalteu reagents in the Assay Kit under the same procedures and conditions. The

samples and standards were tested at a wavelength of 750 nm with an HP 8453E UV-visible spectrophotometer**.** Test samples and protein standards were diluted with sodium acetate buffer (pH=4.8).

2.4 In-situ monitoring of cellulase activity with QCM-D

The QCM instrument used was a Q-Sense D300 from Q-sense (Q-Sense AB, Gothenburg, Sweden). The instrument can monitor both the frequency and dissipation changes of the quartz resonator. During the measurement, the crystal sensor coated with a cellulose film was mounted in the QCM-D chamber, which is build with a temperature control system and provides a rapid exchange of the liquid in contact with one side of the sensor without any disturbance. Cellulose-coated resonators were put in contact with water in the QCM chamber and were hydrated until no appreciable frequency and dissipation shifts were observed. After the stabilization, a cellulase solution was introduced and the QCM was operated in a batch mode. Experiments were terminated when a stable frequency and dissipation plateau was observed in the time-course response from QCM-D. All liquids were degassed and preheated to a temperature close to the desired temperature set for the QCM chamber before they were injected into the system. A syringe pump (Cole-Parmer 74900 series) was employed to inject the solutions into the QCM-D chamber at a flow rate of 0.1 ml/min. 0.5 ml cellulase solutions were injected in each run. Experiments were terminated when a plateau in the respective run was observed. Q-sense D300 recorded frequency and dissipation responses at ca. 5, 15, 25 and 35 MHz, which corresponds to the overtones n=1, 3, 5 and 7, respectively. In this report, the third overtone and dissipation were used for analysis.

3. Results and discussion

3.1 Protein content

The average protein content, expressed as μg protein/mg of the crude cellulases was determined by triplicate and was found to be 520±28.7.

3.2 Monitoring cellulose film hydrolysis

All cellulose films were hydrated until no pronounced frequency and dissipation changes were observed. Figure 4-1 shows a typical QCM-D response to cellulose film hydrolysis by cellulase enzymes in solution. The frequency shift corresponds to the injection of cellulase solution into the QCM-D chamber thereby replacing the buffer solution, in which adsorption may have occurred. After a continuous decrease of frequency for about 5 min, the frequency started to increase rapidly for about 2 hours and then leveled off. The dissipation curve showed an increase until a maximum point was reached. After the maximum point, the dissipation decreased and finally became leveled off as the frequency change slowed down.

Many researchers have believed that the frequency drop was caused by the cellulase adsorption.[10, 11, 13, 19] However, other researchers have reported that liquid properties, especially liquid density and viscosity, can contribute significantly to a change in resonance frequency.[20-22] The frequency drop in response to the cellulase injection may not be interpreted solely as cellulase adsorption, but could be explained as a combination of the effects of both the cellulase solution properties (density and viscosity) in addition to cellulase adsorption onto the cellulose film.

The dissipation curve indicates changes in the viscoelasticity of the cellulose films bound to the silica sensor used in the QCM-D. It can be expected that the increase of dissipation energy is caused by the adsorption and penetration of cellulase enzyme onto and into the cellulose film. As illustrated in Figure 4-1, appreciable cellulase film degradation occurred after the initial frequency drop, which was followed by a large increase of frequency. It can be imaged that several different physical and/or chemical phenomena were occur at this stage. These include the cellulase adsorption on the cellulose film, the penetration of cellulase into the different regions of the cellulose film and the release of soluble products during the cellulose hydrolysis. Cellulase enzyme did not have a maximum interaction until the substrate films became viscous enough, which is indicated by the peak point of the dissipation curve in Fig. 4-1. At this time, the hydrolysis of cellulose film reached its maximum speed, as can be interpreted from the inflection point in the frequency curve in Fig. 4-1, where the frequency curve has its maximum derivative.

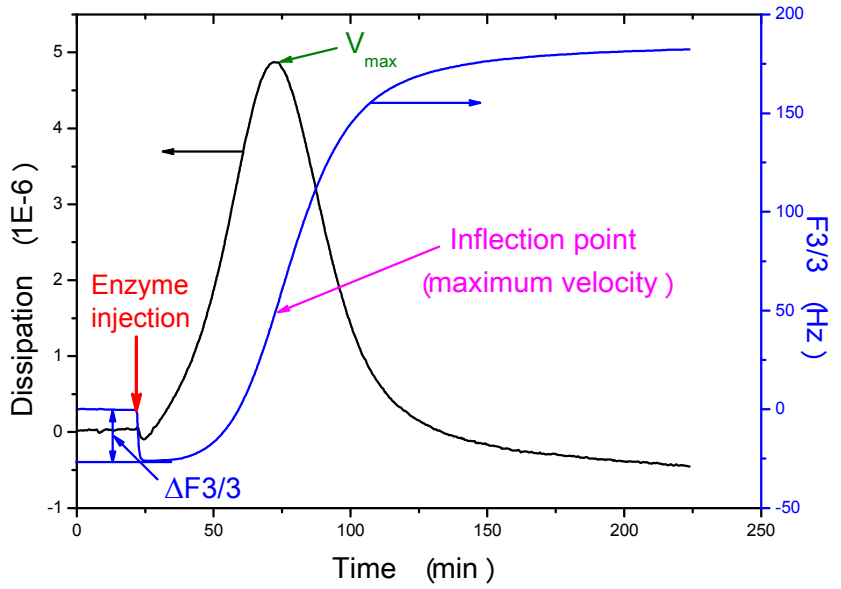

Figure 4-1. QCM-D frequency and dissipation change response in cellulose film hydrolysis by Dyadic EXP cellulase. The cellulose film was made from Avicel®PH101 microcrystalline cellulose. Cellulase concentration: 0.015% in pH 4.8 buffer having an ionic strength of 100 mM. The QCM-D was operated in a batch mode and the records shown here were based on the third overtone. The maximum velocity (V_{max}) is believed to occur when the dissipation curve reaches its peak value, which corresponds to the inflection point (or the maximum slope) in the frequency curve, as indicated by the purple arrow.

It should be pointed out that QCM-D may be less valuable in exploring the Michaelis-Menton kinetics, which has been most broadly used to describe the relationship between the initial velocity and substrate concentration in biological reactions.[23, 24] There are various

limitations that may prevent this application. These limitations would include the determination of substrate concentration in the QCM-D setting. Films produced using the spin-coating technique can have different thickness and surface roughness as reported by various researchers,[17, 25-27] but the modeling of the relationship between surface roughness and cellulose substrated deposited on the silica sensor is one practical issue that should be addressed. Another practical issue would be the change of morphology and the determination of the accessible binding sites on the substrates. As pointed out by Hu et al,[20] the morphology of the native cellulose is altered during the preparation of cellulose films; amorphous cellulose is formed from the DMAc/LiCl procedure,[28, 29] whereas the NMMO/DMSO solutions produce cellulose II.[15]

3.3 Effect of cellulase concentration

The normalized frequency drop (ΔF3/3) as indicated in Fig. 4-1 was obtained for five different cellulase concentrations at 25°C. Figure 4-2 shows the relationship of frequency drop to cellulase concentrations. A Langmuir model was used to fit the frequency drop to the corresponding concentrations. The generated model has a maximum frequency drop of 49.6 Hz and quasi-equilibrium constant of 0.0084 ppm^{-1}. The correlation coefficient is 0.97, which indicates a fairly good fit. A rough estimation using the Sauerbrey equation can give a maximum adsorption of 0.7 μg regardless of the substrate mass. Much research has determined the maximum adsorption for cellulase adsorption on cellulose substrates, [30-32] but it would be difficult to compare the results in this research due to the different techniques employed for parameter determination and because of the difference in substrate morphology.

Meanwhile, the liquid property is expected to affect frequency drop, as reported by Hu et al.[20] and He et al.[21]

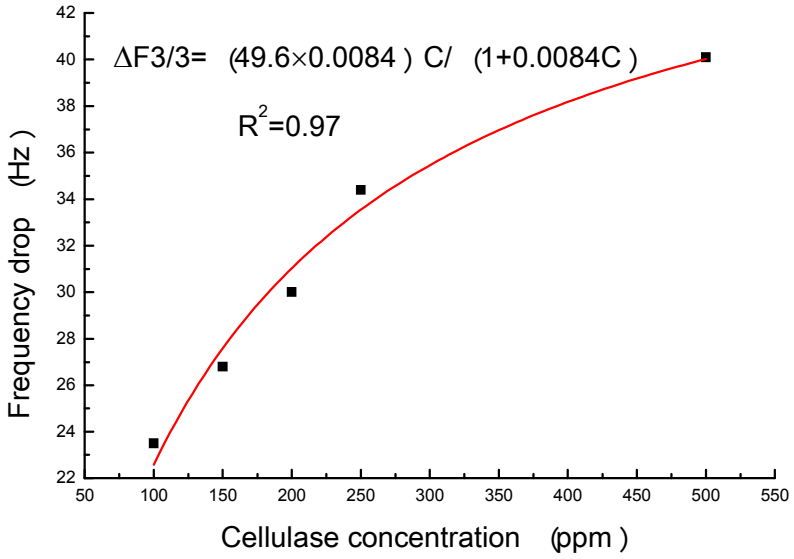

Figure 4-2. QCM-D frequency drop as a function of cellulase concentration at 25°C. A Langmuir equation was employed to fit the frequency (ΔF3/3) and cellulase concentration (C). The fitted equation is $\Delta F3/3 = \frac{(49.6 \times 0.0084)C}{1 + 0.0084C}$ with a correlation coefficient of 0.97. The maximum possible frequency drop is 49.6 Hz with a quasi-equilibrium constant of 0.0084 ppm^{-1}.

According to the cellulase-substrate complex hypothesis, the adsorption constant can indicate how much cellulase enzyme adsorbs on the substrate at the equilibrium state.[32, 33] The adsorption constant shows that only about 0.8% cellulase adsorbed on the substrates upon adsorption equilibrium. This is much lower than amounts reported in previous

investigation. [32, 34-38] However, the enzymatic hydrolysis was obvious from the increase in frequency, as indicated in Fig. 4-1. This may also imply that adsorption is less important in cellulose hydrolysis than believed previously.[39]

3.4 Hydrolysis kinetics

A dose-response model was adopted to investigate the hydrolysis kinetics. Equation 1 shows a typical dose-response equation.

$$\Delta f 3 \big/ 3 = A_1 + \frac{A_2 - A_1}{1 + 10^{P(\log t_0 - t)}} \qquad (3)$$

Where Δf3/3 is the dependent variable, the frequency change during cellulose film hydrolysis and t is the time. A_1 is the bottom asymptote, A_2 is the top asymptote, P is the hill slope and $\log t_0$ is a value corresponding to $\frac{A_1 + A_2}{2}$. Figure 4-3 shows a sigmoidal dose-response fitting of frequency response as a function of time variable. The different parameters for different cellulase concentrations are listed in table 4-1. Each fitting has an adjusted correlation coefficient greater than 0.99, which indicates that the dose-response model can model the frequency/time course data from the QCM fairly well.

The bottom asymptote A_1 can be interpreted as the maximum frequency drop caused by the adsorption of cellulases and their liquid properties, including viscosity and density. The top asymptote A_2 may be used to indicate the maximum substrate mass on the silica sensors. In this investigation, the maximum frequency drop indicated in Fig. 4-2 have the

same trend as the ones shown in table 4-1 for A_1. Different A_2 indicates that the spin coating may have not produced cellulose films with similar thicknesses and masses on different silica sensors.

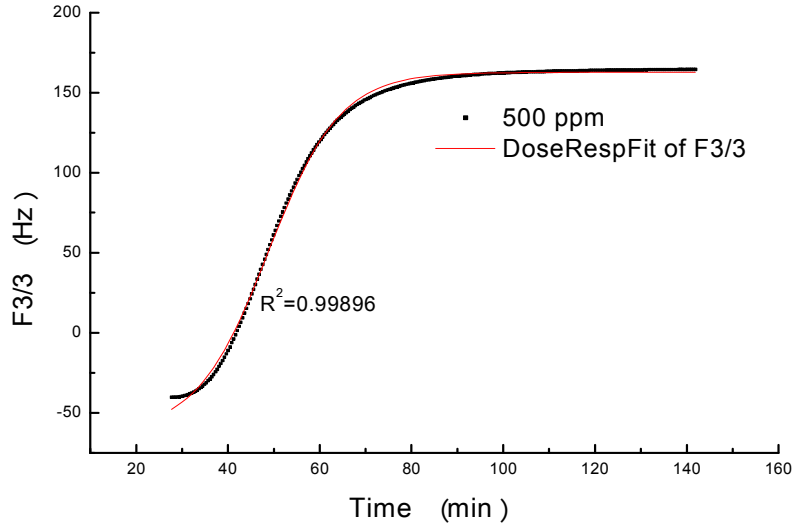

Figure 4-3. A dose-response fit of f3/3 as a function of time during a cellulose film hydrolysis by 500 ppm cellulase solution at 25°C. The fitting was generated using Origin and has an adjusted R^2 = 0.99973. The fitting parameters are A_1 = -61.9 Hz, A_2 = 162.7 Hz, $logt_0$ = 48.8 min, p = 0.56 min^{-1}respectively.

Figure 4-4 shows the fit of A1 as a function of cellulase concentration. The two Langmuir fits (Fig. 4-2 and Fig. 4-4) support each other to some degree and show that QCM-D can be fitted to the Langmuir isotherm. A Langmuir extension model indicates a better fit in Figure 4-4, but the parameter interpretation would be different. A higher power of the

concentration effect can be observed in the Langmuir extension model fitting, which may imply an adsorption model that is not limited to monolayer adsorption.

Table 4-1. Dose-response parameter summary for cellulose film hydrolysis by cellulase solutions at 25°C

Cellulase concentration / Parameters	100 ppm	150 ppm	200 ppm	250 ppm	500 ppm
A_1 (Hz)	-30	-47.5	-53.6	-54.9	-61.9
A_2 (Hz)	166.9	159	213.9	139.7	162.7
Log t_0 (min)	77.2	93.9	66.5	146.5	48.8
P (min^{-1})	0.04	0.013	0.046	0.0077	0.056
Adj. R^2	0.99973	0.99998	0.99927	0.99984	0.99896

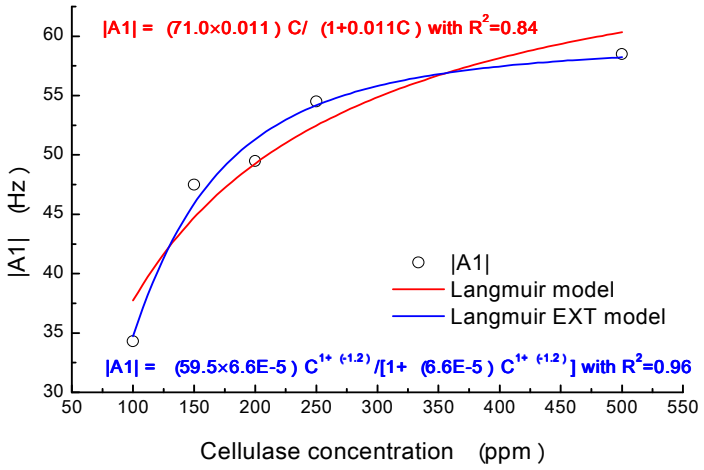

Figure 4-4. Plot of A1 as a function of cellulase concentrations. The Langmuir model and Langmuir extension model were used to fit these data respectively. A Langmuir model produces a fit equation $|A_1| = \frac{(71.0 \times 0.011)C}{1 + 0.011C}$ with a correlation coefficient of 0.84, whereas a Langmuir extension model generates a fit equation $|A_1| = \frac{[59.5 \times (6.6 \times 10^{-5})]C^{1+(-1.2)}}{1 + (6.6 \times 10^{-5})C^{1+(-1.2)}}$ with a correlation coefficient of 0.96.

The $\log t_0$ varied with the running time and the data selected for model fitting. Extended running time increases the value for $\log t_0$, especially as the frequency curve (Fig. 4-1) gradually levels off. These $\log t_0$ would have less practical meaning to expect physical interpretation of these values. However, an accurate control of level-off time can lead to an interpretation of this time as the time needed for cellulase to reach its maximum hydrolysis rate, which is important in the Michaelis-Menten model. P is the maximum slope in the dose-response model. It may be possible to use P to estimate the fastest hydrolysis rate in cellulose

film hydrolysis reaction. Some researchers have reported that the fastest hydrolysis occurred at the beginning of cellulose hydrolysis.[40] The difference may result from the change of morphology of substrates after the regeneration from NMMO/DMSO.

3.5 Temperature effect

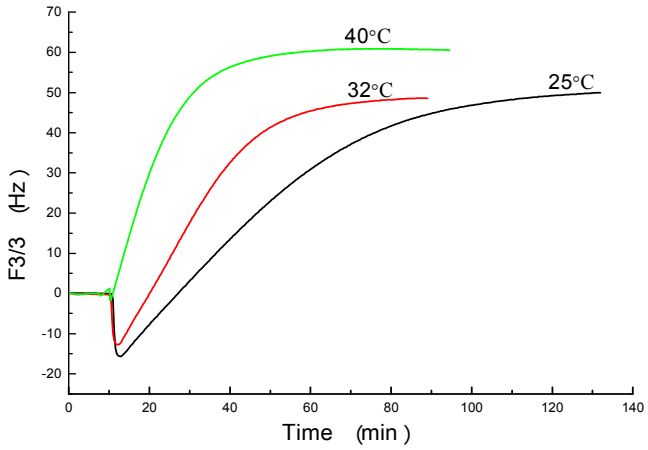

Figure 4-5. QCM-D frequency response for cellulose film hydrolysis at three different temperatures. Cellulase solutions used were Celluclast® from *Trichoderma reesei*, the concentration for the cellulase solution was 500 ppm based on volume ratio from the as-received solution.

The temperature effect was investigated using the cellulase from *Trichoderm reesei*. Figure 4-5 shows the QCM-D frequency response at three different temperatures. It is apparent that higher temperature produced faster hydrolysis from the curve slopes. Table 4-2 shows the dose-response model parameters for the frequency response curves obtained by fitting a dose-response model to Fig. 4-5 (fitting figure not shown).

Table 4-2. Dose response parameters for cellulose film hydrolysis by *T. reesei* cellulase at 25°C in QCM-D chamber (Determined from frequency response curves)

Parameter \ Temperature	25°C	32°C	40°C
A_1 (Hz)	-27.1	-33.2	-81.86
A_2 (Hz)	49.8	48.7	60.76
$\log t_0$ (min)	38.8	24.5	8.3
P (min^{-1})	0.0232	0.0397	0.0478
Adj. R^2	0.99337	0.99996	0.99987

As indicated in Fig. 4-5, the frequency drop became smaller as the temperature increased. However, the fitted A1's show an opposite trend, higher temperature induced greater maximum frequency drop. This contradiction may imply a different model at the lower end for the kinetic fit or a different interpretation for parameter A1. A2 can be used to estimate the mass of the substrate coated on the silica sensors. This was in agreement with the expectation we had from the spin-coating process. The cellulose solutions used in this spin coating were applied in smaller amounts, which should produce cellulose films with lower thickness. Time needed to reach the $\frac{A_1 + A_2}{2}$ showed a decreasing trend, which might also imply a faster hydrolysis rate; however, the substrate mass variation complicates the interpretation. A comparison of the hill slope shows an increasing maximum hydrolysis rate as temperature rose. This temperature effect is in agreement with various reports. [19, 41-43]

3.6 Activation energy of cellulose hydrolysis by Celluclast

The P values in table 4-2 were treated as the maximum hydrolysis rate constant by assuming this cellulolytic reaction is a first order reaction; The calculated activation energy was 37 kJ/mol for Celluclast cellulase to hydrolyze the cellulose film in this research. This was calculated using the simple Arrhenius equation $k = A\ \exp(-\frac{E_a}{RT})$, where k is the rate constant, A is a pre-exponential factor and E_a is the activation energy. This activation energy is lower than the one obtained by He et al,[21] who reported that the activation energy was 52 kJ/mol for enzymatic hydrolysis of CMC. This difference may result from the different enzyme and reaction systems. The linear plot of *ln k* against 1/T gave a correlation coefficient of 0.83 (Figure not shown), which indicates a relatively large error.

4. Conclusions

The quartz crystal microbalance technique with dissipation monitoring was used to investigate the kinetic behavior of cellulose hydrolysis by cellulase enzymes. The maximum frequency drop at various enzyme concentrations followed a Langmuir model and the kinetic data was fitted to a dose-response model. Parameters from both models can be used to obtain the substrate information such as the interfacial adsorption, liquid properties and the hydrolysis rate. In this report, the cellulase was determined to have only about 1% adsorption on the amorphous cellulose film, although the hydrolysis was extensive. This may imply a different concept or mechanism other than the adsorption before hydrolysis hypothesis that

has been believed for decades. The activation of enzymatic hydrolysis by Celluclast® was determined to be 37kJ/mol.

Further research by a combined application of atomic force microscopy, QCM and surface plasmon resonance techniques might be able to provide a more complete understanding of the interfacial and kinetic behavior in cellulose hydrolysis by cellulases.

References

(1) Martin, S. J. Faraday Discuss. **1997**, 107, 463.

(2) Reed, C. E.; Kanazawa, K. K.; Kaufman, J. H. J Appl Phys **1990**, 68, 1993-2001.

(3) Crane, R. A.; Fischer, G. J Phys D Appl Phys **1979**, 12, 2019-2026.

(4) Lu, C.-S. Journal of Vacuum Science and Technology **1975**, 12, 578-583.

(5) Langley, B. a. L., Paul Vacuum technology & coating **2002**, 22.

(6) Ward, M. D.; Buttry, D. A. Science **1990**, 249, 1000-1007.

(7) Bruckenstein, S.; Shay, M. Electrochimica Acta **1985**, 30, 1295-1300.

(8) Wakamatsu, K. Analytical Chemistry **1995**, 67, 3336.

(9) Josefsson, P.; Henriksson, G.; Wagberg, L. Biomacromolecules **2008**, 9, 249-254.

(10) Jeong, C.; Maciel, A. M.; Pawlak, J. J.; Heitmann, J. A.; Argyropulous, D. S.; Rojas, O. J., Auckland, New Zealand, 16-19 MAY 2005.

(11) Rojas, O. J.; Jeong, C.; Turon, X.; Argyropoulos, D. S. ACS Symp. Ser. **2007**, 954, 478-494.

(12) Turon, X., Ahola,S., Österberg, M and Rojas, O.J. Biomacromolecules, in press.

(13) Turon, X.; Rojas, O. J.; Deinhammer, R. S. Langmuir **2008**, 24, 3880-3887.

(14) Rodahl, M.; Hook, F.; Fredriksson, C.; Keller, C. A.; Krozer, A.; Brzezinski, P.; Voinova, M.; Kasemo, B. Faraday Discuss. **1997**, 107, 229-246.

(15) Fält, S.; Wågberg, L.; Vesterlind, E. L.; Larsson, P. T. Cellulose **2004**, 11, 151-162.

(16) Gunnars, S.; Wågberg, L.; Cohen Stuart, M. A. Cellulose **2002**, 9, 239-249.

(17) Fält, S.; Wågberg, L.; Vesterlind, E.-L. Langmuir **2003**, 19, 7895-7903.

(18) Lowry, O. H.; Rosebrough, N. J.; Farr, A. L.; Randall, R. J. J Biol Chem **1951**, 193, 265-275.

(19) Ahola, S.; Turon, X.; Osterberg, M.; Laine, J.; Rojas, O. J. Langmuir **2008**, 24, 11592-11599.

(20) Hu, G.; Heitmann, J. A.; Rojas, O. J. Analytical Chemistry **2009**, 81, 1872-1880.

(21) He, D.; Bao, L.; Long, Y.; Wei, W.; Yao, S. Talanta **2000**, 50, 1267-1273.

(22) Stockbridge, C. D. Vacuum Microbalance Techniques **1966**, 5, 147-178.

(23) Horton, H. R. Principles of biochemistry, 4th ed.; Pearson Prentice Hall: Upper Saddle River, NJ, 2006.

(24) Johnston, D. B.; Shoemaker, S. P.; Smith, G. M.; Whitaker, J. R. Journal of Food Biochemistry **1998**, 22, 301-319.

(25) Eriksson, J.; Malmsten, M.; Tiberg, F.; Callisen, T. H.; Damhus, T.; Johansen, K. S. J. Colloid Interface Sci. **2005**, 284, 99-106.

(26) Turon, X.; Spence, K.; Rojas, O. J., San Francisco, CA, United States, Nov. 12-17 2006; American Institute of Chemical Engineers, New York, NY; 370f/371-370f/376.

(27) Notley, S. M.; Eriksson, M.; Wagberg, L.; Beck, S.; Gray, D. G. Langmuir **2006**, 22, 3154-3160.

(28) Kontturi, E.; Thune, P. C.; Niemantsverdriet, J. W. Langmuir **2003**, 19, 5735-5741.

(29) Kontturi, E.; Thüne, P. C.; Niemantsverdriet, J. W. Polymer **2003**, 44, 3621-3625.

(30) Medve, J.; Ståhlberg, J.; Tjerneld, F. Biotechnology and bioengineering **1994**, 44, 1064-1073.

(31) Stahlberg, J.; Johansson, G.; Pettersson, G. Biochimica Et Biophysica Acta **1993**, 1157, 107-113.

(32) Kim, D. W.; Kim, T. S.; Jeong, Y. K.; Lee, J. K. Journal of Fermentation and Bioengineering **1992**, 73, 461-466.

(33) Rodahl, M.; Hook, F.; Krozer, A.; Brzezinski, P.; Kasemo, B. Review of Scientific Instruments **1995**, 66, 3924-3930.

(34) Kumar, R.; Wyman, C. E. Enzyme and Microbial Technology **2008**, 42, 426-433.

(35) Lu, Y.; Yang, B.; Gregg, D.; Saddler, J. N.; Mansfield, S. D. Appl. Biochem. Biotechnol. **2002**, 98-100, 641-654.

(36) Kim, H.; Ahn, D. H.; Jung, K. H.; Pack, M. Y. Section Title: Enzymes **1997**, 41, 665-677.

(37) Ishihara, M.; Uemura, S.; Hayashi, N.; Jellison, J.; Shimizu, K. Journal of Fermentation and Bioengineering **1991**, 72, 96-100.

(38) Wald, S.; Wilke, C. R.; Blanch, H. W. Biotechnology and Bioengineering **1984**, 26, 221-230.

(39) Lynd Lee, R.; Weimer Paul, J.; van Zyl Willem, H.; Pretorius Isak, S. Microbiology and molecular biology reviews : MMBR **2002**, 66, 506-577.

(40) Lynd, L. R.; Grethlein, H. E. Biotechnology and Bioengineering **1987**, 29, 92-100.

(41) Moniruzzaman, M.; Dale, B. E.; Hespell, R. B.; Bothast, R. J. Appl Biochem Biotechnol **1997**, 67, 113-126.

(42) Jackson, L. S.; Joyce, T. W.; Heitmann, J. A.; Giesbrecht, F. G. J. Biotechnol. **1996**, 45, 33-44.

(43) Kaya, F.; Heitmann, J. A.; Joyce, T. W. J. Biotechnol. **1994**, 36, 1-10.

Chapter 5 Quantification of Cellulase Activity Using the Quartz Crystal Microbalance Technique

Gang Hu, John A. Heitmann, Jr*, Orlando J. Rojas

Forest Biomaterials Science and Engineering, North Carolina State University, Campus Box 8005, Raleigh NC27695-8005

*To whom correspondence should be addressed. E-mail: heitmann@ncsu.edu

Phone: 919-757-8418 FAX: 919-515-6302

Abstract

The development of more efficient utilization of biomass has received increased attention in recent years. Cellulases play an important role in processing biomass through advanced biotechnological approaches. Both the development and the application of cellulases require an understanding of the activities of these enzymes. A new method to determine the activity of cellulase has been developed using a quartz crystal microbalance (QCM) technique. We compare the results from this technique with those from the IUPAC DNS standard method, and also from biccinchoninic acid and ion chromatography methods. It is shown that the QCM technique provides results closer to those obtained by measuring the actual reducing sugars. The elimination of the use of color development in the standard redox methods makes the QCM platform easier to implement; it also allows more flexibility in terms of the nature

of the substrate. Finally, validation of the proposed method was carried out by relating the crystallinity of different substrates and the cellulase activity. Numerical values of cellulase activities measured with the QCM method confirmed that celluloses of higher crystallinity are hydrolyzed slower and to a lower extent than those of lower crystallinity indices for the cellulase mixtures examined.

Keyword: cellulose, cellulase, activity measurement, QCM, biomass

1. Introduction

Cellulases are a group of enzymes mainly consisting of different isozymes, including endoglucanases (EGI and EGII), exoglucanse or cellobio-hydrolyases (CBHI and CBHII), and β-glucosidases, which work synergistically to hydrolyze cellulose into reducing sugars. Cellulases play an important role in the conversion of biomass into energy and chemicals. Significant efforts are being made to develop cellulases of higher efficiency, both from different sources and by transgenic modification, and to explore new fields for their application.

The activity of cellulases is an important parameter since it characterizes their performance and efficiency. A widely used method to measure cellulase activity is the protocol recommended by the International Union of Pure and Applied Chemists (IUPAC), which was published in 1987. [1] According to this method, cellulase activity is determined from the enzyme concentration required to produce a certain amount of reducing sugar in one minute.

The activity is expressed as the micromoles of glucose produced by 1 ml of enzyme in one minute. The amount of sugars produced is typically determined using a spectrophotometric determination under the assumption that all reducing sugars produced after incubation are glucose.

The Filter Paper Activity assay (FPA), which uses Whatman No.1 filter paper (pure cellulose) as substrate, can be applied to determine the overall activity of cellulases. Dinitrosalicylic acid (DNS) is used in the IUPAC-FPA assay as an agent to quantify the amount of reducing sugars released from 50 mg filter paper (Whatman #1) after incubation with the cellulase mixture. In order to obtain reliable results this method requires the preparation of DNS reagent (dinitrosalicylic acid together with phenol are both toxic chemicals[2]) and also demands careful sampling and accurate control of color development. [1]

DNS preparation demands optimal mixing ratios of the different components involved and proper temperature control for color development and color stability.[3] Furthermore, it is known that the decomposition of sugars in the alkaline solution recommended by the IUPAC method causes an increase of (measured) enzyme activity to values higher than the actual ones.[4] Despite efforts to improve the efficiency of IUPAC's filter paper assay[5, 6], the issues indicated before are considered important drawbacks in its utilization.

An alternate method, based on the bicinchoninic acid (BCA) reagent, was proposed by Johnston et al.[7] Here color development from a redox reaction, as in the case of DNS, is used to measure enzyme activity. Many other methods which have been used in the determination

of cellulase activity include viscometric, reducing groups, chromophore or fluorescent group release, chromatographic substrate or product measurement and coupled enzymatic protocols.[7] These methods, including the one based on liquid chromatography for analysis of carbohydrates have been deemed effective.[8, 9] Lacourse et al. provided a technical note covering the use of anion-exchange separation of carbohydrates by pulsed amperometric detection with a pH-selective reference electrode.[10, 11] The use of ion chromatography (IC) to quantify the amount of different sugars produced during cellulase activity measurement provides an accurate way to evaluate the sugar producing ability of cellulases, i.e., the measured sugar content of the hydrolysis product can be used to determine a true cellulase activity in terms of the strict definition of cellulase activity. This method is more used in research due to the sophistication and skills involved in the operation of the instrument and sample preparation.

With an expanded interest in developing reliable protocols to measure enzyme activity, a piezoelectric-sensing technique, the quartz crystal microbalance (QCM) was introduced.[12] QCM utilizes the piezoelectric property of a quartz crystal that is used as an ultrasensitive mass balance. Sauerbrey reported that the changes in frequency of a quartz crystal can be used to measure the mass or thickness of vacuum-deposited metal and researchers have commonly used his equation (the Sauerbrey equation), to quantify changes in such parameters in a number of applications:[12-15] material properties and theoretical models,[16, 17] thin film deposition,[18, 19] electrochemistry,[20, 21] biological/biochemical research,[22-24] as well as adsorption and adhesion. Rojas and col.[15, 17, 25, 26] and Josefsson and col.[27] have reported

recently on the measurement of cellulase behaviors (binding and hydrolysis) with QCM. These efforts have shown that a quartz crystal resonators coated with different types of thin films of cellulose can provide excellent capability for in situ monitoring of enzyme activity, under controlled conditions of temperature, pH, etc. . The most common substrate used in these efforts has been regenerated cellulose which involves the application of a polar solvent to dissolve cellulose before spin coating on the QCM sensors;[14, 17, 25-28] the cellulose crystallinity is therefore completely disrupted in this case. Evaporation of solvent may bring back some hydrogen bonds between cellulose chains, but the morphology of the native cellulose is altered. The activity information obtained after using regenerated cellulose may therefore reflect only part of the information that could be obtained from native cellulose substrates. Recently, nanofibrillar cellulose (NFC) coated on QCM sensors was used to overcome this issue taking advantage of the fact that NFC manifests the crystallinity and morphology at the nanoscale of the native cellulose.[15] However, finding a substrate that truly mirrors the chemical composition, morphology and other characteristics of the cell wall at the micro and nanoscale continues to be extremely challenging.

Furthermore, the use of empirical models ought to be performed to obtain numerical activity results for enzymes acting on surrogate surfaces such as those indicated above, and to be compared with results from other methods.[15] All in all, changes in film mass have been monitored in the efforts cited above but no attempt was made to monitor the changes in solution properties (such as density or viscosity) as the degradation evolved under different incubation conditions.

It should be noted, however, that in 2000, He et al reported on the use of quartz crystal sensors to measure the changes of viscosity of the incubation CMC solution by cellulase; it also pointed out the anticipation of studying cellulose hydrolysis by cellulase as a new method.[29] Nevertheless, this work did not contribute actual exploration of cellulase activities measurement instead of focusing on the kinetic aspects of CMC hydrolysis. Ash et al used also droplet quartz microbalance to measure the viscosities of industrial oils to explore their viscosity properties.[30] Saluja and Kalonia reported the measurement of fluid viscosity from the perspective of a setup of circuit for quartz microbalance.[31] The above efforts have taken advantage of the fact that changes in liquid properties affect the shift of the resonant frequency, as was modeled by Kanazawa and Gordon using a system with wave propagation in the shear mode.[32, 33] Kanazawa and Gordon's model states that the change of resonance frequency due to changes in liquid properties is proportional to the square root of the product of dynamic viscosity and density, as is indicated by equation 1[32, 33]:

$$\Delta f = -\frac{f_0^{3/2}}{\sqrt{\pi\rho\mu}}\sqrt{\rho_L\eta_L} \qquad (1)$$

Where f is the resonant-frequency shift, f_0 the resonant fundamental frequency of the quartz crystal and μ the shear modulus of the quartz crystal, η_L the dynamic viscosity of the liquid, ρ and ρ_L the densities of the quartz crystal and the liquid, respectively. A similar effect was observed and reported twenty years earlier by Stockbridge[34] when exploring the effect of gas pressure on the quartz-crystal microbalance. Stockbridge formulated an expression similar to that in Eq. 1 but considered the resonance overtones (overtone number n):

$$\Delta f = -\sqrt{\frac{n}{\pi}}\frac{f_0^{3/2}}{\upsilon\rho}\sqrt{\rho_L \eta_L} \qquad (2)$$

Where υ is the wave propagation velocity in quartz (3340 m/s) and the other variables have the same meaning as stated before (Eq. 1). Ward and Buttry have pointed out that the fundamental frequency f_0 is a function of tension and mass of the quartz crystal used[23]; also, the gold electrode coat may bring alterations to f_0. Most relevant to our work, Ward and Buttry reported on the QCM frequency response caused by the interaction between glucose and hexokinase bound on polyacrylamide films.[23]

In the present work we propose an alternate protocol to measure cellulase activity by using the QCM. In this method, QCM frequency change is used to measure the solution viscosity and density changes in the solution used to incubate the given cellulose substrate, after enzymatic hydrolysis. The results are then used to quantify the enzyme activity. In order to validate the proposed method and to compare it with the traditional ones, two cellulase enzymes and three different substrates were used. It is worth noting that the proposed method is not limited to any particular type of substrate, in contrast to most standard protocols for which only a given type of cellulose substrate can be used. For the purpose of illustration this fact we document here the cases of three cellulose sources, namely, microcrystalline cellulose powder (MCC), filter paper (FP), and carboxylmethyl cellulose (CMC). The measured activities for the various cellulase enzymess were then compared to values obtained with the DNS, BCA, and chromatographic methods.

2. Experimental

2.1 Materials and Methods

Microcrystalline cellulose (MCC, Avicel®PH-101) was purchased from Fluka. Carboxylmethyl Cellulose (CMC, Mw of ca 90,000 and D.S. of 0.7) and No.1 Whatman Filter Paper (FP hereafter) were purchased from Sigma. DYADIC EXP Cellulase (DEC) was supplied by DyAdic (Jupiter, FL), and a commercial cellulase mixture in powder form was purchased from MP Biomaterial Inc. (MPC thereafter). The Modified Lowry Assay Kit (to determine one protein content) was purchased from Pierce (Rockford, IL). DNS, biccinchoninic acid and cupric sulfate were from Fisher Scientific. Glacial acetic acid and sodium acetate were used in the preparation of buffer solutions (pH 4.8 and ionic strength of 100mM). QCM quartz sensors coated with gold (QSX303) were purchased from Q-Sense (Q-sense, Baltimore, MA).

An HP_8453E_UV_VIS spectrophotometer was used to determine light absorbance in the DNS and BCA methods. A Dionex Ion Chromatography ICS-3000 and IC-500 were used for sugar analysis. CarboPac PA-1 columns were used with both chromatographic instruments. A Q-300 Quartz Crystal Microbalance with Dissipation, QCM-D (Q-Sense, Sweden) was used with Q-tools software for data processing.

X-ray diffraction (Philips XLF ATPS XRD 1000) was used to determine the crystallinity index of the cellulose substrates. The instrument used an OMNI Instruments Inc. customized Automount with a Cu target with λ= 1.5 Å. The quantification of the crystallinity index was based on the method proposed by Segal et al. [35] Finally, a Cannon-Fenske capillary

viscometer was used to determine the viscosity of glucose solutions while their densities were measured by volumetry using a 500ml volumetric flask at 25°C.

2.2 Activity Test of Cellulase

2.2.1 Protein Assay with Lowry Kit

Based on the work by Lowry et al, [36] the modified Lowry protein assay kit (product no. 23240) with bovine serum album (BSA) was applied as a standard for the assay of protein content. Two samples as well as all standard calibration solutions (with a series of different protein concentrations) were treated with the protein assay and Folin-Ciocalteu reagents. For this purpose the assay kit was used following the recommended procedures and conditions noted by Lowry et al.[36] The absorbance was measured at 750nm with an HP spectrophotometer.[36] Test samples and protein standards were diluted with sodium acetate (pH=4.8 and 100 mM ionic strength).

2.2.2 Enzyme Activity using DNS and BCA Methods

Whatman No.1 filter paper (FP), Avicel®PH-101 microcrystalline cellulose (MCC), and carboxymethyl cellulose (CMC) were used as substrates to test cellulase activities. The procedures for filter paper activity (FPase) and CMC activity (CMCase) were applied following the IUPAC method. Activity assays on MCC followed a similar procedure with 50mg substrate mass in each assay. In the case of the BCA assay, incubation was done with test tubes wrapped in aluminum foils to prevent light interference. In order to get accurate

results, the BCA agent, a mixture of bicinchoninic acid and cupric sulfate was freshly prepared before addition to either the standard calibration solution or hydrolysis products. Due to the extreme high sensitivity of BCA agent to reducing end groups in a mixture, the concentrations of standard solutions were in the μg per liter range and the hydrolysis products were therefore diluted by a factor of 500 to 2000. Incubation conditions and the spectrophotometric protocols followed the procedures reported by Johnston et al.[7] Both DNS and BCA methods were used to determine the amount of reducing sugars. The calculation of enzyme activity followed the IUPAC method.[1]

2.2.3 Enzyme Activity using Ion Chromatography

Two sets of standards were prepared to identify all the sugars that were produced after incubation of the substrates. One set included monosaccharides only (arabinose, xylose, glucose, mannose, galactose and fructose). The other set of calibration solutions contained only glucose and cellobiose. In the case of monosaccharide analysis, pure water was the eluent (1.2 ml/min elution rate) while for samples containing cellobiose the eluent consisted of 50 mM potassium hydroxide aqueous solution (elution rate of 1.0ml/min). In all cases fucose was used as an internal standard.

Compared to the hydrolysis samples prepared for both DNS and BCA assays, the samples for IC were vigorously boiled for at least 30 minutes right after the incubation, and then they were filtered through a 0.45-μm nylon membrane syringe filter. Collected samples were diluted by a factor of 50 in a volumetric flask and the fucose internal standard was added. The amount of glucose and glucose equivalent of other reducing sugars were

measured as the sugars produced by enzymatic hydrolysis. At least two concentrations of cellulases were used, so that release sugars were below and above 2.0 mg which is the reference concentration used to calculate cellulase activity.[1]

2.2.4 Enzyme Activity using QCM-D

2.2.4.1 Standard Curve

Glucose solutions were prepared at five different concentrations in buffers of identical pH and ionic strength and used to measure QCM frequency in triplicate runs. The temperature of the QCM chamber was set to 25 °C for all tests and the sequence used in the measurements was randomized. The test procedure is summarized in Figure 5-1. Note that in the case of the standard calibration curves discussed here the third injection shown in Fig. 5-1 consisted of standard glucose solutions instead of the solutions from hydrolysis generally used (see next section).

2.2.4.2 Substrate Hydrolysis

A modified procedure for hydrolysis of the substrates (MCC, CMC, and FP) was applied (see Figure 5-2). A sample of 150 milligrams of each substrate was incubated with enzyme (instead of the 50 mg used in the other methods, see later sections). The relative amounts of both buffer and enzyme solutions were kept the same as in the other methods on. After the incubation of the mixtures, vigorous boiling for 30 minutes was applied to ensure the enzymes were completely denatured and deactivated. Enzyme blanks for each cellulase concentration were boiled together with their corresponding hydrolysis mixtures. No subsequent chemical treatments were adopted for color development (as in the DNS and

BCA methods). The boiled reaction mixtures were then filtered through a 0.45-µm hydrophilic nylon syringe filter to remove protein and cellulose. The filtrates were introduced directly in the QCM-D chamber for frequency detection and therefore to quantify the enzyme activity using the standard curves obtained in 2.2.4.1. (See also Figure 5-1).

For each enzyme, solutions of four different concentrations were prepared to confirm that the produced amount of reducing sugars was linearly related with the respective enzyme concentration. The chosen concentrations were also in a range which was selected to produce 2 mg of reducing sugars (using 0.5 ml of enzyme solution and 60 minutes incubation time). In other situations, the dilution was different in order to have the correct amount of sugar equivalent (0.5 mg in the case of CMC).

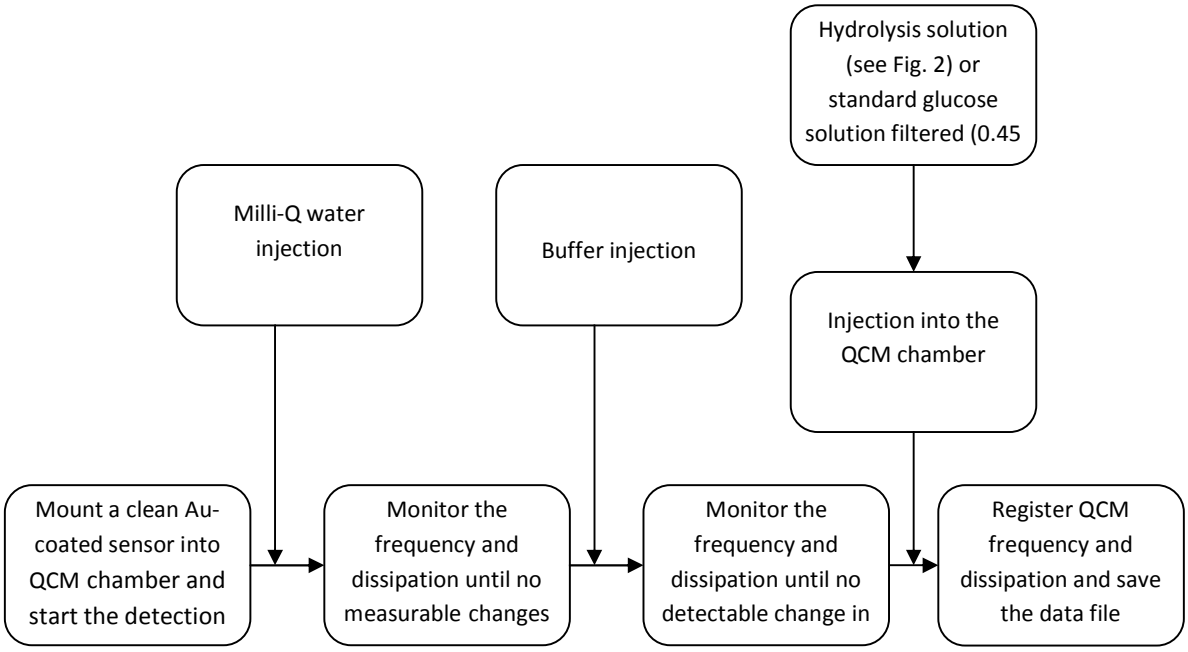

Figure 5-1. QCM protocol to obtain the calibration curves or to test enzymatic activity from measurements with incubation (hydrolysis) solutions

2.2.4.3 Test of Hydrolysis Product with QCM-D

Quartz crystal sensors coated with gold were used for testing both the standard solutions and the hydrolysis products at 25°C. At the beginning, milli-Q water was used in each run to confirm the cleanliness of the sensors and the stability of the base line. After stabilization of the instrument, an injection of buffer solution with a syringe pump followed. All fluids were introduced at very low flow rates to avoid temperature and stress disturbances in the sensor area. After instrument stabilization for at least five minutes, the injection of the hydrolysis products was initiated. Each run was terminated once the frequency variation was less than 0.1 Hz over a five-minute period. Finally, a surfactant solution was injected to clean the tubing and QCM chamber (see Figure 5-1).

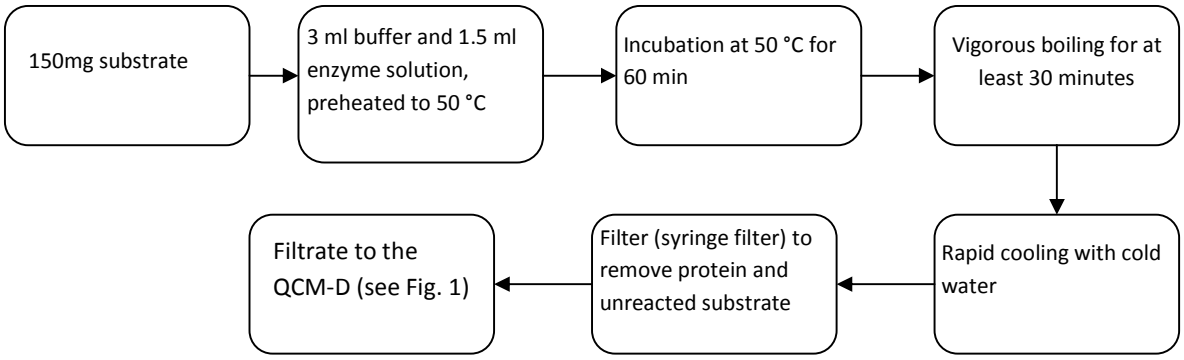

Figure 5-2. General procedure followed to measure enzymatic hydrolysis of the substrate in the QCM method

3. Results and Discussion

3.1 Verification of separation interferences

Ion chromatography was used to verify which sugars were contained in the filtrates

from incubation of Whatman No. 1 filter paper used in the QCM experiments (see also Figs. 5-1 and 5-2).Besides the first negative noise signal, three peaks were detected (see Figure 5-3), which corresponded to fucose (internal standard), glucose and cellobiose. Therefore, only these two sugars were present in the filtrate of the hydrolysis products. It is apparent that the process of boiling the reaction mixtures successfully coagulated the cellulase proteins and did not produce any interference species passing through the syringe filter that otherwise could have been detected. Since the cellulase enzymes used in this research were received as powders, no stabilizing reagents, such as sorbitol were expected as was confirmed by their absence in the IC chromatograms. The same experiments were performed using the substrates CMC and MCC and a second cellulase (MPC). Only peaks for the internal standard fucose and glucose were obtained. Several experiments were also performed for up to 2 hours elution time under the same operation conditions as show in Figure 5-3. No peaks other than those for fucose, glucose and cellobiose were observed (chromatograms not shown).

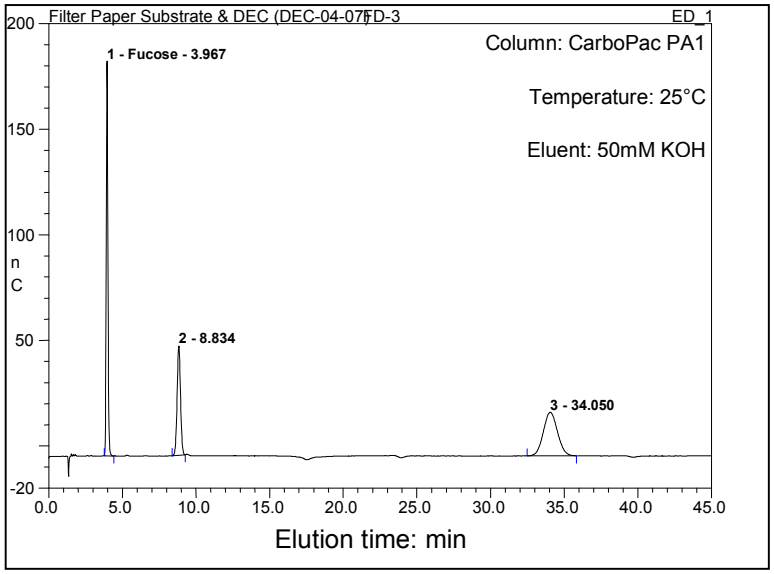

Figure 5-3. Chromatogram of hydrolysis solution after boiling and filtration. Incubation was performed at 50°C for 60min using Whatman No. 1 filter paper substrate and Dyadic Experimental Cellulase (DEC).

3.2 Protein Content and Enzyme Activity from DNS and BCA Methods

As noted before, we used a protein standard consisting of bovine serum album (BSA) to measure the protein content of the enzymes used in this investigation. The average protein content, expressed as μg protein/mg of the crude cellulases from triplicate measurement were 520±28.7 and 210.5±20.5 for DEC and MPC, respectively.

For the purpose of comparison, filter paper (Whatman No. 1), which has a high degree of crystallinity; microcrystalline cellulose (MCC), a cellulose with higher crystallinity and amorphous carboxylmethyl cellulose (CMC), were used as substrates in our experiment. The measured activities are presented in Table 5-1 that includes results from all methods used, as will be discussed below.

3.3 Cellulase Activity via Ion Chromatography

IC results showed that products of hydrolysis from DEC and MPC treatments yield different carbohydrate species. DEC produced both glucose and cellobiose, whereas MPC produced only glucose. This distinctive difference is explained by the fact that MPC contains relatively larger amounts of β-glucosidase which was capable of degrading cellobiose units into glucose as soon as it is produced during incubation. The amount of total carbohydrates produced (glucose and cellobiose) were factored in obtaining cellulase activities, as explained earlier. Cellulase activity was calculated following the IUPAC method.[1]

3.4 Cellulase Activity via QCM-D

3.4.1 QCM Frequency and Glucose Concentration

Figure 5-4 shows a time profile of the QCM third overtone frequency after introduction of different solutions into the resonator chamber (see Figure 5-1). The first flat section of the QCM frequency corresponds to milli-Q water in contact with the sensor. Upon injection of buffer solution, the frequency dropped abruptly to a plateau while dissipation increased. These changes may be explained by the change in bulk density and viscosity of the

buffer solutions relative to the milli-Q water. The overshoot signal is the result of temporal stresses in the resonator upon injection and is disregarded in any calculation. Injection of buffered glucose solution followed (second drop in QCM frequency shown in Fig. 5-4). Once the temperature stabilized at 25 °C, both the frequency and dissipation curves leveled out.

The frequency and dissipation changes were calculated numerically by subtracting the value corresponding to the buffer from that corresponding to the buffered glucose solution. Glucose solutions of five different concentrations, each run in triplicate, were tested following the procedure explained above. The normalized change in QCM frequency (f) and dissipation (D) as a result of changes in glucose concentrations (C_{gl}) were fitted using linear regression, yielding the following expressions: $\Delta f = 0.59C_{gl} + 0.15$ for frequency change with an $R^2 = 0.99$ and $\Delta D = 0.22C_{gl} + 0.03$ for dissipation change with an $R^2 = 0.98$. See Figure 5-5 for the frequency calibration curves.

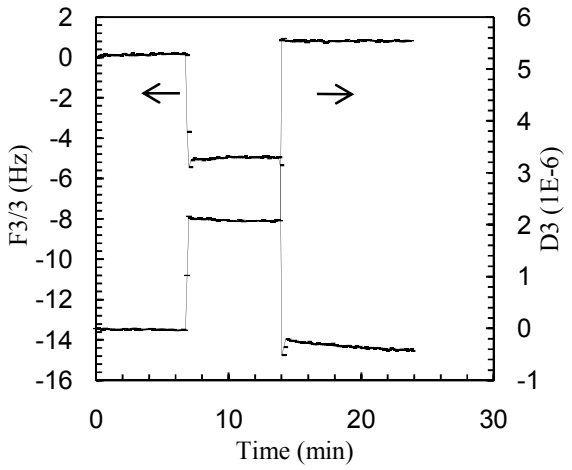

Figure 5-4. Frequency profile following the injection of buffer (7 min time) and glucose solution (14 min). The primary vertical axis on the left indicates the normalized 3rd overtone frequency while the one on the right indicates the corresponding change in dissipation. The first plateau corresponds to water in the QCM chamber, the second one to buffer solution and the third to a 2.5 mg/ml glucose solution in buffer. Tests were performed at 25°C.

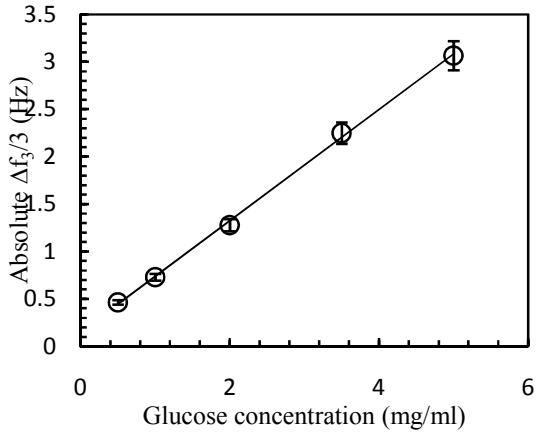

Figure 5-5. Calibration curve of absolute change of normalized frequency vs glucose concentration. Measurements were performed at 25°C using a gold-coated quartz crystal sensor (each condition was run in triplicate).

3.4.2 Cellulase Activity from the QCM-D Method

The protocols followed for standard glucose solutions explained before were applied to the hydrolysis products after incubation of filter paper with DEC enzymes at different concentrations and the QCM changes in frequency corresponding to these experiments were collected. The difference between Δf from filtrates from enzymatic hydrolysis and their corresponding blanks were used as the net Δf contribution from hydrolysis products, Δf_n. The observed changes in QCM frequency for the various hydrolysis solutions are the result of different concentrations of glucose produced and therefore different densities and viscosities of the bulk solution measured by the QCM sensor. It should be noted, however, that any other monomeric or oligomeric degradation product that may be small enough to pass through the syringe filter can also contribute to the measured signal. The contribution from

these units is accounted for by subtracting the frequency change for an enzyme "blank". Figure 5-6a shows a plot of Δf_n against DEC concentration.

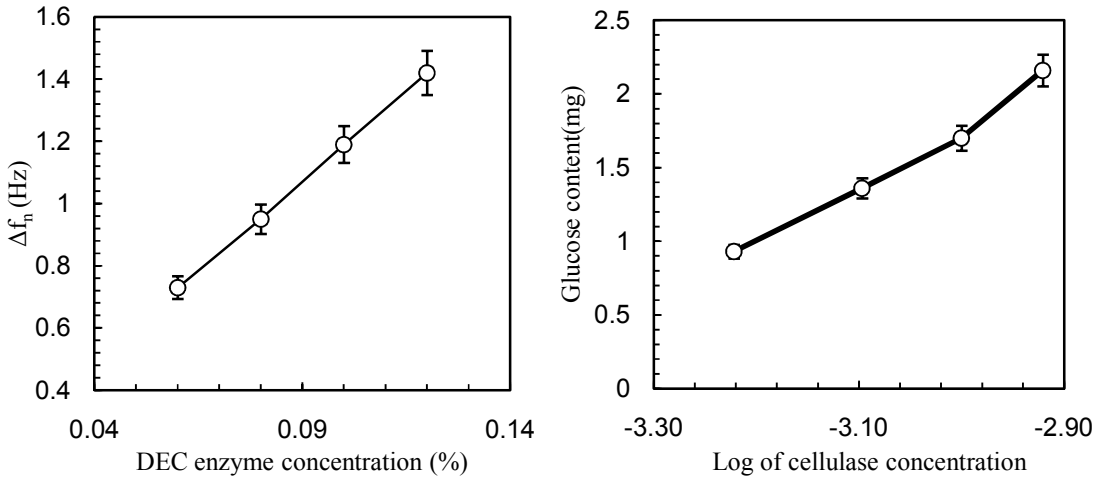

Figure 5-6. a) (Left plot) QCM frequency change as a function of DEC cellulase concentration. **Δf** is the absolute value of adjusted frequency change. Best fitted curve is $\Delta f_n = 1189.4 C_{dec}$. **b.) (Right plot)** Glucose content as a function of the logarithmic value of DEC enzyme on FP substrate. The best fitted equation: glucose content = 3.98 Log(Cdec) + 13.73 with a correlation coefficient of 0.98, where Cdec is the cellulase concentration.

The frequency values in Fig. 5-6a were converted to glucose content using the calibration curve (Fig. 5-5) and then plotted against the logarithmic values of the respective cellulase concentration used during the incubation (see Figure 5-6b for DEC enzyme used to hydrolyze filter paper substrate). The glucose concentration measured in the solution after incubation of the substrate with the enzyme was shown to have a logarithmic relationship with the cellulase concentration [1]. The dilution factor of the enzyme solution that would be

required to produce 2 mg of glucose was obtained from Fig. 5-6b, and from this value the cellulase activity was calculated according to Ghose[1, 2]. The resulting activity values are shown in Table 5-1 that includes DEC activity on filter paper and also for other substrates and for MPC enzyme. (see Table 5-1).

Table 5-1. Cellulase activity (µmol per mg per min) for DEC and MPC determined from the four techniques used, DNS, BCA, IC and QCM-D.

Enzyme & Method / Substrate	Dyadic Experimental Cellulase (DEC)				Commercial Cellulase from MP (MPC)			
	DNS	BCA	IC	QCM-D	DNS	BCA	IC	QCM-D
MCC	286	130	84	173	72	*Failed to eliminate protein contribution*	60	120
FP	417	252	389	329	185		84	171
CMC	5873	2482	1082	6458	1779		837	3244

*Protein interference in the case of MPC cellulase (with BCA method) prevented accurate determination of activity. The units for activity were units per mg of cellulase instead of units per ml, as recommended by Ghose. [1]

3.4.3 Density and Viscosity Effects on QCM Frequency

Table 5-2 includes values for the density and viscosity of glucose solutions; it also shows the expected QCM frequency changes if such solutions were tested with the QCM in response to bulk liquid density and viscosity, as calculated from equation 2 (using a quartz density and wave velocity of 2649 kg/m^3 and 3340m/s, respectively) [34]. The fundamental frequency used in the calculations is 2.5MHz, which equals one half of the first overtone as indicated by the QCM-D used in this research. [37] The two slopes in Fig. 5-7 are approximately the same within experimental errors. The pronounced difference at 5.0 mg/ml

glucose concentration may come from experimental error produced in determining its dynamic viscosity. Compared to the description by Ward and Buttry,[23] the fundamental frequency of a 1 mm thick AT-cut quartz crystal sensor would be 3.3MHz, with shear modulus of 2.947×10^{11} dyne/cm^2 and density of 2.648 g/cm^3. The difference between these fundamental frequencies is probably due to the gold coating on the crystal sensors because gold has different shear modulus and density from crystal. A plot of the experimental values versus the predicted frequency changes for different glucose concentrations gives an excellent linear relationship (R^2= 0.99) and the plot of calculated Δf vs. glucose concentration is also very linear with R^2=0.98 (Fig. 5-7).

Table 5-2. Density, viscosity and predicted Δf based on Stockbridge equation

Glucose Conc.(mg/ml)	Density* (g/ml)	Dynamic Viscosity* (Ns/m^2)	Calculated Δf (10^6 Hz)	Calculated Δf relative to buffer (Hz)$^{\Delta}$	Experimental Δf (Hz)$^{\uparrow}$
0	1.00166	1.132E-03	457.9±0.1	0.0	0
0.5	1.00178	1.133E-03	458.2±0.4	0.3	0.46±0.07
1	1.00202	1.135E-03	458.6±0.5	0.7	0.73±0.05
2	1.00246	1.137E-03	459.1±0.4	1.2	1.29±0.06
3.35	1.00304	1.141E-03	460.1±0.5	2.2	2.25±0.10
5	1.00376	1.142E-03	460.4±0.4	2.5	3.07±0.17
6.67	1.00450	1.146E-03	461.4±0.4	3.5	----

*Both density and dynamic viscosity values are average of three replicates.

$^{\Delta}$The relative confidence intervals for calculated Δf relative to buffers are less than ±5% and not shown in the table (the ±5% relative intervals have counted the accumulative property of errors).

[↑]The experimental Δf indicated in the table with 95% confidence interval. The design of experiments for experimental Δf was generated using a software pack JMP from SAS Institute Inc.

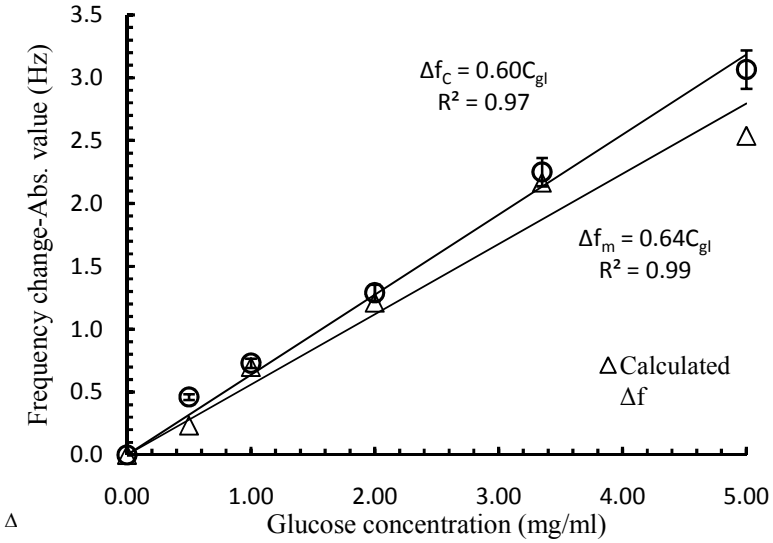

Figure 5-7. Plot of calculated **Δf** using equation (2) and experimental Δf against glucose concentration. Both have very good linear relationship. The fit equation for calculated frequency change is $\Delta f_C = 0.60C_{gl}$ with a correlation coefficient of 0.97 while that for measured frequency change is $\Delta f_m = 0.64C_{gl}$ with a correlation coefficient of 0.99.

3.5 Enzymatic Activity from the Different Methods

Table 5-1 summarizes the enzyme activities for the different substrates. These results demonstrate that the activity of enzymes applied on CMC was by far the highest, followed by filter paper and MCC activities. This observation is probably explained by the difference in substrate crystallinity, as measured by X-ray crystallography: The crystallinity index of Whatman No.1 filter paper was 78% while Avicel PH-101 MCC was 84% (Figure 5-8). The crystallinity index of MCC was similar to that obtained by Fan et al[38], whose crystallinity

index for MCC was 84.5%[36]. Compared to the crystallinity index obtained by Nidetzky et al for filter paper (45%)[39], our experimental result shows a higher value (78%). However, Banka and Mishra showed a wide range of values between 57% to 96% for the same substrate after being ball-milled for different times.[40] Our results for enzyme activities for the different substrates are consistent with the fact that a substrate with higher crystallinity is expected to be hydrolyzed slower.[38, 40] The large variance of cellulase activity on carboxymethyl cellulose is the result of its complete solubility (non crystalline nature) in water. However, there was also research work that pointed out that the crystallinity index has no relationship to hydrolysis rate.[41] It's worthwhile doing research to explore this difference.

Examination of table 5-1 also shows that DNS and QCM-D yielded the highest enzyme activity values, whereas ion chromatography gave the lowest values. The difference in the measured activity is explained by the fact that the DNS method is sensitive to all reducing end groups, including those from substrate, cellulase enzyme and product, while QCM-D detects only contributions from sugars (since it is expected that the enzyme blank can eliminate effects from any small molecules that pass through the syringe filter) Ion chromatography, however, detects the contribution from sugars depending on the species used in the preparation of the standard calibration. Here the results are based on the contribution from glucose and cellobiose only. Finally, the BCA technique is very sensitive to any possible protein contained in the test solutions.

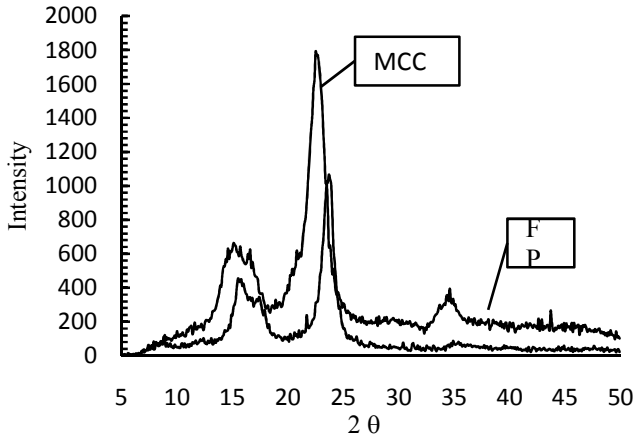

Figure 5-8. X-ray diffractogram for Microcrystalline cellulose (MCC) and Whatman No. 1 filter paper (FP). The calculated MCC crystallinity index was 84 % while that for FP was 78%.

Fig. 5-9 shows the correlation of cellulase activities from QCM-D, DNS and BCA with respect to those obtained from the IC method. It is reasonable to believe the IC results more closely represent the actual, overall ability of a cellulase enzyme to produce reducing sugars, especially based on the definition from Ghose[1]. IC results combine both the contribution of glucose and cellobiose while it eliminates other interferences such as proteins, under the premise that those substances were removed by the nylon filter, as demonstrated in the chromatograms such as that presented in Fig. 5-3. A higher correlation coefficient between QCM-D and IC activities was found compared to that of the DNS method. This can be explained by the fact that the syringe filter used in the QCM-D and IC methods was able to remove most interfering substances that are produced during hydrolysis and the major components detected by both QCM and IC are sugars. Since the DNS method has been the

most widely used one to measure cellulase activity, we compared the IC, QCM and BCA methods against it and noted that QCM-D gave a relatively good correlation (R^2=0.955). However, the correlation between IC and DNS is not as good, which can be explained by the different relative amounts of glucose and cellobiose produced for the different substrates. This was in fact observed in experiments with DEC after analyzing the chromatograms (not shown). A high correlation between BCA and DNS was observed, as expected from the fact that both methods are based on redox reactions, and also because they use the same detection technique (UV-vis spectroscopy).

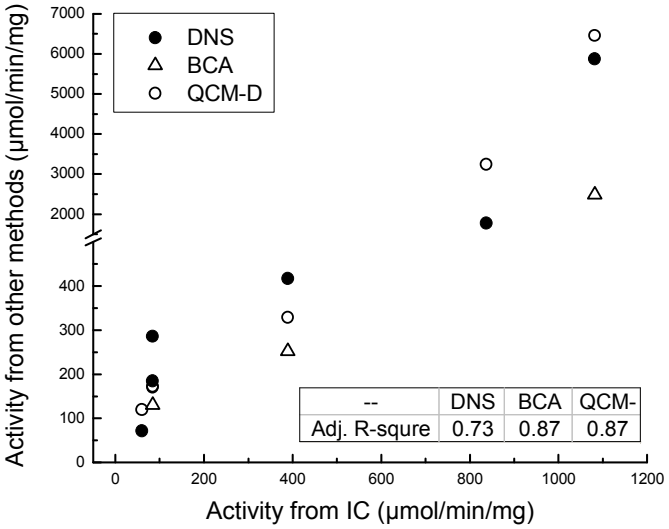

Figure 5-9. Correlation of enzyme activity measured with DNS, BCA and QCM-D methods compared to IC results.

QCM-D is an advanced technique that involves simple operation and does not involve application and disposal of color-developing (redox) chemicals. Compared to the more sophisticated ion chromatography, it involves less advanced skills. The standard calibration

curve shows good reproducibility with a correlation coefficient as high as 0.99 (see 3.4.1). When hydrolyzing complex substrates such as lignocellulosics, the DNS and BCA methods can suffer from interfering substances in color development or measurement. This is in contrast to QCM that has no limitation in terms of the type of substrate used. With the IC technique sample preparation may be involved and possible column contamination could cause interference.

4. Conclusion

A new method to measure enzyme activity is proposed that measures the change in frequency of a gold-coated quartz sensor when exposed to hydrolysis solutions after substrate incubation. The quantification of cellulase activity is based on the Stockbridge relation for different concentrations of degradation products. Validation of the proposed method was accomplished by the use of three different substrates, with different crystallinities. Lower enzyme activities were measured in the case of substrates with high crystallinity. Comparisons were carried out with other methods, including IUPAC's DNS method.

In contrast to methods requiring color development and possible exposure to toxic reagents, the QCM activity protocols do not entail the use of any chemical that would be critical to its reproducibility. Results from the four different techniques tested (QCM, DNS, BCA and IC) showed that the QCM-D method produced results closer to the true sugar production activity of cellulase enzymes. The skill required and the cost and maintenance needed in ion chromatography prevent its use as a routine method to quantify cellulase activity, whereas QCM-D is a promising application in quantification of cellulase activity

with a simple operation principle. Finally, the QCM technique can be applied to situations where substrates other than pure cellulose are to be used. This opens the possibilities for analysis of complex lignocellulosic matrices such as whole biomass substrates.

Acknowledgement

This research was carried out in part with financial aid support from Procter & Gamble.

References

(1) Ghose, T. K. Pure and Applied Chemistry 1987, 59, 257-268.

(2) Coward-Kelly, G.; Aiello-Mazzari, C.; Kim, S.; Granda, C.; Holtzapple, M. Biotechnology and Bioengineering 2003, 82, 745-749.

(3) Miller, G. L. Anal Chem 1959, 31, 426-428.

(4) Gilman, H. Organic Chemistry, Advanced Treatise, 2nd ed.; Wiley: New York, 1943.

(5) Decker, S. R.; Adney, W. S.; Jennings, E.; Vinzant, T. B.; Himmel, M. E. Appl Biochem Biotechnol 2003, 105, 689-703.

(6) Xiao, Z.; Storms, R.; Tsang, A. Biotechnology and bioengineering 2004, 88, 832-837.

(7) Johnston, D. B.; Shoemaker, S. P.; Smith, G. M.; Whitaker, J. R. Journal of Food Biochemistry 1998, 22, 301-319.

(8) Baust, J. G.; Lee, R. E., Jr.; Rojas, R. R.; Hendrix, D. L.; Friday, D.; James, H. J. Chromatogr. 1983, 261, 65-75.

(9) Cataldi, T. R. I.; Campa, C.; Margiotta, G.; Bufo, S. A. Anal. Chem. 1998, 70, 3940-3945.

(10) LaCourse, W. R.; Mead, D. A.; Johnson, D. C. Anal. Chem. 1990, 62, 220-224.

(11) Generoso, M.; De Rosa, M.; De Rosa, R.; De Magistris, L.; Secondulfo, M.; Fiandra, R.; Carratù, R.; Cartenì, M. Journal of Chromatography B 2003, 783, 349-357.

(12) Jeong, C. M., A.M.; Pawlak, J.J.; Heitmann, J. A.; Argyropulous, D. S.; and Rojas, O.J. , Auckland, New Zealand, 16-19 MAY 2005 2006; New Generation Print & Copy,14 Barkly Street, Brunswick East, Victoria, 3057 Australia Telephone: 03 9380 9166.

(13) Buttry, D. A.; Ward, M. D. Chemical Reviews 1992, 92, 1355-1379.

(14) Turon, X.; Spence, K.; Rojas, O. J. AIChE Annual Meeting, Conference Proceedings, San Francisco, CA, United States, Nov. 12-17, 2006 2006, 370f/371-370f/376.

(15) Ahola, S.; Turon, X.; Österberg, M.; Laine, J.; Rojas, O. J. Langmuir 2008, 24, 11592-11599.

(16) Sauerbrey, G. Zeitschrift fuer Physik 1959, 155, 206-222.

(17) Turon, X.; Rojas, O. J.; Deinhammer, R. S. Langmuir 2008, 24, 3880-3887.

(18) Reed, C. E.; Kanazawa, K. K.; Kaufman, J. H. J Appl Phys 1990, 68, 1993-2001.

(19) Crane, R. A.; Fischer, G. J Phys D Appl Phys 1979, 12, 2019-2026.

(20) Lu, C.-S. Journal of Vacuum Science and Technology 1975, 12, 578-583.

(21) Langley, B. a. L., Paul Vacuum technology & coating 2002, 22.

(22) Bruckenstein, S.; Shay, M. Electrochimica Acta 1985, 30, 1295-1300.

(23) Ward, M. D.; Buttry, D. A. Science 1990, 249, 1000-1007.

(24) Wakamatsu, K. Analytical Chemistry 1995, 67, 3336.

(25) Rojas, O. J.; Jeong, C.; Turon, X.; Argyropoulos, D. S. ACS Symp. Ser. 2007, 954, 478-494.

(26) Turon, X.; Spence, K.; Rojas, O. J., San Francisco, CA, United States Nov. 12-17, 2006; American Institute of Chemical Engineers, New York, NY; 370f/371-370f/376.

(27) Josefsson, P.; Henriksson, G.; Wagberg, L. Biomacromolecules 2008, 9, 249-254.

(28) Gunnars, S.; Wågberg, L.; Cohen Stuart, M. A. Cellulose 2003, 10, 185-185.

(29) He, D.; Bao, L.; Long, Y.; Wei, W.; Yao, S. Talanta 2000, 50, 1267-1273.

(30) Ash, D. C.; Joyce, M. J.; Barnes, C.; Booth, C. J.; Jefferies, A. C. Measurement Science and Technology 2003, 1955.

(31) Saluja, A.; Kalonia, D. AAPS PharmSciTech 2004, 5, 68-81.

(32) Kanazawa, K. K.; Gordon, J. G. Anal. Chem. 1985, 57, 1770-1771.

(33) Kanazawa, K. K.; Gordon, J. G. Analytica Chimica Acta 1985, 175, 99-105.

(34) Stockbridge, C. D. Vacuum Microbalance Techniques 1966, 5, 147-178.

(35) Segal, L.; Creely, J. J.; Martin, A. E., Jr.; Conrad, C. M. Textile Research Journal 1959, 29, 786-794.

(36) Lowry, O. H.; Rosebrough, N. J.; Farr, A. L.; Randall, R. J. J Biol Chem 1951, 193, 265-275.

(37) Young, H. D.; Freedman, R. A. University physics: with modern physics; Addison-Wesley: San Francisco, 2000.

(38) Fan, L. T.; Lee, Y.-H.; Beardmore, D. H. Biotechnology and Bioengineering 1980, 22, 177-199.

(39) Nidetzky, B.; Steiner, W.; Hayn, M.; Claeyssens, M. Biochemical Journal 1994, 298, 705-710.

(40) Banka, R. R.; Mishra, S. Enzyme and Microbial Technology 2002, 31, 784-793.

(41) Grethlein, H. E. Nat Biotech 1985, 3, 155-160.

Chapter 6 Comparison of water retention of microcrystalline cellulose (MCC) and hardwood pulp (HW)

Abstract

Much research has been performed on the interaction between cellulase enzyme and model cellulose substrates such as microcrystalline celluloses; less attention has been paid to the interaction between water and these substrates. In this research, three model microcrystalline celluloses (Avicel®PH101, PH102 and PH105) were used to study their interactions with water. Unbeaten and beaten hard wood pulp were used as well for comparison. X-ray diffraction was employed to measure the crystallinites and a laser scattering particle analyzer was used to determine their particle sizes and surface areas. Both the particle sizes and crystallinities were correlated with the water retention values. The results show that surface area is a major factor affecting water retention value at given crystallinity. Lower crystallinities are associated with higher water retention values.

Key words: Hard wood pulp, microcrystalline cellulose, crystallinity, water retention value, surface area, crystallinity

1. Introduction

Enzymatic hydrolysis of cellulose has become a significant research area due to its

potential to provide a sugar feedstock for fermentation into ethanol[1]. The enzymatic decomposition of cellulose to simple sugars is performed by the breakdown of glycosidic bonds within the cellulose chains, with the different isozymes involved making the overall hydrolysis reaction very complex.[2-5] The hydrolysis reaction involves both celluloses and water molecules as substrates; although most research on enzymatic reaction considered water molecules only as a solvent.

Adsorbed water on the surface of cellulose is very different from that in the bulk solution. Within the cellulose matrix, water is subject to a number of different interactions caused by the physiochemical composition of cellulosic materials. Water involved in the interaction with the cellulose surface may therefore have different states and properties due to the different environments and degree of confinement.[1] It is worthwhile knowing the different status and locations of the water involved in the interaction with cellulose substrates. Among the research work reported for the cellulase-cellulose interaction, hydration of a model cellulose (Avicel, Solka Floc and filter paper) was investigated.[6-9] On the other hand, most research work on absorption and hydrolysis of pulps, have paid little attention to the role of water.[10-12] The adsorption behavior, as well as the hydrolysis rate by cellulase enzymes might be altered due to water hydration.

As pointed out by Febly et al,[1] the different structures of the lignocellulosic matrix affect the water state from the molecular to the micro scales. At the molecular scale, the free hydroxyl groups on the cellulose surface readily form hydrogen bonds with water molecules. At a nano-scale along the lignocellulose surface, confined water may form ordered layers or

clusters that reflect the crystalline structure of the cellulose. This water is denoted as primary bound water by Matthews et al.[13] This packed water may be part of the so-called hard-to-remove water, as proposed by Part et al.,[14] which can be quantified as part of the water retention value. [14, 15] Other water molecules interacting with cellulose are comprised of such types as the bound water within confined spaces in the lignocelluloses substrates. This type of water is confined either by capillary forces or by hydrogen bonds to hydroxyl groups of hemi-cellulose and lignin, or by hydrogen bonds to water that is bound to the surface. This bound water is usually classified as secondary bound water.[16] The secondary bound water, as well as the primary bound water comprises the major part of water present when the saturation level is about 25%~30%. In the process of enzymatic hydrolysis of cellulase, the primary bound water matters, as reported by Felby et al.[1] The primary bound water content increases as enzymatic hydrolysis proceeded as indicated by the time-domain NMR relaxation time T2, which corresponds to a spin-spin state. It was also concluded that this response was different for different isozymes; EG's showed an effect while CBH's did not. This difference was speculated to be due to the catalytic activity of these isozymes based on their experimental data.[1] It was also concluded that the application of Celluclast increased the porosity and water bonding capacity of filter paper cell walls, which may have caused a higher amount of bound water. Some researchers have studied the role of water during the enzymatic hydrolysis of cellulose,[17] others have studied the different aspects of enzyme-substrate interactions,[18-20] but paid little attention to the interaction between water and the substrates. Water retention values have long been used to characterize the swelling behavior

and hydratation of cellulosic materials.[16, 21-23] Little research has been performed to give a comprehensive evaluation of how the water retention value changes with crystallinity and surface area. We studied the relation of cellulose hydration to crystallinity and surface area in terms of their water retention value by using three different microcrystalline celluloses (Avicel®PH101, PH102 and PH105) and two bleached hard wood kraft pulps (unbeaten and beaten HW).

2. Experimental

2.1 Materials and methods

Microcrystalline celluloses (Avicel®PH 101, PH102 & PH105) were a gift from of FMC BioPolymer Inc. The nominal particle sizes were 50 μm, 90 μm and 20 μm, respectively. A cellulase powder (*Aspergillus niger*) was purchased from MP Biomedical Inc. Eucalyptus bleached kraft hardwood pulp was purchased from NIST (US Department of Commerce, National Institute of Standards and Technologies, Gaithersburg, MD 20899).

2.2 Pulp Beating and MCC hydration

The pulp was disintegrated using a disintegrator and denoted hereafter as unbeaten pulp (UP). Part of this pulp was beaten for 40 min using a valley beater following TAPPI method T 200 sp-96 Laboratory Beating of Pulp (valley beater method)[24], this was denoted as beaten pulp (BP) and had a freeness of 130 ml. All pulps were washed using sodium acetate buffer (pH 4.8, ionic strength=100 mM) three times and then stored in a cold room at 4°C. All micrystalline celluloses used for this research were soaked in sodium acetate buffer (pH 4.8, ionic strength I=100 mM) and stored in a cold room at °C.

2.3 Crystallinity Index Measurement

X-ray diffraction (Philips XLF ATPS XRD 1000) was used to determine the crystallinity index of the cellulose substrates. The equipment used an OMNI Instruments Inc. customized Automount with a Cu target with λ= 1.5 Å. The crystallinity index is defined as the ratio of crystalline cellulose to the total sample used. The Segal method was used to calculate the crystallinity indexes of the samples,[25] as illustrate in equation (1):

$$CrI = \frac{(I_{002} - I_{am})}{I_{002}} \times 100 \qquad (1)$$

where CrI expresses the relative crystallinity degree in %, I_{002} is the maximum intensity of the 002 lattice diffraction, which represents both crystalline and amorphous materials and I_{am} corresponds to the amorphous peak.

Handsheets of both beaten and unbeaten pulp were prepared according to TAPPI Method T205 to measure their crystallinities.[26] For MCC powders, pellets were employed.

2.4 WRV and Particle size measurement

The WRV of cellulose samples was determined according to Tappi UM 256.[27] Using this method, cellulose pads were first formed by applying vacuum and then centrifuged at 900g for 30 min. The samples were weighed in the wet centrifuged state, oven-dried to constant weight, and then weighed in the dry state. The WRV was calculated using equation (2):

$$WRV = \frac{W_1 - W_2}{W_2} \qquad (2)$$

Where W_1 is the wet weight of the samples (g); W_2 is the dry weight of samples (g). An Eppendorf® Centrifuge (5702) was used for the determination of WRV. The centrifugal

filters were Millipore-Centriplus® centrifugal devices. A Horiba LA 300 Laser scattering particle size analyzer was used to determine particle sizes. The transmittance range was set at 70~90% for the particle analyzer. The light source was a 650-nm laser diode with a power of 5 mW. Tests were performed at 23°C with three replications, with ultrasonic both on and off.

3. Results and Discussion

3.1 Crystallinity of microcrystalline cellulose and hard wood pulp

Figure 6-1 shows the x-ray spectrum for MCC PH 105. Following equation 1, the crystalliity index calculated from this figure was 80.9. A summary of the crystallinity indices is shown in table 6-1. The crystallinities of the three MCCs were basically the same, but higher than the value obtained by Wang et al. for the same substrates[28] Our results for MCC_S were close to the crystallinities reported by Fan et al (CrI for MCC was 84.5),[6] and Lee et al (80.3-82.9 for MCC PH102), depending on different swelling time.[29]

Unbeaten and beaten pulps showed a pronounced difference in their crystallinities with both lower than those of microcrystalline cellulose. The crystallinity of unbeaten pulp was very close to the crystallinity reported by Cheng et al,[30] but higher than the value reported by Park in the case of softwood pulp.[31] These differences may come from different species used. Beating is supposed to fibrillate the fiber, and decrease fiber crystallinity. As opposed to MCC, most of the amorphorous region of the fibers remains intact; this results in lower crystallinities for the pulp.

3.2 Particle sizes and water retention value

The size distribution of MCC follows a typical log normal distribution. Figure 6-2 shows the distribution of Avicel®PH105 with a mean diameter of 28.7μm and standard deviation of 14.4μm. The Horiba LA-300 assumes the particles in the suspension of spherical shapes and either Rayleigh scattering or Fraunhofer diffraction is adopted to calculate the geometry of particles depending on their relative size and the wave length (Horiba LA300 Manual). As shown in Figure 6-3, the measured particle size increases as the transmittance detected by the laser detector increases. For accurate representation of particle size, all tests were performed under the conditions that the transmittance received by the detector was in the range of 70~90%. The instrument also calculated the specific surface area of particles in terms of area to volume ratio.

Table 6-1. The crystallinities of microcrystalline celluloses and unbeaten and beaten hardwood pulps by XRD

Sample	Crystallinity index		
	Replicate 1	Replicate 2	Mean
Unbeaten Pulp	68.4	68.7	68.6
Beaten Pulp	59.7	63.9	61.8
MCC PH101	82.6	---	82.6
MCC PH102	81.2	83.5	82.3
MCC PH105	80.9	84.9	82.9

Handsheets of unbeaten and beaten pulp were prepared for the x-ray diffraction measurement following Tappi Method T 205 and microcrystalline celluloses were pelletized for this measurement.

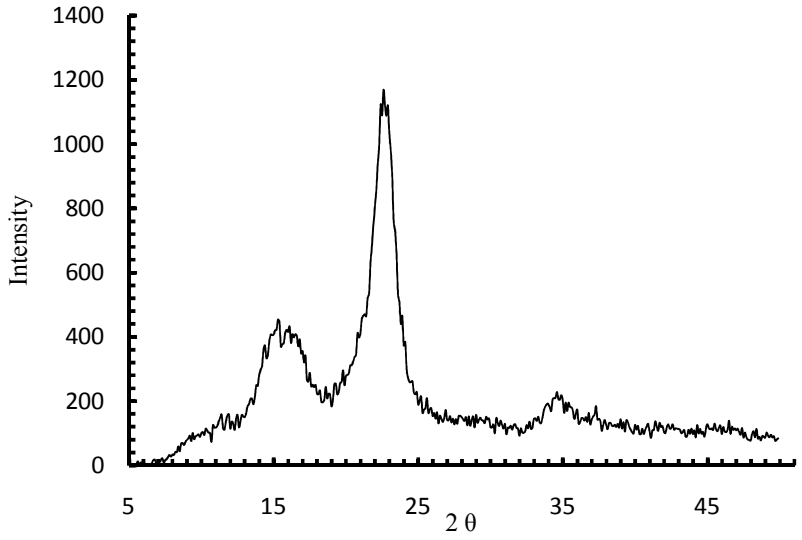

Figure 6-1. XRD of pelletized microcrystalline cellulose (Avicel® MCC PH105) .

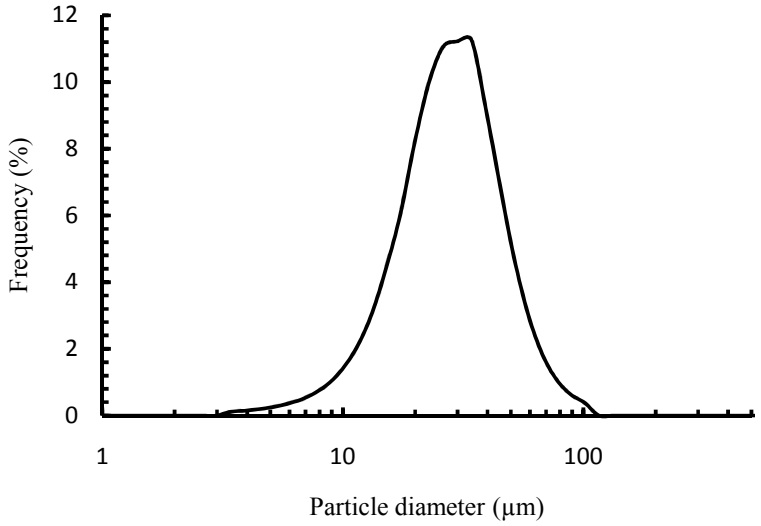

Figure 6-2. Particle diameter distribution of microcrystalline cellulose MCC PH 105. The particle diameter follows a log normal distribution with a mean of μ=28.7μm and standard deviation σ=14.4μm. (Data obtained through Horiba LA 300 software and re-plotted using Excel 2007)

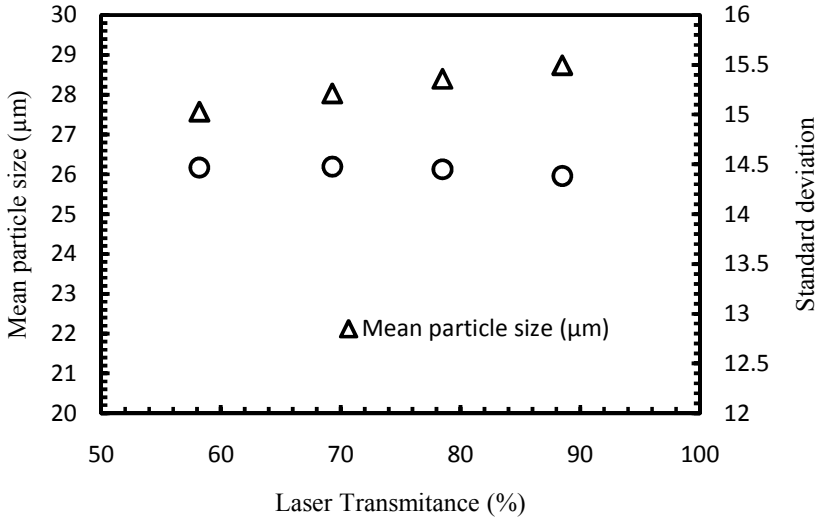

Figure 6-3. The mean particle size and standard deviation of microcrystalline cellulose, Avicel® PH105, as a function of laser transmittance under the test conditions. The test chamber of the Horiba LA300 was first filler with water, then Avicel®PH105 powder was added gradually to achieve the observed later transmittance as shown in the figure.

Tests were performed both in sodium acetate buffer and DI water. No significant differences were observed. Table 6-2 summarizes the particle sizes of all three microcrystalline celluloses and both the unbeaten and beaten hard wood pulp used in this research. The results correspond to the ones obtained in DI water. It is noteworthy that the particle sizes of different species vary depending on whether the MCC granules were added directly into the test chamber or whether a slurry was used. In the latter case, the slurries were made in DI water in advance and were hydrated overnight. No significant differences were observed statistically, except the surface areas for Avicel®PH102 in the form of a slurry and a powder.

Table 6-2 also shows no pronounced difference in the particle sizes of unbeaten and beaten hard wood pulps, although the degree of beating was appreciable as judged by the CSF (560 ml for unbeaten pulp as compared to 127 ml for beaten pulp). This may be interpreted as no significant fiber cutting during the beating process, whereas fibrillation did not affect either the specific surface area or the particle sizes. The possible reasons may come from the buffer since the beating was performed in a buffer with pH 4.8 and ionic strength 100mM. The acid condition and the presence of sodium and carboxylic ions helped the swelling of fibers.

Table 6-2. Particle sizes of microcrystalline cellulose, unbeaten hard wood pulp and beaten hardwood pulp

	PH101	PH102	PH105	Unbeaten HW	Beaten HW
Nominal size(μm)	50	90	30	-----	------
Measured specific surface area (cm^2/cm^3)					
Slurry	1169.0±68.2	1127.0±133.4	3238.4±356.7	1570.4±92.9	1529.3±112.0
Powder	1207.2±65.1	626.5±59.5	2860.6±148.0	-----	------
Measured particle size (μm)					
Slurry	74.2±6.1	123.9±9.7	25.2±2.0	103.5±2.6	101.0±1.7
Powder	73.0±4.7	151.8±13.2	27.4±2.2	-----	-----

Nominal sizes are the sizes found on the label of samples

All results were averages of five replicates for each. The ranges are based on 95% confidence intervals.

Water retention values were measured following Tappi UM-256.[32] Table 6-3 summarizes the water retention values of the three MCCs and pulps. A lot of work has been done to measure water retention values of different pulps. Our water retention values are close to the value obtained by Zhang.[33] In his thesis, a water retention value of 212.6% for never-dried pulp and 166.7% for recycled pulp was reported. The latter case was similar to our system since the pulp was obtained in a dry form from NIST. The WRV for beaten pulp in this work was higher than the one obtained by Greenwood et al[21] (2.675 g/g vs 3.34 g/g in our work), but lower than the value obtained by Park et al[31]. This is reasonable, since the freeness of the pulp in the work of Greenwood et al was 190 ml whereas the WRV value from the work of Park et al was obtained from contributions from fines. For MCCs, the water retention value showed a smaller values compared to Wang et al; their values ranged from 130.5~175.2%.[28] Compared to the WRV obtained by Cheng et al,[30] ranging from 71~230%, the results here are in reasonable agreement. These differences can be partly related to the crystallinity for the different microcrystalline celluloses used. Wang et al used MCCs with a crystallinity index which ranged from 54.56 to 62.42 after a treatment using ultrasonic activation[28], whereas the crystallinity index of the cellulose Cheng et al used was 72.4, where the cellulose was actually Lyocell fiber (provided by Lenzing) passed through a screen of 1 mm in diameter in a Willey mill.[30] In our situation, the microcrystalline celluloses have not been treated and show a high crystallinity index as shown in table 1.

Table 6-3. Water retention values for microcrystalline cellulose and hard wood pulps

	WRV in buffer (g/g)	WRV in water (g/g)
MCC PH101	1.01±0.07	1.29±0.15
MCC PH102	0.96±0.06	1.03±0.13
MCC PH105	1.43±0.13	1.38±0.10
Unbeaten HW pulp	1.73±0.11	
Beaten HW pulp	3.34±0.17	

The water retention values in the table were average of three replicates, ranges show a 95% confidence interval.

Water retention values showed a distinctive trend with the particle size (surface area of MCCs). Figure 6-4 plots WRVs as a function of specific surface areas of MCCs. It is apparent that the surface area plays a significant role in water retention for MCC surfaces since their crystallinities were essentially the same for all three microcrystalline celluloses. A hypothesis would be that all water retained as measured by the water retention value could be bound water; no trapped water may have contributed in our test conditions. Another possibility is that all the bound water is primary water with same number of layers on the surfaces of these microcrystalline celluloses.

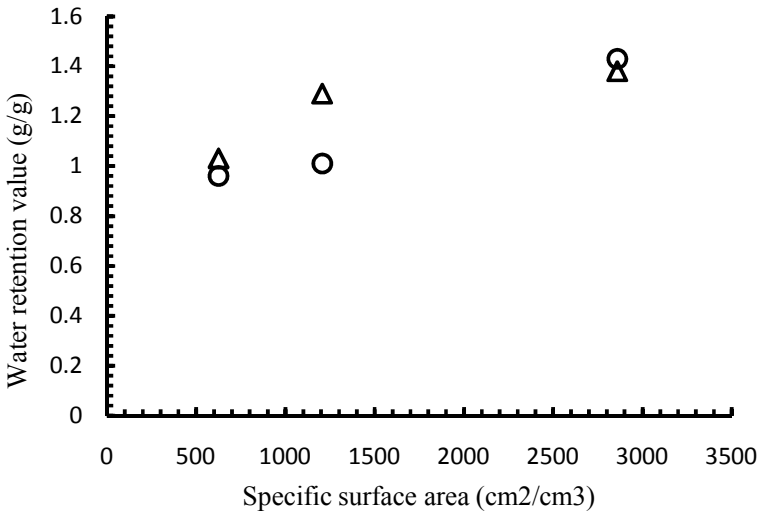

Figure 6-4. Water retention values as a function of specific surface area. (Circle: WRV tested in buffer, triangle: WRV tested in DI water; From left to right, MCC PH102, MCC PH101, MCC PH105)

4. Conclusion

The beating of hardwood pulp did not cut much the fiber in the presence of ions from sodium acetate buffer. Fiber fibrillation during beating caused the decrease of crystallinities of hard wood pulps, which in turn produced a higher water retention value. The difference in the surface area of the three microcrystalline celluloses created the difference in water retention value; the similar crystallinities of these microcrystalline celluloses may suggest the free hydroxyl groups on microcrystalline cellulose are directly related to the surface area.

References

(1) Felby, C.; Thygesen, L.; Kristensen, J.; Jørgensen, H.; Elder, T. *Cellulose* **2008**, *15*, 703-710.

(2) Sinnott, M. L. *Chemical Reviews* **1990**, *90*, 1171-1202.

(3) Ryu, D. D. Y.; Kim, C.; Mandels, M. *Biotechnology and Bioengineering* **1984**, *26*, 488-496.

(4) Wood, T. M.; McCrae, S. I.; Bhat, M. K. *The Biochemical journal* **1989**, *260*, 37-43.

(5) Rabinovich, M. L.; Melnick, M. S.; Bolobova, A. V. *Biochemistry (Moscow)* **2002**, *67*, 850-871.

(6) Fan, L. T.; Lee, Y.-H.; Beardmore, D. H. *Biotechnology and Bioengineering* **1980**, *22*, 177-199.

(7) Turon, X.; Spence, K.; Rojas, O. J., San Francisco, CA, United States Nov. 12-17, 2006; American Institute of Chemical Engineers, New York, NY; 370f/371-370f/376.

(8) Dourado, F.; Mota, M.; Pala, H.; Gama, F. M. *Cellulose* **1999**, *6*, 265-282.

(9) Rehfeldt, F.; Tanaka, M. *Langmuir* **2003**, *19*, 1467-1473.

(10) Suurnäkki, A.; Tenkanen, M.; Siika-aho, M.; Niku-Paavola, M. L.; Viikari, L.; Buchert, J. *Cellulose* **2000**, *7*, 189-209.

(11) Bhardwaj, N. K.; Bajpai, P.; Bajpai, P. K. *J. Biotechnol.* **1996**, *51*, 21-26.

(12) Gerber, P.; Joyce, T.; Heitmann, J.; Siika-Aho, M.; Buchert, J. *Cellulose* **1997**, *4*, 255-268.

(13) Matthews, J. F.; Skopec, C. E.; Mason, P. E.; Zuccato, P.; Torget, R. W.; Sugiyama, J.; Himmel, M. E.; Brady, J. W. *Carbohydrate Research* **2006**, *341*, 138-152.

(14) Park, S.; Venditti, R. A.; Jameel, H.; Pawlak, J. J. *Tappi J.* **2007**, *6*, 10-16.

(15) Park, M. S. *Macromolecules* **2002**, *35*, 8466.

(16) Hartley, I. D.; Kamke, F. A.; Peemoeller, H. *Wood Sci. Technol.* **1992**, *26*, 83-99.

(17) Capitani, D.; Emanuele, M. C.; Segre, A.; Fanelli, C.; Fabbri, A. A.; Attanasio, D.; Focher, B.; Capretti, G. *Nord. Pulp Pap. Res. J.* **1998**, *13*, 95-100.

(18) Kim, D. W.; Yang, J. H.; Jeong, Y. K. *Appl. Microbiol. Biotechnol.* **1988**, *28*, 148-154.

(19) Henrissat, B. *Cellulose* **1994**, *1*, 169-196.

(20) Mattinen, M. L.; Kontteli, M.; Kerovuo, J.; Linder, M.; Annila, A.; Lindeberg, G.; Stahlberg, J.; Drakenberg, T. *Bulletin of Magnetic Resonance* **1995**, *17*, 268-309.

(21) Greenwood, M. S.; Panetta, P. D.; Bond, L. J.; Mccaw, M. W. *Ultrasonics* **2006**, *44*, E1123-E1126.

(22) Khan, F.; Pilpel, N.; Ingham, S. *Powder Technology* **1988**, *54*, 161-164.

(23) Luukkonen, P.; Maloney, T.; Rantanen, J.; Paulapuro, H.; Yliruusi, J. *Pharmaceutical Research* **2001**, *18*, 1562-1569.

(24) TAPPI In *Test Methods T 200 sp-96*; TAPPI: Atlanta, GA, United States, 1998, pp 9.

(25) Segal, L.; Creely, J. J.; Martin, A. E., Jr.; Conrad, C. M. *Textile Research Journal* **1959**, *29*, 786-794.

(26) TAPPI In *TAPPI Test Method T 205 om-88*; United States, 1988, pp 6.

(27) TAPPI In *TAPPI Useful Methods UM 256*; United States, 1991; Vol. 1991, pp 54-56.

(28) Wang, X. L.; Fang, G. Z.; Hu, C. P.; Du, T. C. *Journal of Applied Polymer Science* **2008**, *109*, 2762-2767.

(29) Lee, S. B.; Kim, I. H.; Ryu, D. D.; Taguchi, H. *Biotechnol Bioeng* **1983**, *25*, 33-51.

(30) Cheng, Q.; Wang, S. Q.; Rials, T. G.; Lee, S. H. *Cellulose* **2007**, *14*, 593-602.

(31) Park, S.; Venditti, R. A.; Abrecht, D. G.; Jameel, H.; Pawlak, J. J.; Lee, J. M. *Journal of Applied Polymer Science* **2007**, *103*, 3833-3839.

(32) TAPPI In *TAPPI Useful Test Method UM 256*; United States, 1981, pp 3.

(33) Zhang, M., North Carolina State University, Raleigh, NC, 2003.

Chapter 7 Effects of crystallinity, particle size and surface area on cellulase adsorption

Abstract

Environmentally friendly utilization of lignocellulosic biomass usually involves the hydrolysis of the cellulosic components of these substrates by cellulases. In many cases, the adsorption of cellulase to substrates is believed to be a prerequisite for hydrolysis to occur. In this research, we studied the adsorption isotherms of an *Aspergillus niger* cellulase on several different cellulose substrates, including three microcrystalline celluloses and both unbeaten and beaten hardwood pulps. Adsorptions were performed at 4°C, 25°C and 50°C. Crystallinity indices were measured using X-ray diffraction. Laser scattering and BET nitrogen adsorption were employed to determine the particle sizes and surface areas of these substrates. It was found that greater adsorption occurred at lower temperature for all substrates and that MCC substrates with a smaller particle size had a higher adsorption. Beating was found to increase surface area and adsorption. Our findings supported the belief that crystallinity plays a significant role in cellulase adsorption to cellulosic substrates; particle size and surface area affects cellulase adsorption when crystallinities were the same.

Key words: biomass; cellulose; pulp; cellulase; cellulase adsorption; cellulase desorption; adsorption isotherm

1. Introduction

Hydrolysis by cellulases is an economical and environmentally friendly method to obtain simple sugars, which can then be fermented to produce ethanol from lignocellulosic biomass.[1, 2] Cellulase adsorption is a prerequisite for cellulose hydrolysis. Due to the complexity of the solid substrates and that of cellulase enzyme systems, understanding heterogeneous enzymatic reactions is more challenging compared to homogeneous (enzymatic) reactions.[3]

Previous publications have reviewed mechanisms of cellulose hydrolysis by cellulase enzymes.[4, 5] Cellulase adsorption to cellulose is affected by several factors, including those related to the enzyme systems, the physiochemical properties of the substrates and media through which the enzyme and substrate contact each other. Other factors such as degree of mixing and shear, presence of electric fields and special chemical environment may also have an effect.[6-8] The nature of the heterogeneous reactions makes the study associated interfacial phenomena very complicated. Numerous studies reported on the effect of temperature, pH, ionic strength, surfactants etc. on the interaction between cellulase systems and their cellulose substrates. [9-12] Cellulases from different sources showed some different specific features in their adsorption behaviors but the adsorption isotherm was described by a Langmuir model: [13-16]

$$W_{ads} = \frac{W_{ads,\max} K_p C}{1 + K_p C} \qquad (1)$$

Where W_{ads} is the amount of cellulase or protein adsorbed per unit weight of substrate

(mg/g), $W_{ads,max}$ is the maximum amount of cellulase/protein that can be absorbed (mg/g), C is the free cellulase or protein concentration (mg/ml) in equilibrium and K_p is the adsorption constant (ml/mg).[16]

In the study of substrate effects on cellulose hydrolysis, there is general agreement about how the substrate chemical composition affects the hydrolysis;[17] however, there is no consensus on the effect of physical properties such as particle sizes, surface area, porosity and crystallinity. Several reports state that such properties affect the hydrolysis rate in terms of cellulose accessibility to cellulase enzymes.[18-20] On the other hand, conflicting opinions exists regarding the influence of substrate crystallinity. The general belief seems to be that crystallinity prevent hydrolysis, but some author has downplayed its relevance compared to that of assigned to the particle size, surface area and porosity.[21] A similar situation is observed in the case of cellulase critical adsorption, particle size, surface area or crystallinty? Therefore, this report discusses the effect of such variables on cellulase adsorption.

2. Experimental

2.1 Materials

A commercial cellulase enzyme powder *Aspergillus niger* was purchased from MP Biomedical Inc. (referred to as MPC thereafter). Microcrystalline celluloses (Avicel®PH 101, PH102 and PH105) were received as a gift from of FMC BioPolymer Corporation. Their nominal particle sizes were 50, 90 and 20μm, respectively. Eucalyptus bleached Kraft pulp was purchased from NIST (US Department of Commerce, National Institute of

Standards and Technologies, Gaithersburg, MD 20899). Some additional pulp was disintegrated using a disintegrator and designated as unbeaten pulp (UP hereafter). Another batch of cellulose pulp was beaten using a valley beater to (TAPPI method T 200 sp-96 Laboratory beating of pulp)[22] to 130 ml CSF freeness –designated thereafter as beaten pulp (BP) as compared to unbeaten pulp with 560 ml freeness. All pulps were washed using sodium acetate buffer (pH 4.8 and ionic strength of 100mM) three times and then stored in a cold room at 4°C.

2.2 Crystallinity measurement

X-ray diffraction was employed to determine the crystallinity indices of the cellulose substrates. The instrument used was a Philips XLF ATPS XRD 1000 with an OMNI Instruments Inc. customized automount and a Cu target with λ= 1.54 Å. The calculation of crystallinity indices was based on the method proposed by Segal et al. [23] according to equation (2):

$$CrI = \frac{I_{002} - I_{am}}{I_{002}} \times 100 \qquad (2)$$

where CrI is the relative crystallinity-index (%), I_{002} is the maximum intensity of the 002 lattice diffraction and I_{am} is the intensity of diffraction in the same units at $2\theta = 18°$. Handsheets of both beaten and unbeaten pulp were prepared by following TAPPI method T 272 sp-97 (Forming handsheets for reflectance testing of pulp−sheet machine procedure) for crystallinity measurement.[24] For MCC powders, pellets were employed.

2.3 Particle size and surface area measurement

Two different instruments were used to measure the particle sizes and surface areas of MCCs and pulps. These included a COULTER^{TM} SA3100^{TM} Surface Area and Pore Size Analyzer (Coulter Corporation, Miami, Florida 33196) and a Horiba Laser Scattering Particle Size Distribution Analyzer LA-300.

In the COULTER^{TM} SA3100^{TM} we used nitrogen as the adsorbate. An isotherm was constructed from the quantity of condensed nitrogen and the resultant sample pressure. The isotherm data was used to calculate the sample specific surface area according to liberalized BET (Brunauer, Emmett and Teller) model (3):

$$\frac{P_S}{V_A(P_0 - P_S)} = \frac{1}{V_M C} + \left[\frac{C-1}{V_M C}\right] \times \frac{P_S}{P_0} \qquad (3)$$

where P_s = sample pressure, P_0 = saturation pressure, V_A = volume of nitrogen adsorbed, V_M = volume of monolayer nitrogen on sample surface, C = constant related to the enthalpy of adsorption.

A plot of $\frac{P_S}{V_A(P_0 - P_S)}$ against $\frac{P_S}{P_0}$ gives a straight line having a slope of $\frac{C-1}{V_M C}$ and intercept $\frac{1}{V_M C}$, from which V_M can be obtained. The BET surface area can be obtained following equation (4):

$$S_{BET} = \frac{V_M \times N_A \times A_M}{M_V} \qquad (4)$$

where S_{BET} is the BET surface in m^2/g, N_A is Avogadros number, A_M is the cross sectional

area occupied by each nitrogen molecule, and M_V is the standard P and T molar volume (22.4 l/mol). The cross-sectional area of nitrogen is assumed to be 0.162 nm^2 (COULTER^{TM} SA3100^{TM} Series Surface Area and Pore Size Analyzer Product Manual). Samples were washed using milli-Q water and freeze dried using a Labconco freeze dry/shell freeze system before measurement.

The particle size distribution was quantified with a Horiba LA-300 Laser Scattering Particle Size Distribution Analyzer measures the particle size distribution by angular light scattering techniques. When light encounters a spherical particle of radius r, three types of light will be emitted, as shown in Fig. 7-1. The LA-300 we used uses a 600 nm incident light. The Mie scattering theory can be used to precisely determine the particle geometry, but it is difficult to use.[25] In practice, a simple approximation is generally used. When the particle size is considerably larger than the wavelength λ of the incident ray, the Fraunhofer diffraction is involved, which is illustrated in Fig. 7-2. In this approximation, the scattered light intensity of a particle can be expressed by equation (5):

$$I = I_0 \left(\frac{2J_1(x)}{x} \right)^2 \qquad (5)$$

where I is the scattered light intensity, I_0 is the intensity at the center of the diffraction pattern shown in Fig. 7-2. J_1 is the first order spherical primary Bessel function. By applying the x obtained from equation (5), the particle radius can be calculated using equation (6):

$$r = \frac{x\lambda f}{2\pi s} \qquad (6)$$

where r is the radius of particle, λ is the wavelength of incident light, f is the focal length of the lens and s is the radial distance as measured from the optical axis. A more detailed description can be found in Absorption and Scattering of Light by Small Particles by Bohren and Huffman.[26] In this research, sample slurries of MCCs and pulps were prepared in sodium acetate buffer and then placed in the test chambers to determine the size distribution, mean particle size and specific surface area using the principle of Fraunhofer diffraction.

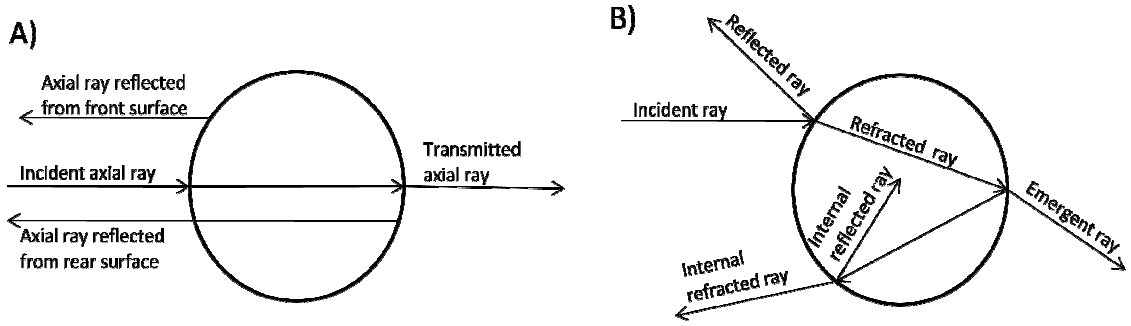

Figure 7-1. Schematic presentation of light scattering by a spherical particle. A represents a spherical geometry showing an axial ray while B represents a spherical geometry showing scattered rays in a non-axial optical path.

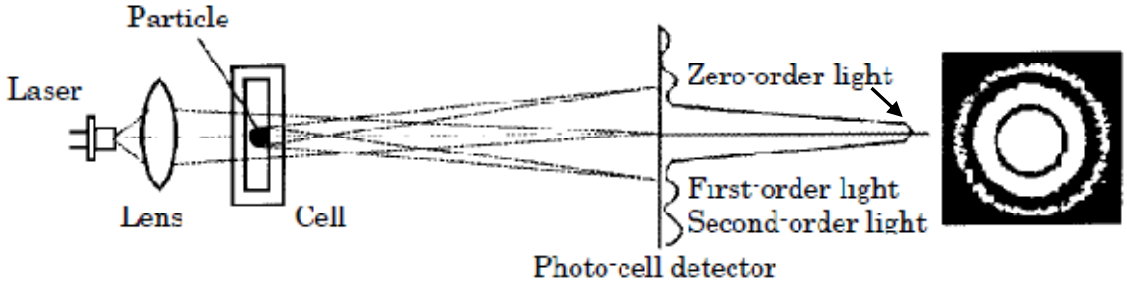

Figure 7-2. Fraunhoefer diffraction

2.4 Adsorption/desorption measurement

A Beckman Model TJ-6 centrifuge was used to separate the solid and liquid phases of enzymatic reaction mixtures. A Lambda XLS spectrophotometer was then used to determine protein concentration in the liquid phase by measure the absorbance at 280 nm wavelength.

Adsorption was determined by using the depletion method, in which the original cellulase protein was determined using the absorbance method at 280 nm.[27] Enzymatic reaction was performed at a 5% substrate consistency at different temperatures (4, 25 & 50 °C) using a Labline Incubator-Shaker. Adsorption experiments at 4°C were performed in a cold room. An incubation time of 60 minutes for the system to reach equilibrium was determined from preliminary experiments and therefore. This time was used in all experiments.

After the adsorption procedure, the separated solid substrates were directly washed using either buffer or caustic water (pH 10, 0.1 mM/L) for 10 min using the same condition of temperature used during the adsorption experiments. Centrifugal separation for 20 minutes at 1400 rpm was used to remove solid phase. The supernatants were collected for protein assay. Figure 7-3 illustrates the procedure employed in our experiments.

3. Results and discussion

3.1 Crystallinity index of microcrystalline cellulose and HW pulps

Figure 7-4 shows the X-ray spectrum for the beaten HW pulp which is in agreements with previous reports.[28, 29] Table 7-1 summarizes the cyrstallinity indexes (CrI, calculated from Eq. 1) for samples used in this research. The crystalline index of AVICEL®PH102 was higher than the ones the reported values by Ardizzone et al and Nakai et al,[29, 30] (CrI of 65%

and 63% respectively; but closer to that reported independently by Plonka and Sottys et al, i.e., 75%.[31, 32] However, these differences in CrI for this substrate may be simply explained by the different experimental approaches used. Our results for the MCCs were in agreement with the crystallinity obtained by Fan et al. and Lee et al, of 84.5%[3] and 80.3~82.9%,[33] respectively. Unbeaten and beaten pulps showed significantly lower crystallinities than microcrystalline celluloses. The crystallinity of unbeaten pulp was very close to the crystalliinity by Cheng et al,[34] and higher than the value by Park for softwood pulps.[35] Luukkonen et al. reported higher crystallinity indexes for pulps, all of which were higher than 80%.[36] The spreading in CrI cited in these reports obviously related to the fact that different wood pulp types were used. In comparing the CrI for MCC and the pulp samples it should be noted that beating process induces fibrillation, which decreases the crystallinity of the fiber. Meanwhile, most of the amorphorous regions of fibers remain intact, which gives lower crystallinities to the pulp.

Figure 7-5 shows the crystallinities of all three microcrystalline celluloses and unbeaten and beaten pulps. A microscopic examination of the samples showed that there was no fibrillation of cellulose fibrils in MCCs (only pictures for Avicel®PH101 and Avicel®PH105 are shown), whereas there were an appreciable number of cellulose fibrils in the sample consisting of beaten HW fibers (see Figure 7-6). The same figure showed appreciable crystalline structures and no fibrillation for MCCs whereas the beaten HW eucalyptus pulp showed no crystalline regions but did show fibrillation. These observations support the findings that that microcrystalline cellulose has a higher ratio of crystallinity indexes than

pulps do. Beating decreases the crystallinity index because the crystalline regions are mechanically destroyed or decreased in size. This has been previously reported by Fan et al.,[3] who showed the effect of ball milling on the crystallinity index of the samples. Another factor causing higher crystallinity indexes for MCC is the extensive hydrolysis of amorphous region during the manufacturing of the MCC.

The crystallinity of the cellulose substrate is believed to be an important factor that affects the rate of hydrolysis.[3, 37, 38] However, less work has been reported on the effect of crystallinity on the adsorption and binding of enzymes. This issue is to be discussed in later sections of this report.

Table 7-1. Crystallinity indexes of microcrystalline cellulose and hard wood pulps.

Sample species	Crystallinity index ($CrI = \frac{I_{002} - I_{am}}{I_{002}} \times 100$)		
	Sample 1	Sample 2	Mean
Unbeaten Pulp	68.4	68.7	68.6
Beaten Pulp	59.7	63.9	61.8
AVICEL® PH101	82.6		82.6
AVICEL® PH102	81.2	83.5	82.3
AVICEL® PH105	80.9	84.9	82.9

I_{002} is the maximum intensity of the 002 lattice diffraction and I_{am} is the intensity of diffraction in the same units at $2\theta = 18°$ as stated in the experimental section.

3.2 Surface area of microcrystalline cellulose and HW pulps

Surface areas of the microcrystalline celluloses and HW pulps were measured by using two techniques and are summarized in table 7-2. The measured particle sizes of AVICEL®PH101 and AVICEL® PH102 by Horiba LA-300 were greater than their nominal sizes whereas(as reported by the manufacturer) that of Avicel®PH105 was smaller than its nominal value. The calculated specific surface was based on an assumption that all the particles are spherical and assuming a cellulose density of 1.5 g/cc. No attempt was made to use this approximation in the case of HW fibers, although a shape factor may be defined and thereby to approximate these values for fibers.[39] The Horiba LA-300 yields a specific surface area in cm^2/cm^3. The measured surface areas of Avicel®PH101 and AVICEL®PH102 were in agreement with the calculated values from the nominal sizes while no such agreement was observed in the case of AVICEL®PH105. These differences may be due to the internal scattering of laser light within the cellulose particles. The larger particles of Avicel®PH101 and Avicel®PH102 produce larger internal scattering due to more or larger pores compared to the case of AVICEL® PH105; however, further verification may be needed for this statement. Little literature has been found to measure MCC particle sizes using laser scattering techniques, although there are some data reported for the measurement of the size distributions using different techniques.[40-42]

Table 7-2. Particle sizes and surface areas measured for microcrystalline celluloses and unbeaten and beaten hardwood pulps

	Particle size (μm)				
	PH101	PH102	PH105	Unbeaten HW	Beaten HW
Nominal size	50	90	30	-----	------
LA-300	74.2±6.1	123.9±9.7	25.2±2.0	103.5±2.6	101.0±1.7
	Specific surface area (m^2/g)				
Calculated from nominal size	0.078	0.042	0.13	-----	------
LA-300	0.078±0.005	0.042±0.004	0.216±0.024	0.105±0.006	0.102±0.007
BET	1.428	1.286	1.707	1.164	1.239

All experimental results in the above table are the average of three replicates; the ranges are based on a 95% confidence interval using a t-distribution critical value with 3 degree of freedom.

The BET surface area obtained for AVICEL® PH101 is higher than those reported by Badawy et al.[43] and Luukkonen et al,[36] whose values were 1.09 m^2/g and 1.14 m^2/g respectively; Gustafsson et al reported a 1.36 m^2/g specific surface area for Avicel®PH101 using krypton (Kr) as adsorbate. The specific surface areas of unbeaten and beaten pulps are within the range found in the literature.[44] However, the beating in this work did not increase the specific surface area to a large extent even though we measured a large change in the freeness value. The literature shows reports in which surface areas were greatly increased by refining.[45] The existence of the sodium acetate buffer in this work may have reduced the change of surface areas during refining.

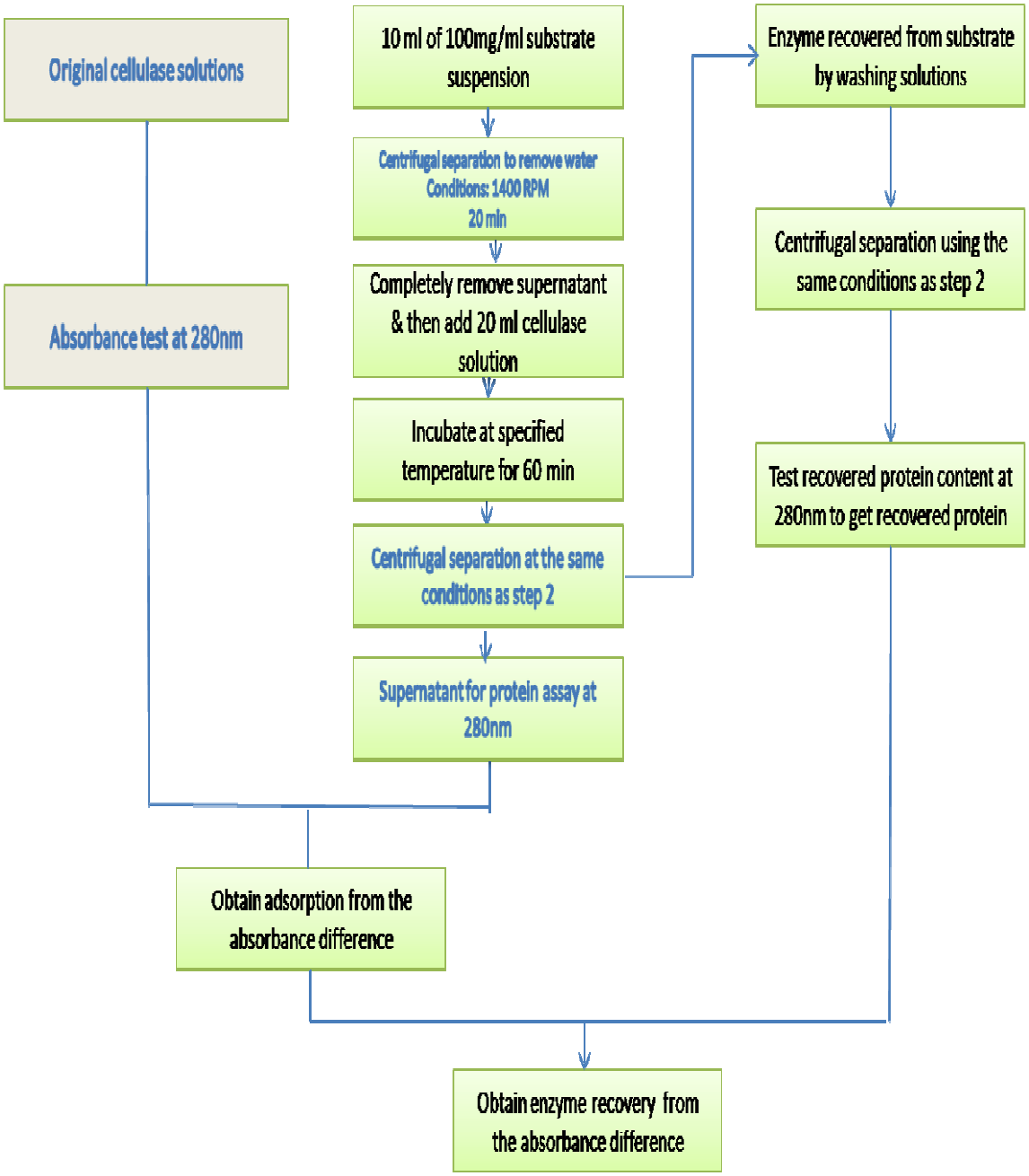

Figure 7-3. Schematic description of procedure used to determine protein adsorption in cellulase solutions

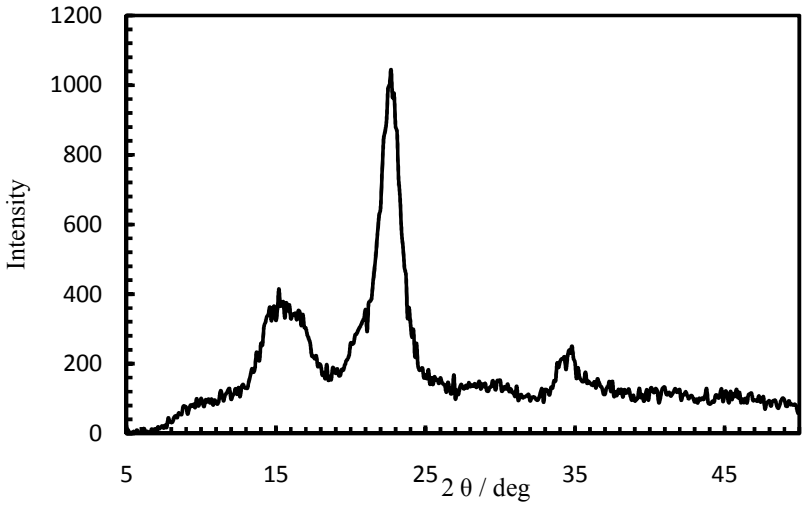

Figure 7-4. X-ray diffraction spectrum for beaten hard wood pulp. The crystallinity index for this pulp is 59.7% (see table 1).

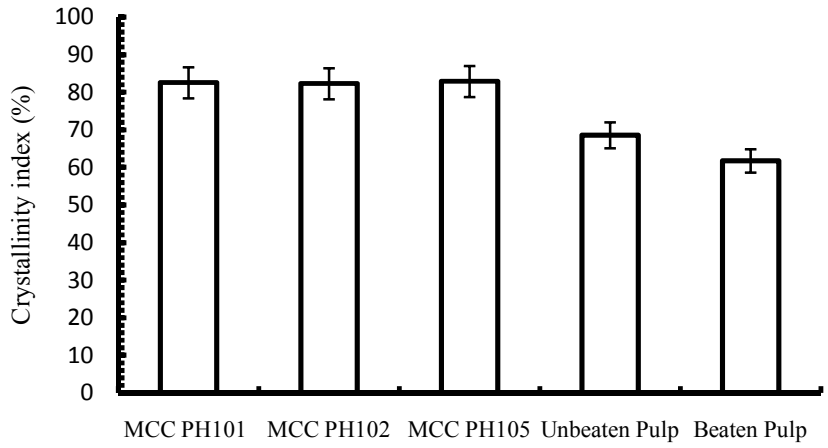

Figure 7-5. Comparison of crystallinities of cellulose samples used in this research. The different types of microcrystalline cellulose area in the range of 82.3-82.9 and do not show significant differences in their crystallinity indexes. Pulps generally have lower crystallinities. Beating decreased the crystallinity of hardwood pulp from 68.6 to 61.8.

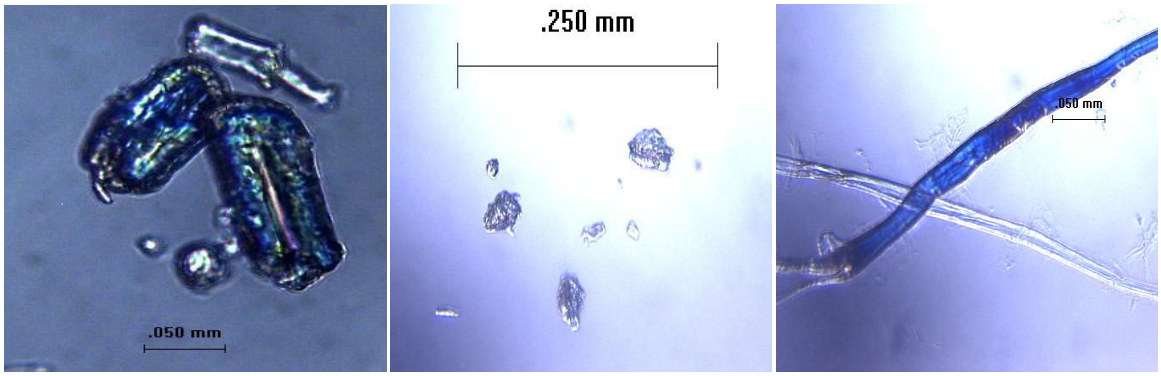

Figure 7-6. Microscopic picture of MCCs and beaten HW pulp. **Left,** AVICEL® PH101; **Center,** AVICEL® PH105; **Right,** beaten HW Eucalyptus pulp. No fibrillation of cellulose fibril is observed in MCC microscopy; instead, pronounced crystalline structure can be observed, which implies a higher crystallinity index for MCCs than for pulp.

3.3 Adsorption isotherms

A cellulase adsorption curve on Avicel®PH101 is shown in Fig. 7-7. AVICEL®PH101 was incubated with a 0.75 mg/ml cellulase solution at 25°C, for various incubation time to indentify the time needed for adsorption equilibrium. In the depletion method, the difference between initial concentration (at time zero) and equilibrium concentration at any time gives the amount of cellulase absorbed on the substrate. Figure 7-7 shows that the equilibrium concentration did not change significantly after 2 min of incubation. All equilibrium cellulase concentrations were fundamentally the same from 2 min to 60 min, with about 87% of the original cellulase protein staying in the solutions. This indicates a very fast dynamics in adsorption. The time needed for equilibrium is shorter than reported by others who used the quartz crystal microbalance technique,[46, 47] where the equilibrium time stated to be about 5

min by using the quartz crystal microbalance technique. Jackson reported a 5 to 30 min time for equilibrium in the case of different isozymes.[48] It is worth noting that the difference of our results from those of Jeong et al may be caused by the different morphology and states of substrates used whereas the difference from Jackson's work may be due to the lack of synergism in his system since only individual isozymes were used in his systems. The different solvency and enzyme types may also produce these differences. It is also worth noting that the cellulase adsorption and cellulose degradation are supposed to occur at the same time during this period, this would complicated this discussion. Figure 7-7 also shows that about 13% of the original cellulase was adsorbed onto the Avicel®PH101 after reaching equilibrium. The other substrates, Avicel®PH102, Avicel®PH105 and unbeaten and beaten HW pulps showed similar adsorption equilibrium time (Figures not shown). To ensure fully equilibrated systems, a 60 min incubation time was chosen in the experiments to be presented nexted. This was also the time interval used by Fan et al.[3] Ghose has reported a 4% degradation of substrate in a one-hour incubation at 50°C.[49]

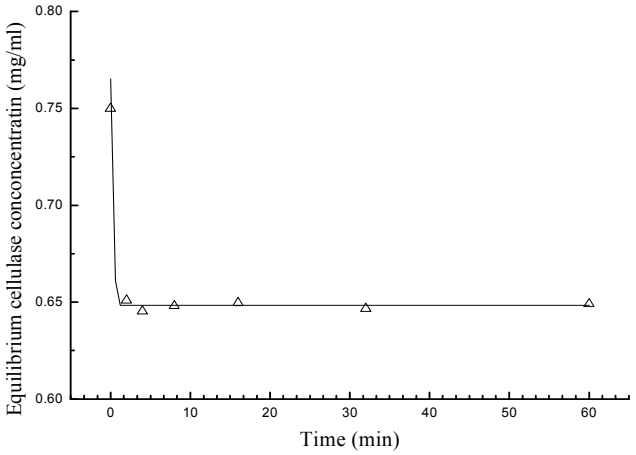

Figure 7-7. Adsorption kinetics of cellulase on Avicel® PH101 at 25°C to find the time needed to reach adsorption equilibrium. The cellulase employed was MPC at 0.75 mg/ml concentration. Substrate consistency was 5% in a solution having pH 4.8 and ionic strength of 100 mM. All incubations were conducted in the Labline Incubator-Shaker at 180 rpm.

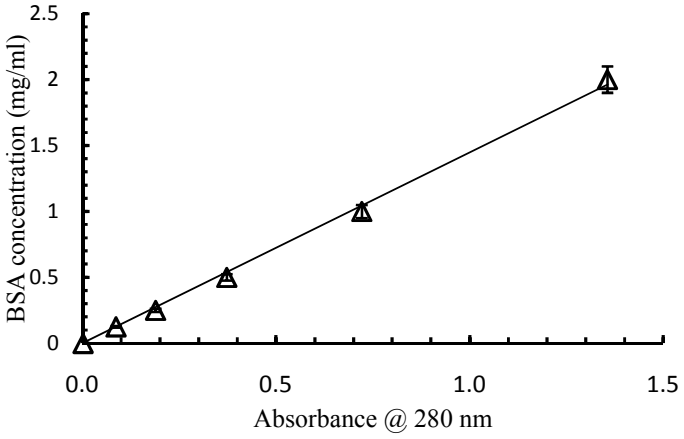

Figure 7-8. Calibration curve of protein standards using bovine serum albumin. UV absorbance was measured at room temperature. The fitted equation is Concentration = 1.45*Absorbance with a correlation coefficient of 0.998.

A standard calibration curve was made using bovine serum albumin (BSA) for the determination of protein concentrations in solutions. Figure 7-8 is the calibration curve obtained at a wavelength of 280 nm using Lambda XLS UV-vis. Both equilibrium and original concentrations were obtained using the calibration curve in Fig. 7-8; appropriate dilutions were performed if the tested absorbance of any solutions were out of the working range.

Figure 7-9 shows adsorption isotherms for MP cellulase on Avicel®PH102 at 4, 25 and 50°C. As can be seen in this figure**,** higher incubation temperatures produced lower cellulase adsorption, which is typical in Langmuir adsorption. No appreciable adsorption was observed at 50°C. These results are in agreement with the results obtained by others.[48, 50, 51] The other substrates investigated showed similar temperature effects (date not shown).

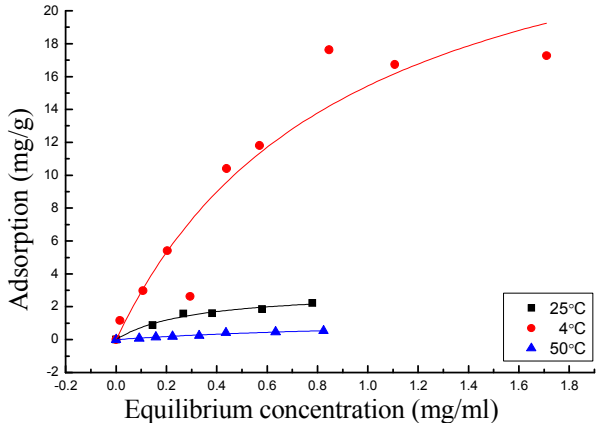

Figure 7-9. Adsorption isotherms for MCC PH102 at 4°C, 25°C and 50°C. The maximum adsorption $W_{ads,max}$ and adsorption constant K_p at 4°C are 29.56 mg/g-substrate and 2.32 ml/mg respectively. The constants at 25°C are shown in table 3. No appreciable adsorption occurred at 50°C.

The different adsorption levels at different temperatures can be explained by looking into the activation energy. Higher temperature favors the high energy state, which therefore creates a low adsorption ratio. Cellulase adsorption has been demonstrated to be an exothermic process, in which high temperature favors desorption. In terms of molecular motion, the cellulase proteins tend to cluster on the surface of substrate at lower temperatures, thereby forming an adsorption complex with the substrates. This produces higher adsorption at different cellulase concentrations until the binding sites are occupied. At higher temperature, the cellulase molecules become active and start to catalyze the hydrolysis of substrates. Another factor is that the release of simple sugars may reduce the adsorbed amount due to the reduced binding sites as hydrolysis continues. When the temperature reaches the optimum condition for cellulase activity, the adsorption would probably be low due to the molecular motion of cellulase molecules and the incessant rapid release of reducing sugars; this may explain why we did not observe appreciable cellulase adsorption at 50°C.

Isotherms for cellulase adsorption on microcrystalline celluloses and unbeaten and beaten HW pulps at 25°C are presented in figure 10. Langmuir isotherms were fitted using equation (1). Table 7-4 shows the maximum amount of adsorption, $W_{ads,max}$ (mg/g), the adsorption constant, K_p (ml/mg), and correlation coefficients for Langmuir fittings. The fitted correlation coefficients show a good Langmuir type adsorption for every substrate used except for the one for unbeaten HW pulp. In the case of microcrystalline celluloses, the amount of adsorbed cellulase increased as the surface area of the substrate increased.

Avicel®PH105 had the highest adsorption at the smallest particle size and largest BET specific surface area. Both the unbeaten and beaten HW pulps showed much higher adsorption than MCCs, which can be explained by a higher content of amorphous region in the pulps. The maximum adsorption $W_{ads,max}$ for all the substrates followed this trend. The maximum adsorption and adsorption constants change in opposite directions, which is in agreement with other investigations.[50-52] The maximum adsorptions were smaller and the equilibrium constants were greater than the values obtained by Peitersen et al. for Avicel®PH102, whose adsorption constants K_p and maximum adsorption $W_{ads,max}$ ranged from 0.53 to 1.67 ml/mg and 0.029 to 0.082 mg protein per mg cellulose at the temperature range of 20°C to 50°C, and Kim et al. for Avicel PH101, who investigated the adsorption of CMCase and Avicelase and three mixtures of these isozymes in different proportions at five temperatures (see table 3 from the work of Kim et al. [51, 53]). A cellulase from *Trichoderma viride* was used in both of these studies as opposed to the cellulase from *Aspergillus niger* used in this research. The difference between this work and these previous results may partially be caused by the different methods used. Peitersen et al.[51] used the Folin procedure to determine protein adsorption while Kim et al.[53] used the Lowry method to determine the enzyme (protein) amount. No previous research has been found which studied adsorption on Avicel®PH105. A Langmuir fitting of Jackson's data[48] on dried hardwood pulp gave maximum adsorptions at 4°C for CBH I and EG II of 16.07 mg/g and 24.02 mg/g, while the maximum adsorptions at 50°C was 10.13 mg/g and 17.18 mg/ml. The adsorption constants obtained are 53.91 ml/mg and 8.67 ml/mg for CBHI and EGII at 4°C and those at 50°C are

21.61 ml/mg and 9.54 ml/mg. The adsorption constants from his work are higher than those in this report. It can also be speculated that the actual adsorption for isozyme mixtures in his work would be higher than results obtained in this report. These differences may have come from the different types of cellulase enzymes used, since cellulase from *Trichoderma reesei* was used in Jackson's work.

Table 7-3. Langmuir constants at various temperature in the work of Kim et al.[53]

Temp. (°C)	CMCase		Avicelase		CMCase and Avicelase mixture					
					r=0.43		r=1		r=2.33	
	A_{max}[b]	K_{ad}[c] × 10^3	A_{max}[b]	K_{ad}[c] × 10^3	A_{max}[b]	K_{ad}[c] × 10^3	A_{max}[b]	K_{ad}[c] × 10^3	A_{max}[b]	K_{ad}[c] × 10^3
25	56.8	41.2	62.9	57.2	57.8	52.3	63.8	49.7	60.9	50.1
30	47.5	52.2	52.2	64.3	45.3	60.6	54.1	52.0	51.5	55.0
35	30.3	68.3	41.0	71.8	33.8	68.8	41.6	54.1	39.1	67.1
40	18.4	94.5	30.7	84.3	22.0	82.3	34.5	58.6	24.7	79.9
45	12.1	110.9	20.7	95.2	14.0	96.9	22.1	61.3	13.1	98.1

[a] r is mass ratio of CMCase to Avicelase.

[b] Maximum adsorption amounts of cellulase (mg/g cellulose).

[c] K_{ad} is adsorption equilibrium constant (l/mol).

Table 7-4. Langmuir adsorption constants for microcrystalline celluloses and pulps at 25°C

	Avicel® PH101	Avicel® PH102	Avicel® PH105	Unbeaten HW pulp	Beaten HW pulp
K_p (ml/mg)	3.13	3.28	3.03	1.52	1.32
$W_{ads,max}$ (mg/g)	4.10	3.01	5.03	28.89	36.80
Adj. R-square	0.97	0.98	0.96	0.89	0.98

Kp = adsorption constant, $W_{ads,max}$ = maximum adsorption amount

Adj. R-squares were obtained using OriginPro 8, which describes the goodness of fit. Higher values indicate better fits.

It is worth noting no census found in literature regarding the different effects of crystallinity and surface areas on cellulase adsorption. In this research, the cyrstallinity of substrates played a more significant role than their surface areas (Figure 7-11). The maximum enzyme adsorption for all substrates used correlated linearly with the crystallinity indexes, regardless of the surface areas and morphology (Figure 7-11 A); furthermore, at a similar crystallinity level, surface areas also showed a linear relationship (Figure 7-11 B). It can be expected that surface area plays a significant role in cellulase adsorption provided the substrates have the same crystallinity. Figure 7-12 shows BET surface areas as a function of cellulose crystallinity index. There is no linear relationship between surface areas and crystallinity indexes for the substrate studied. It may therefore be concluded that crystallinity plays a more significant role than surface area does. This is in agreement with the claim of Fan et al.[3] Comparing the adsorption for microcrystalline celluloses and HW pulps, the former had a higher surface area and higher crystallinity but lower adsorption. This shows that crystallinity may play a more important role than surface area in determining the adsorption of cellulase to a cellulose substrate. This finding is different from the work of Grethlein,[21] who reported that crystalliniy has less impact than the substrate surface areas.

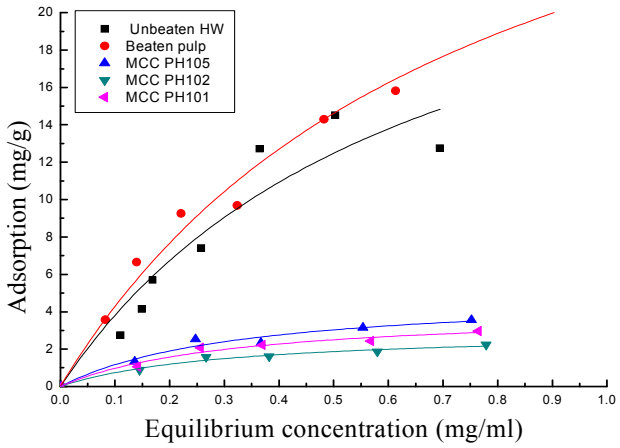

Figure 7-10. Adsorption isotherms for MPC on microcrystalline celluloses and unbeaten and beaten hardwood pulps at 25°C. The plotted values were average of three replicates in all situations.

The production of microcrystalline cellulose involves acid hydrolysis of the amorphous region of cellulose between the microcrystallites. Because of this, the degree of crystallinity can be very high.[16, 38] From the perspective of cellulose structures, accessible sites for cellulase may be much less due to the existence of hydrogen bonding between and within cellulose chains.[54] Cellulase molecules can more easily attach themselves to the amorphous regions than to crystalline ones through hydrophobic forces. Research from the ball milling of cellulose and filter papers for cellulose hydrolysis supports this conclusion.[38]

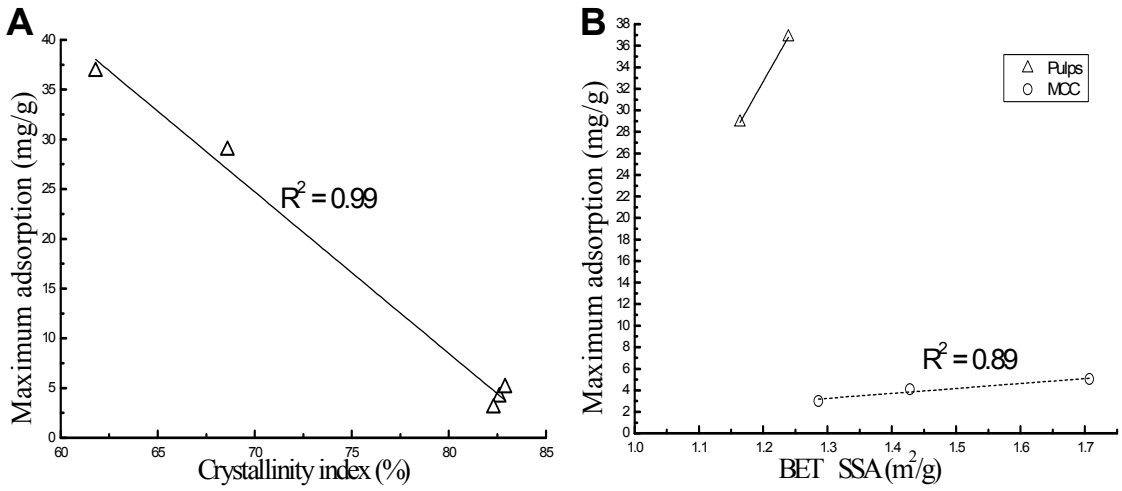

Figure 7-11. **(A)** Maximum adsorption of MPC cellulase enzyme at 25°C as a function of crystallinity. **(B)** Maximum adsorption of cellulase enzyme as a function of specific surface area. The surfaces areas for MCCs in the lower line follow a sequence of from left to right: Avicel® PH102 (Smallest), Avicel® PH101 (Medium), Avicel® PH105 (Largest). The two dots in the upper line correspond to unbeaten and beaten hardwood pulps respectively from left to right; no correlation coefficient can be generated due to the lack of more data points.

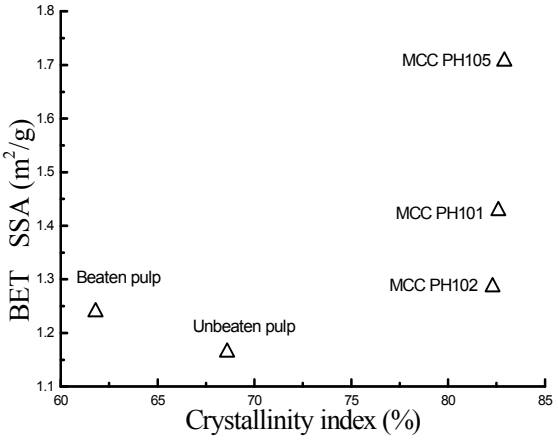

Figure 7-12. Plot of BET specific surface area as a function of crystallinity index.

4. Conclusions

Temperature affects adsorption inversely; higher temperature produced lower cellulase adsorption to cellulose. The BET surface areas measured all accessible surfaces and represent a more generally accepted description of the surfaces that cellulase molecules can approach. Higher surface area produced a relatively higher cellulase adsorption and higher maximum adsorption. However, crystallinity played a more important role in cellulose adsorption; lower crystallinity substrates (more amorphous material) produced much higher adsorption. Beating increased the adsorption significantly by changing the substrate crystallinity. For all substrates used, the maximum adsorption is inversely related to adsorption constant. An increase in maximum adsorption correlated with a decrease in adsorption constant.

References

(1) Hu, G.; Heitmann, J. A.; Rojas, O. J. BioResouces **2008**, 3, 270-294.

(2) Bin Yang, C. E. W. Biofuels, Bioproducts and Biorefining **2008**, 2, 26-40.

(3) Fan, L. T.; Lee, Y.-H.; Beardmore, D. H. Biotechnology and Bioengineering **1980**, 22, 177-199.

(4) Lynd Lee, R.; Weimer Paul, J.; van Zyl Willem, H.; Pretorius Isak, S. Microbiology and molecular biology reviews : MMBR **2002**, 66, 506-577.

(5) Himmel, M. E. Biomass recalcitrance : deconstructing the plant cell wall for bioenergy; Blackwell Pub.: Oxford, 2008.

(6) Eriksson, J.; Malmsten, M.; Tiberg, F.; Callisen, T. H.; Damhus, T.; Johansen, K. S. J. Colloid Interface Sci. **2005**, 284, 99-106.

(7) Azevedo, H.; Bishop, D.; Cavaco-Paulo, A. Enzyme and Microbial Technology **2000**, 27, 325-329.

(8) Sinitsyn, A. P.; Larionova, T. B.; Yakovenko, L. V. Biotekhnologiya **1988**, 4, 476-486.

(9) Gerber, P. J.; Joyce, T. W.; Heitmann, J. A.; Siika-Aho, M.; Buchert, J. Cellulose **1997**, 4, 255-268.

(10) Kaya, F.; Heitmann, J. A.; Joyce, T. W. J. Biotechnol. **1994**, 36, 1-10.

(11) Jackson, L. S.; Joyce, T. W.; Heitmann, J. A.; Giesbrecht, F. G. J. Biotechnol. **1996**, 45, 33-44.

(12) Kaya, F.; Heitmann, J. A.; Joyce, T. W. Cellulose Chemistry and Technology **1999**, 33, 203-213.

(13) Ooshima, H.; Burns, D. S.; Converse, A. O. Biotechnology and Bioengineering **1990**, 36, 446-452.

(14) Converse, A. O.; Girard, D. J. Biotechnol. Prog. **1992**, 8, 587-588.

(15) Lee, S. B.; Shin, H. S.; Ryu, D. D. Y.; Mandels, M. Biotechnology and bioengineering **1982**, 24, 2137-2153.

(16) Ooshima, H.; Sakata, M.; Harano, Y. Biotechnology and Bioengineering **1983**, 25, 3103-3114.

(17) Chernoglazov, V. M.; Ermolova, O. V.; Klyosov, A. A. Enzyme and Microbial Technology **1988**, 10, 503-507.

(18) Gilbert, I. G., Purdue University, Indiana, 1982.

(19) Ryu, D. D. Y.; Lee, S. B.; Tassinari, T.; Macy, C. Biotechnology and Bioengineering **1982**, 24, 1047-1067.

(20) Inglesby, M. K.; Zeronian, S. H. Cellulose **1996**, 3, 165-181.

(21) Grethlein, H. E. Nat Biotech **1985**, 3, 155-160.

(22) TAPPI In Test Methods T 200 sp-96; TAPPI: Atlanta, GA, United States, 1998, pp 9.

(23) Segal, L.; Creely, J. J.; Martin, A. E., Jr.; Conrad, C. M. Textile Research Journal **1959**, 29, 786-794.

(24) TAPPI In TAPPI Test Methods TAPPI Press: Atlanta, GA, United States, 1997; Vol. T 272 sp-97, pp 6.

(25) Kerker, M. The scattering of light, and other electromagnetic radiation; Academic Press: New York, 1969.

(26) Bohren, C. F.; Huffman, D. R. Absorption and Scattering of Light by Small Particles; John Wiley & Sons, Inc., 1983.

(27) Peterson, G. L.; Hirs, C. H. W.; Serge, N. T. In Methods in Enzymology; Academic Press, 1983; Vol. Volume 91, pp 95-119.

(28) Hoshino, E.; Kanda, T.; Sasaki, Y.; Nisizawa, K. Section Title: Enzymes **1992**, 111, 600-605.

(29) Ardizzone, S.; Dioguardi, F. S.; Mussini, T.; Mussini, P. R.; Rondinini, S.; Vercelli, B.; Vertova, A. Cellulose **1999**, 6, 57-69.

(30) Nakai, Y. Chemical & pharmaceutical bulletin **1977**, 25, 96-101.

(31) Plonka, A. M. Cellulose chemistry and technology **1982**, 16, 473-483.

(32) Sottys, J.; Lisowski, Z.; Knapczyk, J. Acta pharmaceutica technologica **1984**, 30, 174-181.

(33) Lee, S. B.; Kim, I. H.; Ryu, D. D.; Taguchi, H. Biotechnol Bioeng **1983**, 25, 33-51.

(34) Cheng, Q.; Wang, S. Q.; Rials, T. G.; Lee, S. H. Cellulose **2007**, 14, 593-602.

(35) Park, S.; Venditti, R. A.; Abrecht, D. G.; Jameel, H.; Pawlak, J. J.; Lee, J. M. Journal of Applied Polymer Science **2007**, 103, 3833-3839.

(36) Luukkonen, P.; Schaefer, T.; Hellen, L.; Juppo, A. M.; Yliruusi, J. International Journal of Pharmaceutics **1999**, 188, 181-192.

(37) Gama, F. M.; Mota, M. Section Title: Enzymes **1997**, 15, 237-250.

(38) Banka, R. R.; Mishra, S. Enzyme and Microbial Technology **2002**, 31, 784-793.

(39) Hamer, R. J. Paper Technology **1974**, 15, 263-270.

(40) O'Neil, A. J.; Jee, R. D.; Moffat, A. C. Analyst **1998**, 123, 2297-2302.

(41) O'Neil, A. J.; Jee, R. D.; Moffat, A. C. Analyst **1999**, 124, 33-36.

(42) Ek, R.; Alderborn, G.; Nystrom, C. International Journal of Pharmaceutics **1994**, 111, 43-50.

(43) Badawy, S.; Gray, D.; Hussain, M. Pharmaceutical Research **2006**, 23, 634-640.

(44) Herrington, T. M.; Petzold, J. C. Cellulose **1995**, 2, 83-94.

(45) Risén, J.; Hultén, A. H.; Paulsson, M. Journal of wood chemistry and technology **2004**, 24, 289 - 306.

(46) Jeong, C.; Maciel, A. M.; Pawlak, J. J.; Heitmann, J. A.; Argyropulous, D. S.; Rojas, O. J., Auckland, New Zealand, 16-19 MAY 2005.

(47) Rojas, O. J.; Jeong, C.; Turon, X.; Argyropoulos, D. S. ACS Symp. Ser. **2007**, 954, 478-494.

(48) Jackson, L. S., North Carolina State University, Raleigh, North Carolina, USA, 1996.

(49) Ghose, T. K. Pure and Applied Chemistry **1987**, 59, 257-268.

(50) Kim, D. W.; Yang, J. H.; Jeong, Y. K. Appl. Microbiol. Biotechnol. **1988**, 28, 148-154.

(51) Peitersen, N.; Medeiros, J.; Mandels, M. Biotechnology and Bioengineering **1977**, 19, 1091-1094.

(52) Beltrame, P. L.; Carniti, P.; Focher, B.; Marzetti, A.; Cattaneo, M. Journal of Applied Polymer Science **1982**, 27, 3493-3502.

(53) Kim, D. W.; Kim, T. S.; Jeong, Y. K.; Lee, J. K. Journal of Fermentation and Bioengineering **1992**, 73, 461-466.

(54) Wada, M.; Nishiyama, Y.; Chanzy, H.; Forsyth, T.; Langan, P. Powder Diffraction **2008**, 23, 92-95.

Chapter 8 Differentiation of cellulase isozyme adsorption and desorption by SDS-PAGE

Abstract

Sodium dodecyl sulfate polyacrylamide gel electrophoresis (SDS-PAGE) is a broadly used analytical and preparative tool in enzymology, biochemisty and related areas. In this research, SDS-PAGE was employed to study the sorption behavior of cellulase isozymes to two microcrystalline celluloses (Avicel® PH102 and PH105) and beaten bleached kraft pulp. Two cellulases, one from *Aspergillus niger* and the other from *Trichoderma reesei*, were used to investigate the adsorption and desorption behaviors. The desorption operations were conducted at 25°C using a recycling process with three different recycling agents at pH 4.8, pH 7 and pH 10, respectively. The original isozyme proteins, equilibrium proteins and desorbed proteins were analyzed using SDS-PAGE gels. Gel images were scanned and analyzed using ImagePro. The molecular weights of isozymes in both cellulases were determined by comparing their migration distance to a protein marker consisting of seven known proteins. It was observed that the cellulase from *Trichoderma reesei* had a higher adsorption on all substrates studied compared to the cellulase system from *Aspergillius niger*, and higher pH favored a larger desorption. Experimental results also demonstrate a uniform adsorption and desorption in proportion to their concentrations for the isozymes determined by SDS-PAGE.

Keywords: electrophoresis, SDS-PAGE, cellulases, isozymes, cellulase adsorption, cellulase desorption

1. Introduction

Gel electrophoresis is a relatively simple, rapid and highly sensitive tool to study the properties of proteins. The separation of proteins by electrophoresis is based on the fact that charged molecules will migrate through a support matrix upon application of an electric field usually provided by immersed electrodes.[1] Agarose and polyacrylamide gels are the major support matrixes broadly used. Agarose gels are usually used for the separation of larger macromolecules such as nucleic acids whereas polyacrylamide gels are widely used for protein separation. Polyacrylamide gel electrophoresis can be employed to determine the size, amount and purity of proteins or polypeptides. There are a variety of different polyacrylamide gel electrohphoresis methods developed for different applications in analytical chemistry, biochemistry and molecular biology. Among these methods, sodium dodecyle sulfate polyacrylamide gel electrophoresis (SDS-PAGE), which was originally described by Laemmli,[2] is the most widely used system. In this system, the proteins are denatured and hence the separation is strictly based on their sizes.[2] The PAGE-gels are polymerized from monomeric acrylamide and N,N'-methylene-bisacrylamide (bisacrylamide), with the latter as a cross linker. Figure 8-1 shows the chemical structures of the monomers and the polymer. During the process of gel polymerization, ammonium persulphate or a light source is used to initiate the reaction. Polyacrylamide usually makes a

small-pore gel which is used to separate proteins ranging in molecular weight from smaller than 5,000 to larger than 200,000 kD. Pore sizes are determined by the total solids content (%T) and the ratio of cross-linker to acrylamide monomer (%C):

$$\begin{aligned} \%T &= \frac{(\text{Acrylamide} + \text{bisacrylamide})/g}{100\ \text{ml}} \times 100 \\ \%C &= \frac{\text{bisacrylamide}/g}{(\text{Acrylamide} + \text{bisacrylamide})/g} \times 100 \end{aligned} \qquad (1)$$

The driving force of electrophoresis is the voltage applied to the gel system. The speeds of movement of molecules are directly related to the voltage gradient applied. Ohm's law shows the relationship of voltage, current and resistance (equation 2):

$$I = \frac{V}{R} \text{ or } V = IR \qquad (2)$$

Where V, I and R stand for voltage, current and resistance and are measured in volts (V), amperes (A) and ohms (Ω), respectively. Another significant equation is the power equation, which describes the heat that is produced in a circuit (equation 3):

$$P = VI = I^2R = \frac{V^2}{R} \qquad (3)$$

Where P denotes power and is measured in watts (W). The heat produced according to equation 3 is also called Joule heat. In an electrophoresis circuit, the voltage and current are supplied by a DC current and the electrodes, buffers and gels all act as simple resistors. In the SDS-PAGE electrophoresis system, the overall resistance increases as the run progresses while the buffer resistance declines with the increasing temperature produced by the Joule heating. Depending on which parameter is set constant, voltage or current, the Joule heat may

increase or decrease with temperature.

In enzymology, SDS-PAGE has been broadly employed to determine the molecular weight of various proteins. Cellulase is one of the extensively researched enzymes, existing in nature to degrade cellulosic materials. Scientific research has attempted to find various different microbial sources for cellulase enzymes. SDS-PAGE plays an important role in characterizing the enzymes produced by these sources. However, in the applied research on cellulase enzymes, SDS-PAGE is less commonly used, especially in the study of interaction between cellulases and cellulose. In this report, by assuming that the gel band density in a gel would be proportional to the protein loaded, we used commercial pre-casted SDS-PAGE gels to compare the adsorption and desorption of different isozymes in cellulases. Two cellulases, one from *Asperigllus niger* and the other from *Trichoderma reesei*, were used on three substrates, Avicel® PH102 and PH105 and as well as on a beaten hardwood pulp. The desorptions were conducted using direct washing by sodium acetate buffer (pH 4.8), pure water and caustic water (pH 10, 0.1 mM/L). Gel images were scanned and analyzed using ImagePro software.

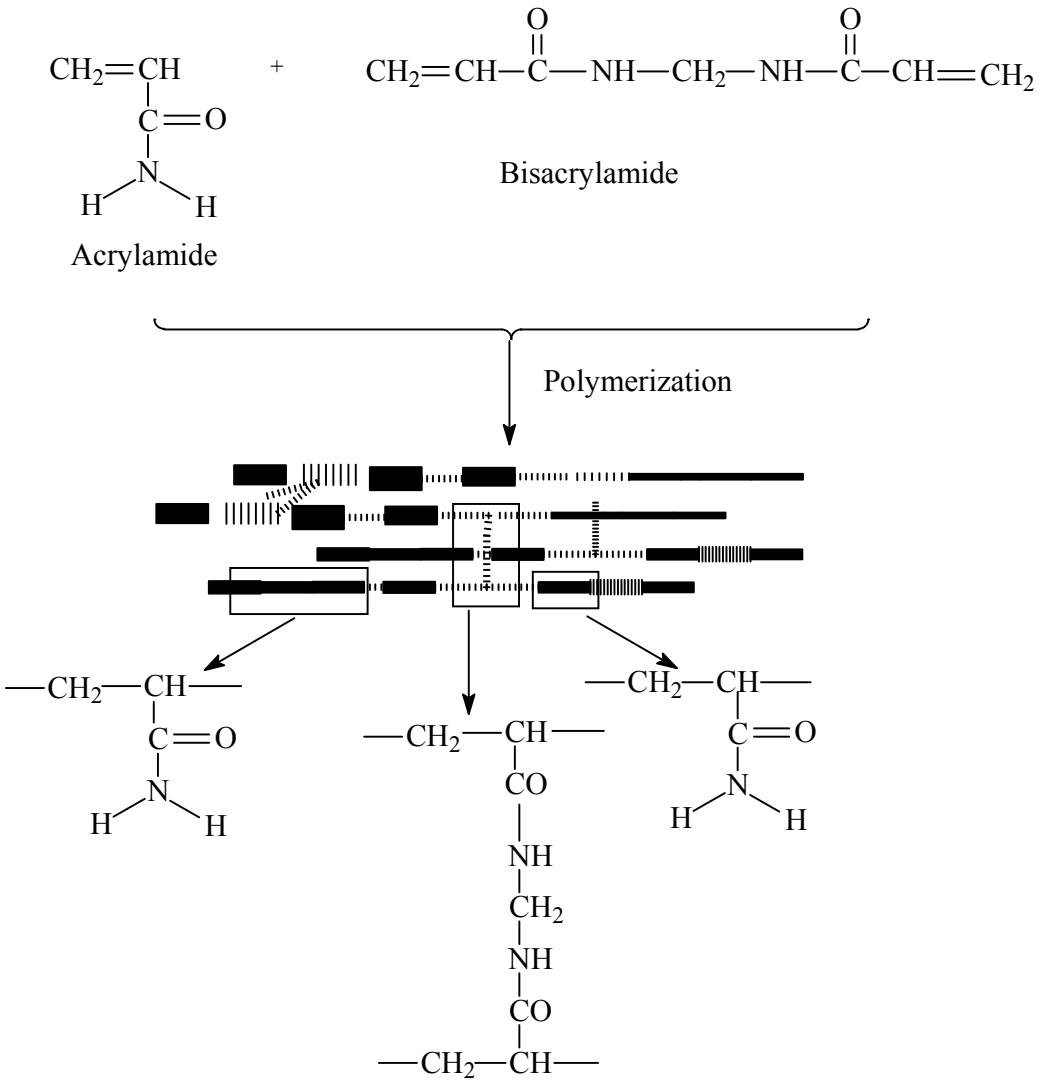

Figure 8-1. The chemical structures of acrylamide, bisacrylamide and polyacrylamide gel.[1]

2. Experimental

2.1 Materials and instruments

Commercial cellulases were purchased from MP Biomedical Inc. and Sigma Aldrich Co. The cellulase from MP Biomedical Inc. (MPC hereafter) was a yellow dry powder from

Aspergillus niger. The cellulase from Sigma Aldrich (SAC) was an amber viscose liquid *Trichoderma reesei*. Microcrystalline celluloses (Avicel® PH 102 and Avicel® PH 105) were a gift from of FMC BioPolymer Inc. Their nominal particle sizes were 90 μm and 20 μm, respectively. Eucalyptus bleached kraft pulp was purchased from NIST (US Department of Commerce, National Institute of Standards and Technologies, Gaithersburg, MD 20899). After disintegration, the pulp was beaten using a valley beater following TAPPI Method T 200.[3] All pulp were thoroughly washed using sodium acetate buffer (pH 4.8, ionic strength 100 mM) and stored in a cold room at 4°C.

Pre-cast polyacrylamide mini gels, 4~20% Precise™ Protein Gels and 12% Precise™ Protein Gels, ImmunoPure™ Lane Marker Reducing Sample buffer, BupH (tm) Tris-HEPES-SDS Running Buffer, Imperial™ Protein Stain, SilverSNAP® Stain Kits and Fisher BioReagents EZ-Run Protein Marker, were purchased from Thermo Fisher Scientific Inc. A homemade drying agent was made using ethanol, glycerol and milli-Q water. Concentrations of ethanol and glycecol were 20% and 3% by volume, respectively.

A Hoefer SE-260 mini-vertical gel electrophoresis unit coupled with an Electrophoresis Power Supply EPS 301(Amersham Biosciences) was employed for electrophoresis. A 12 cm × 12 cm Thermo Scientific* Owl* Gel-Dying Kit was applied for gel drying using cellophane membrane. An Umax PowerLook III scanner was used for gel scanning. The Image-Pro Plus (Version 4.5.1.22) from Media Cybernetics Inc. was employed to conduct gel band density analysis. Line profile was selected for image decomposition.

2.2 Sample preparation

MP cellulase powders were dissolved in the sodium acetate buffer at a concentration of 20 mg/ml, and then diluted to the target concentrations using buffer solutions. Sigma cellulases were handled similarly but the concentrations were denoted as a volume ratio, the stock solution had a concentration of 2% v/v. All solution preparations were conducted in volumetric flasks to ensure accuracy. All microcrystalline celluloses were hydrated overnight and then centrifugally separated following TAPPI Method UM-256 to remove unbound water.[4]

2.3 Adsorption and desorption

Adsorptions were performed using the procedure shown Figure 8-2. Incubations were performed at a 5% substrate consistency using 1 g of substrate mixed with 20 ml cellulase solution. A LAB-LINE® Incubator-shaker was employed to incubate the samples at 25°C. When incubated at 4°C, a water-ice bath was employed. After a one hour incubation, the samples were centrifugally separated using an Eppendorf Centrifuge 5702 following TAPPI Useful Method UM 256 [4] and supernatants were collected for SDS-PAGE and the remaining solid substrates were washed using buffer, milliQ water and caustic water (pH 10, 0.1 mM/L), respectively. A 30 min washing was performed in the A LAB-LINE® Incubator-shaker and then the mixtures were centrifugally separated to collect the desorbed liquid phases for SDS-PAGE experiments. Before recycling from the incubated beaten hardwood pulp, five Kimwipes® were used twice to press the pulp to ensure that no appreciable residual liquid cellulase solutions were present to interfere with the recycling determination.

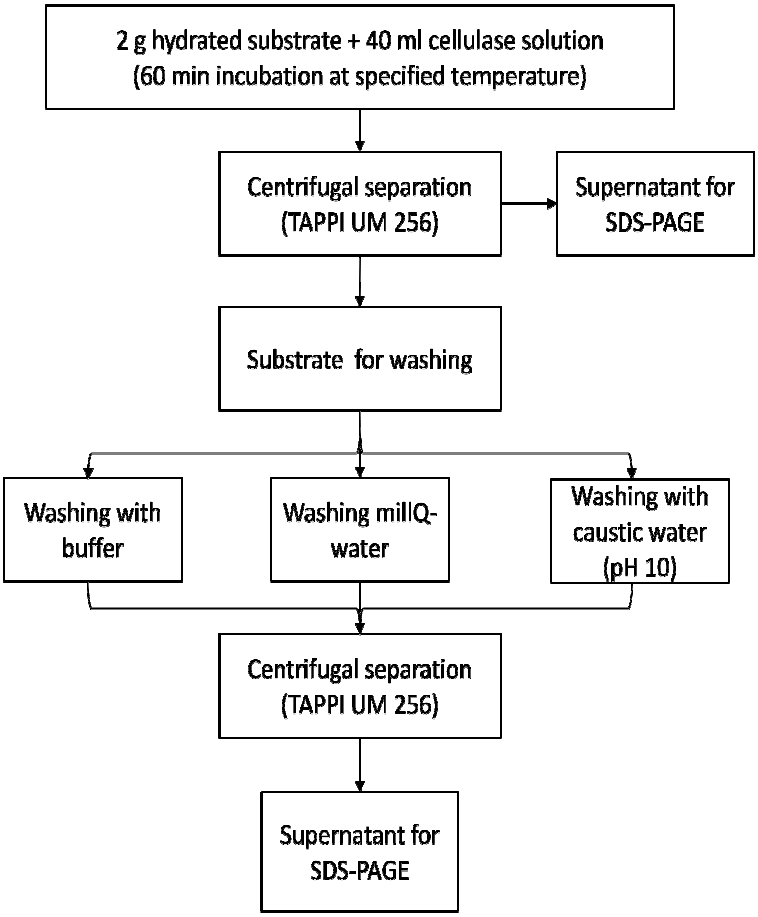

Figure 8-2. A schematic illustration of cellulase adsorption/desorption experiments to get samples for sodium dodecyle sulphate polyacrylamide gel electrophoresis.

2.4 Electrophoresis

Four parts of liquids, including the equilibrium solutions, washing agent, and the original cellulase solutions were mixed with one part of the ImmunoPure^{TM} Lane Marker Reducing Sample buffer, which was used to denature enzyme proteins, increase sample densities as well as to be an indicator (red color) signaling the front ends during gel running. These

mixtures were boiled for 5 min to denature the proteins. After cooling the samples to room temperature, 10 μl samples were placed in gel wells. A control (blank) and a protein marker were placed in two wells respectively when needed. A 5~10 min settling was allowed and then the power was applied to the gel. A water circulation was employed to prevent a overheating of the gel apparatus. Two gels were run simultaneously under 150 V voltage (constant voltage), 240 mA initial current, and 90 min running time. Gel running was discontinued if the red front reached the bottom of the gels before the end of the time. Gels were washed for about 1 hr by gently shaking in a shaker bath to remove surfactant, which followed by gel staining using Imperial™ Protein Stain (Coomassie blue) and SilverSNAP® Stain Kits respectively. Sample volumes varied for different staining methods. Stained gels were washed several times to completely remove the staining agents and then dehydrated for at least 30 min by soaking in a homemade drying agent. Thereafter, the gels were air-dried overnight. The dry gels were scanned using the Umax PowerLook III scanner and images were analyzed using the Image-Pro Plus software. Figure 8-3 summarizes the SDS-PAGE process used in this research.

3. Results and discussion

3.1 Analysis of gel images and molecular weights of isozymes

The molecular weight of isozymes in MPC and Celluclast were obtained by comparing their migration distance to a protein marker that had 7 proteins. Table 8-1 contains the protein names, the sources for these proteins and their molecular weights. Figure 8-4 shows the image of a gel that was employed to check the molecular weights of different isozymes in

MPC and the relationship between the densities of isozyme bands and the concentrations of sample loadings. A line profile was used to measure the migration distance and transmitted light density of the scanned image (Figure 8-5). The fifth column in table 8-1 lists the migration distance of different isozymes in MPC.

Table 8-1. Proteins, protein sources and their molecular weights in the protein marker.

Protein	Source	Molecular Weight, kDa	Log (MW)	*Migration distance
β-galactosidase	E. Coli	116	2.064	184
Bovine serum albumin	Bovine plasma	66.2	1.821	312
Ovalbumin	Chicken egg white	45	1.653	424
Lactate dehydrogenase	Porcine muscle	35	1.544	513
Restriction endonuclease Bsp981	E. Coli	25	1.398	629
β-lactoglobulin	Bovine milk	18.4	1.265	735
Lysozyme	Chicken egg white	14.4	1.158	789

The above information came from the manufacturer's instructions for protein marker.

*Migration distance was measured on a line profile using ImagePro software.

A correlation of the logarithmic value of molecular weights of proteins in the protein marker to the migration distances produced a linear fitting equation $Log(MW_{MPC}) = -0.00143\,D_M + 2.28913$ with a correlation coefficient R^2=0.993 for MPC and $Log(MW_{Celluclast}) = -0.00171\,D_M + 2.40717$ with a correlation coefficient R^2=0.993 for Celluclast (Figure 8-6). The molecular weights in both MPC and Celluclast were obtained by

applying their migration distances (see Fig. 8-4 for MPC) respectively to the fitting equations observed in Fig 8-6. Table 8-2 shows the molecular weights for different isozymes in both MPC and Celluclast.

Table 8-2. Molecular weights of proteins in both MPC and Celluclast

	Isozymes	I	II	III	IV	V	VI	VII	VIII
MW (kDa)	MPC	110.0	92.2	60.2	47.9	37.6	33.5	29.4	24.6
	Celluclast	117.7	98.2	60.0	50.2	37.7	28.8	23.3	18.1

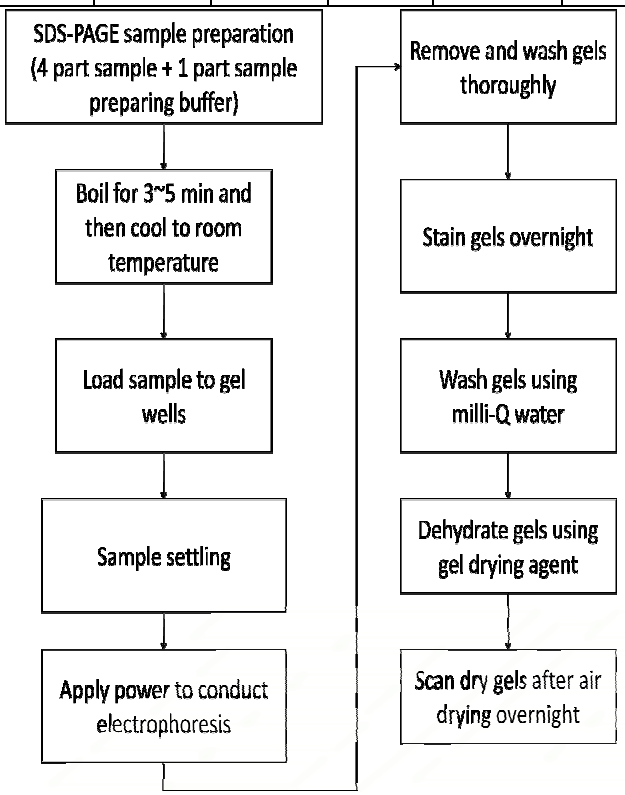

Figure 8-3. A schematic illustration of sodium dodecyle sulfate polyacrylamide gel electrophoresis process

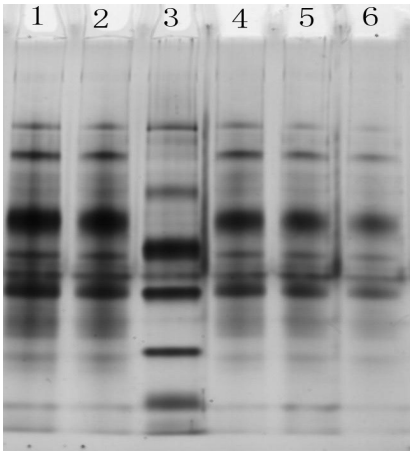

Figure 8-4. Measurement of molecular weights of isozymes in MPC cellulase and the relationship of isozyme band density versus sample loading concentration. MPC cellulase concentrations in well 1 to 2 and 4 to 6 were 0.625 mg/ml, 0.5 mg/ml, 0.4 mg/ml, 0.3 mg/ml and 0.2 mg/ml. Well 3 was the protein marker.

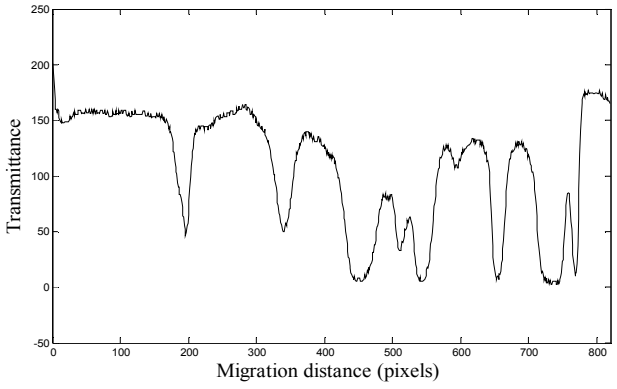

Figure 8-5. Line profile generated using ImagePro for the protein marker. The migration distance was measured from the top of the gel wells where sample loading occurred. Peak transmittances correspond to the density of isozyme bands. Higher transmittance means lower band density, which is equivalent to a lower amount of isozyme.

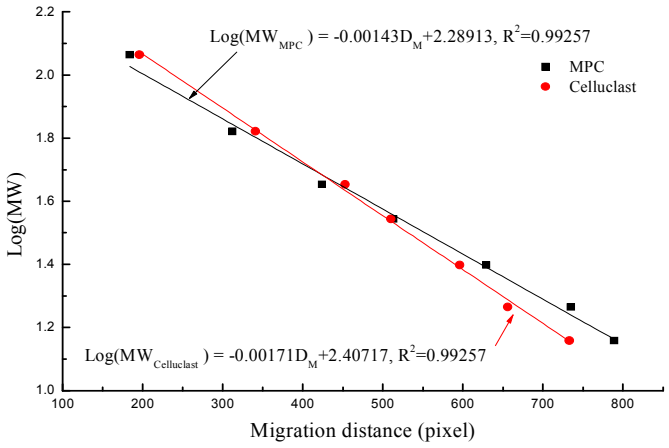

Figure 8-6. Migration distances of proteins in the protein marker as a function of molecular weights under the respective running conditions for both MPC and celluclast.

The molecular weights of isozymes IV in table 8-2 are close to those for EGII reported by Goyal et al. [5] and those of isozymes III are close to the molecular weights of CBHII reported by Kyriacou et al.[6] The smallest molecules detected by the PAGE gel may correspond to xylanase, but further information is needed to confirm this. The number of isozymes obtained by coomasie blue staining was 6 for MPC and 3 for celluclast. However, the silver stain kit produced gel images that showed 8 isozymes for both cellulase enzymes. This difference can be explained by the different sensitivity of these two staining methods. Coomassie can only detect and develop color for protein at a scale of micro-gram level while the silver stain kit can develop color for protein in the gel at a scale of lower than 1 nano-gram (gel images not shown). This produced information about the proportions of different isozymes. The celluclast probably contained lower amounts of isozymes with a molecular weight lower than

50 kD. These results are different from those described by Goyal,[5] who reported the molecular weights were in a range of 45 kD to 100 kD for *Trichoder reesei* cellulases.

3.2 Adsorption on different substrates

Cellulase adsorptions on three substrates, Avicel®PH102, Avicel®PH105 and beaten hardwood pulp were performed at 25°C. Figure 8-7 shows the information before and after the adsorptions of cellulases on those substrates. The one on the left shows that information on Celluclast and the right one shows that on MPC. It is apparent that Celluclast displayed a higher adsorption on all three substrates than MPC. These higher adsorptions occurred with most of the isozymes having a molecular weight greater than 30 kD. MPC shows a different behavior; the adsorbed amounts were much less. It can also be observed that both enzymes adsorbed highest on the beaten hardwood pulp whereas lowest adsorption occurred on Avicel®PH 102. This is consistent with the results that we obtained using the depletion method where the protein contents were determined by UV-Vis at a wavelength of 280 nm.

Much research has focused on the effect of physical properties on cellulase adsorption and cellulose hydrolysis.[7-11] Some researchers have shown that the crystallinity plays a more significant role than surface areas,[10] whereas some others have pointed out that surface area or porosity is the leading factor in terms of cellulose hydrolysis.[9] Our current research supports the opinion that both surface areas and crystallinity affect the cellulase adsorption but that crystallinity matters more, since both Avicel®PH 102 and Avicel®PH 105 had a crystallinity of about 82% whereas the crystallinity for beaten hardwood pulp was about 62% (X-ray diffraction spectrum and calculation of crystallinity can be referred from our previous

work). It can also be observed that most of the isozymes in cellulase mixtures showed a uniform adsorption proportional to their concentration on the substrates employed in this investigation.

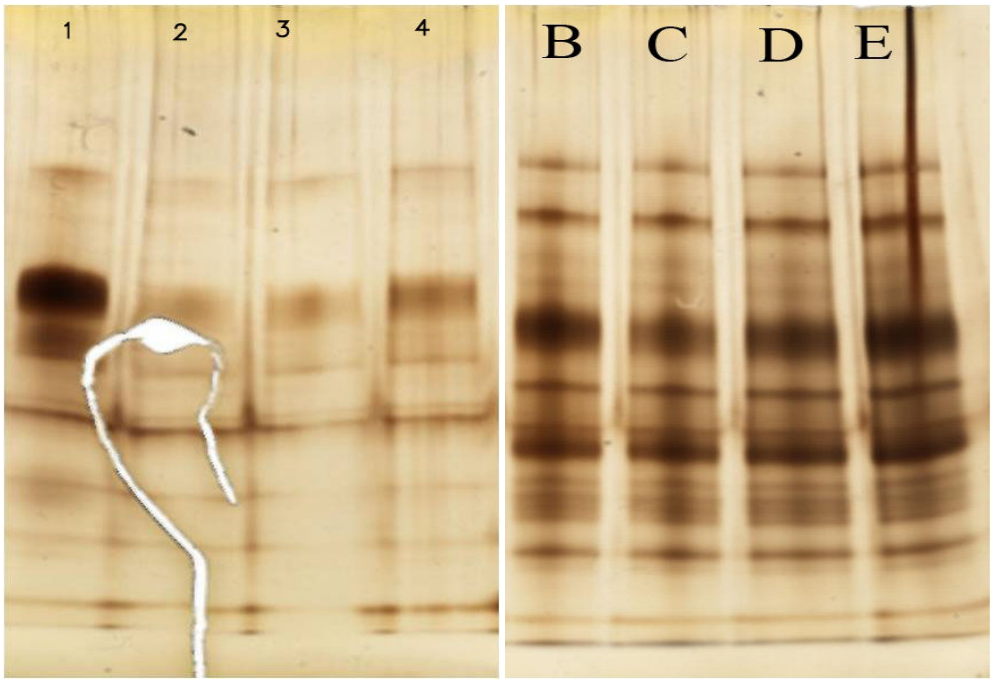

Figure 8-7. Adsorption effect of isozymes on three substrates Avicel®PH102, Aveicel®PH105 and beaten hardwood pulp. The original cellulase concentration for Cellullast was 2% v/v and that for MPC was 5 mg/ml. All substrate consistencies were 5% based on weight ratio. The solutions were diluted by a factor of 10 before loading into gel wells. 1, B= original cellulase solution 2, C=equilibrium solution from beaten hardwood pulp 3, D=equilibrium solution from Avicel®PH105 4, E=equilibrium solution from Avicel®PH102. Left: Celluclast. Right: MPC

3.3 Desorption and pH effect

The investigation of desorption was conducted on the three substrates at 25°C, using the method shown in Fig. 8-2. Figure 8-8 shows information about the adsorption and subsequent desorption/recycling of both MPC and Celluclast from the substrate Avicel®PH105. The original and equilibrium solutions were both diluted by a factor of 10 to ensure legible band separation. Since the recycling regents were only half of the amounts used for the adsorptions, the same band density from both original and equilibrium solutions would represent a concentration 20 times greater than those for the recycling. The equilibrium band densities supported the previous observation that Celluclast adsorbed more than MPC did on the same substrate and that there was uniform adsorption for all isozymes in the cellulase solutions.

Figure 8-8 also shows pH played an important role in recycling. It is obvious that higher pH produced higher desorption from Avicel®PH 105 for both cellulase enzymes. This was true for the other two substrates, Avicel®PH 102 and beaten hardwood pulp (Figures not shown). A hypothesis for the underlying desorption mechanism would be that pH 4.8 determined the best environment for the interaction between cellulase isozymes and the cellulosic substrate. The washing of substrates therefore could allow a continuation of the hydrolysis process once buffer solutions were added; however, the zero concentration of cellulase in the fresh buffer solutions would rebalance the dynamic equilibrium in the desorption direction (to the left direction). This agrees with the optimum pH range for cellulose hydrolysis by celluase. At pH 7, the buffer conditions for cellulase to fold into its

optimum tertiary or quarternatury structure may be less, the binding domain or even the catalytic domains may lose their capability to some extent. This would favor a change of protein structure that may cause the cellulases a loss of interaction with the cellulose substrate. At a higher pH, the hydroxide ions in the recycling reagent would probably have chemical interactions with the side chains of amino acid residues within the protein chains. These interactions with basic or acidic groups would be more pronounced, which may turn into a disruption of either hydrogen bond interaction or hydrophobic interaction with the substrates.

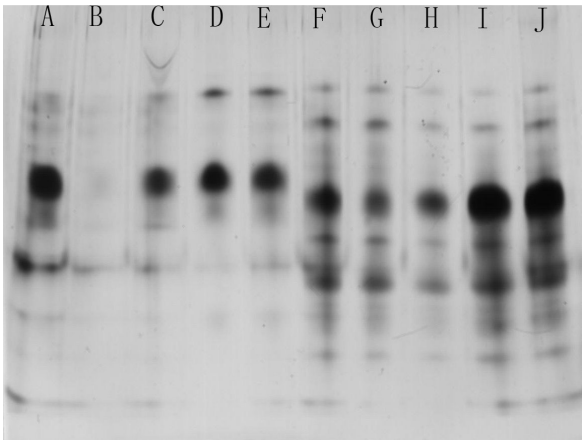

Figure 8-8. Adsorption on and desorption from Avicel®PH 105 by cellulases (MPC and Celluclast). Both adsorption and desorption were performed at 25°C. A~E: Celluclast, F~J: MPC. A, F =original solution with a concentration of 2%v/v and 5 mg/ml respectively; B, G = equilibrium solution; C, H = recycled at pH 4.8 using sodium acetate buffer; D, I = recycled at pH7 using milli-Q water; E, J = recycled at pH10 using a caustic water (pH 10, 0.1 mM/L).

3.4 Relationship of band intensity with cellulase concentration

The band intensity of isozyme from gel image was analyzed using the Matlab 2008b software. The intensities of isozyme bands for 4 different cellulase concentration (Fig. 8-4) were determined from their line profile (Figure similar to Fig. 8-5 but not shown). The five isozymes that have the most appreciable bands were analyzed. Figure 8-9 shows the correlation of the band intensities of the 5 isozymes to the concentration of their original cellulase solutions. The correlation coefficients for the five isozymes are 0.98, 0.97, 0.97, 0.98 and 0.94 respectively. It can be noticed that the isozymes with higher concentrations, which can be determined from higher band intensity, gave a better correlation to the original concentration of the cellulase solutions in which they existed. No similar technique has been found in the literature, especially involving the use of a simple scanner to determine the gel image intensity from which the relative ratios of different isozymes can be obtained and therefore provide information about adsorption and desorption depending on the prior experimental settings.

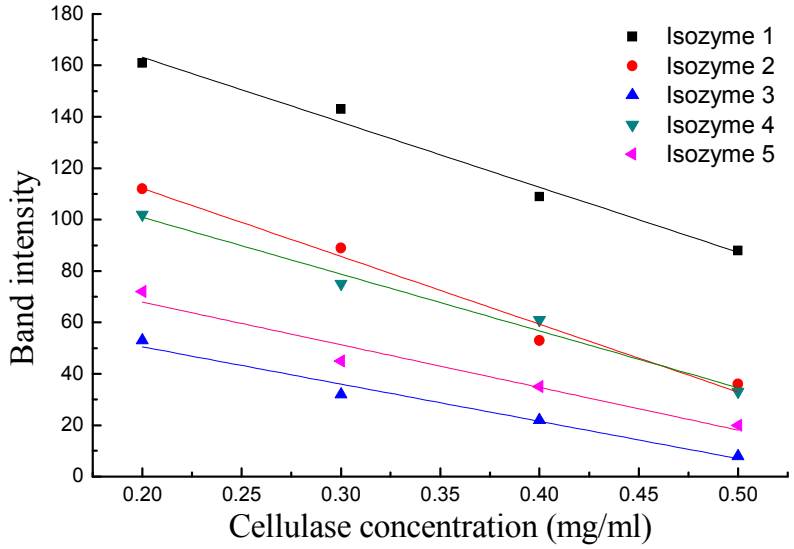

Figure 8-9. Relationship of isozyme band intensity with cellulase concentration. The four concentrations correspond to the well 2, 4, 5 and 6 in Figure 4. Correlation coefficients for isozyme 1 to isozyme 5 are 0.98, 0.97, 0.97, 0.98 and 0.94 respectively. Only the most appreciable 5 isozymes were analyzed in terms of the relationship of band intensity to cellulase concentration.

4. Conclusion

The molecular weights of cellulases from both *Trichoderma reesei* and *Aspergillus niger* ranged from 18 kDa to 110 kDa. The relative ratios of isozymes are different from each other. *Trichoderma reesei* cellulases contained three major components while the other isozymes were present in trace amounts. The *Aspergillus niger* cellulases contained more evenly distributed isozymes for all eight detected. All isozymes were uniformly adsorbed in proportion to concentration on three substrates, but the isozymes from *Trichoderma reesei*

showed much greater adsorption than the ones from *Aspergillus niger*. Microcrystalline cellulose with higher surface area produced higher adsorption for isozymes. Nevertheless, the degree of crystallinity had a much more pronounced effect on adsorption. The beaten hardwood pulp with a lower crystallinty gave the highest adsorption among the substrates used. All isozymes desorbed some at the three pH values, but the degree of desorption was different. The buffer desorbed cellulase least whereas the caustic water (pH 10, 0.1 mM/L NaOH) desorbed most among the three recycling agents. The analysis of the relationship of band intensity to cellulase concentration implies a potential broad application of sodium dodecyle sulfate gel electrophoresis that is useful in studies such as this.

References

(1) Hames, B. D.; Rickwood, D. Gel electrophoresis of proteins: a practical approch, 2nd edition ed.; Oxford University Press, 1990.

(2) Laemmli, U. K. Nature **1970**, 227, 680-685.

(3) TAPPI In Test Methods T 200 sp-96; TAPPI: Atlanta, GA, United States, 1998, pp 9.

(4) TAPPI In TAPPI Useful Methods UM 256; United States, 1991; Vol. 1991, pp 54-56.

(5) Goyal, A.; Ghosh, B.; Eveleigh, D. Bioresource Technology **1991**, 36, 37-50.

(6) Kyriacou, A.; MacKenzie, C. R.; Neufeld, R. J. Enzyme and Microbial Technology **1987**, 9, 25-32.

(7) Jackson, L. S.; Heitmann, J. A., Jr.; Joyce, T. W. Progress in Paper Recycling **1994**, 3, 32-41.

(8) Jackson, L. S., North Carolina State University, Raleigh, North Carolina, USA, 1996.

(9) Grethlein, H. E. Nat Biotech **1985**, 3, 155-160.

(10) Fan, L. T.; Lee, Y.-H.; Beardmore, D. H. Biotechnology and Bioengineering **1980**, 22, 177-199.

(11) Fan, L.; Lee, Y.-H.; Beardmore, D. In Advances in Biochemical Engineering, Volume 14, 1980, pp 101-117.

Chapter 9 General summary and conclusions

This dissertation began with a review of the chemical structures of lignocellulosic materials and cellulase enzyme systems. Direct research work included in-situ monitoring of cellulase activities using the quartz microbalance technology. It was hoped that this would lead to a new and more accurate cellulase assay and technique. In follow-up research a method was developed for determining cellulase activity using the quartz microbalance technique to measure changes in hydrolysis liquid products. The substrates used in this work were characterized using water retention value, crystallinity and surface area by a variety of techniques. Adsorption behavior was analyzed using a Langmuir isotherm model and the effect of substrate properties on adsorption was compared based on the Langmuir constants and the substrate properties. The final research work focused on the differentiation of isozyme adsorption by using sodium dodecyle sulphate polyacrylamide gel electrophoresis. Desorption phenomena were also investigated in this work. The following list summarizes the most important findings in this research:

1. Based on the adsorption constant and maximum adsorption obtained from the in-situ monitoring, adsorption may not be as important as previously believed in the hydrolysis of amorphous cellulose films by cellulase enzymes. The time course frequency change in QCM-D can be modeled by a dose-response model and the model parameters provide significant information about the substrate, the interfacial interaction, the liquid properties and the kinetics. (Chapter 4)

2. By measuring the liquid properties, such as density and viscosity of the hydrolysis products after removing the protein and other macromolecules, a QCM-D technique was developed to quantify the cellulase activities. Comparison of activity results from QCM-D with DNS, BCA and IC indicated that QCM-D can be a new and more accurate cellulase assay. The technique is relatively simple and it eliminates the difficult color development in redox based methods, and the use of toxic chemicals and the advance skills needed for ion chromatography operation. (Chapter 5)

3. Water retention value, particle size and surface areas, and crystallinity of the cellulosic substrates used in this work were characterized using the TAPPI UM 256 method, laser scattering and BET nitrogen adsorption, and X-ray diffraction respectively. It was found that surface area have a positive correlation with water retention value for the microcrystalline cellulose. (Chapter 6, Chapter 7)

4. Cellulase protein adsorption isotherms were developed using the depletion method. The isotherms followed Langmuir adsorption model and the Langmuir constants were obtained. The correlation of maximum adsorption to surface area and crystallinity implies that both cellulose crystallinity and surface areas are important to cellulase adsorption. The cellulase activity values from Chapter 5 help to support that cellulose crystallinity also plays an important role in cellulose hydrolysis.

5. Cellulase isozyme adsorption and desorption determined by SDS-PAGE indicated that isozyme adsorptions are uniform in proportion to their relative concentrations. It

was also found that the isozyme adsorption of cellulase from *Trichoderma reesei* on the same substrates was higher than the cellulase system from *Aspergillus niger*. The isozyme desorption and recovery increased at higher pH levels, with buffer (pH 4.8) giving least recovery and caustic water (pH 10, 0.1 mM/L NaOH) giving the highest. Image analysis of SDS-PAGE bands showed a concentration of band intensity with isozyme concentrations. This may be developed into a simple method to quantify gel analysis.

Chapter 10 Recommendations for future research work

Although this dissertation has developed results which contributed significantly to scientific knowledge in the field, future work is suggested to address the following issues and make further contributions:

1. A method should be developed to measure porosity and surface areas of cellulose and other polymer films prepared using spin-coating. A direct method to measure the crystallinity of cellulose films made using spin-coating and other techniques should also be developed. Actually this could be very simple if the casted films can be removed and put into an X-ray instrument.
2. A method should be developed to characterize the film thickness using a quartz microbalance technique. This method should be flexible and easy to use and interpret. For this research, AFM and other spectroscopic methods should be included for a comparison. A method might be developed using the QCM-D time course response to characterize cellulose film thickness.
3. A better understanding of the cellulase adsorption mechanism should be developed using piezoelectric techniques. The quartz microbalance techniques can shed light on the basic mechanism and whether that cellulase adsorption is a prerequisite for cellulose hydrolysis.
4. The mechanism behind the frequency drop in QCM-D research should be addressed to differentiate the contribution of the different factors, the

adsorption of cellulase, change in properties of the film, or change in the properties of cellulase solution.

5. A more direct way to measure the cellulase protein adsorption can be developed using a precipitation of protein in the cellulase solution. Both the proteins in the original solutions and that in equilibrium solutions can be precipitated. Adsorption may be obtained by direct weighing of the amount differences of proteins. A re-dissolution of these proteins can be adopted for the differentiation of isozyme adsorption.
6. A qualitative UV-visible technique can be used to indirectly determine the relative ratio of cellulose isozyme adsorption. This may be developed as a general method to maximize the effect of using recycled cellulase.
7. The synergism of different isozymes deserves further investigation. Gel electrophoresis could be employed to separate isozymes before and after adsorption experiments.